ACTA PROTOZOOLOGICA

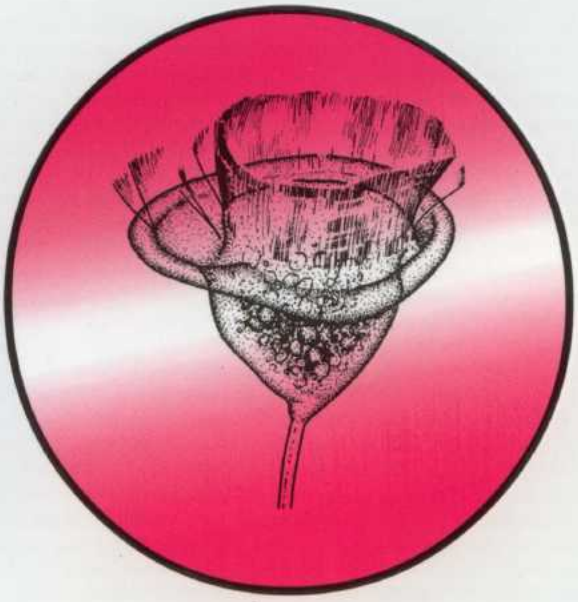

NENCKI INSTITUTE OF EXPERIMENTAL BIOLOGY
WARSAW, POLAND
2001
VOLUME 40 NUMBER 2
ISSN 0065-1583

Polish Academy of Sciences
Nencki Institute of Experimental Biology
and
Polish Society of Cell Biology

ACTA PROTOZOOLOGICA
International Journal on Protistology

ACTA PROTOZOOLOGICA appears quarterly.

The price (including Air Mail postage) of subscription to ACTA PROTOZOOLOGICA at 2001 is: US $ 200.- by institutions and US $ 120.- by individual subscribers. Limited numbers of back volumes at reduced rate are available. TERMS OF PAYMENT: check, money oder or payment to be made to the Nencki Institute of Experimental Biology account: 111-01053-401050001074 at Państwowy Bank Kredytowy XIII Oddz. Warszawa, Poland. For matters regarding ACTA PROTOZOOLOGICA, contact Editor, Nencki Institute of Experimental Biology, ul. Pasteura 3, 02-093 Warszawa, Poland; Fax: (4822) 822 53 42; E-mail: jurek@ameba.nencki.gov.pl For more information see Web page **http://www.nencki.gov.pl/ap.htm**).

Front cover: Song W. and Warren A. (2000) A redescription of *Pseudovorticella patellina* (O. F. Müller, 1776) nov. comb., a Peritrichous ciliate (Protozoa: Ciliophora: Peritrichida) isolated from mariculture biotopes in North China. *Acta Protozool.* **39:** 43-50

This publication is supported by the State Committee for Scientific Research

Desktop processing: Justyna Osmulska, Data Processing Laboratory of the Nencki Institute
Printed at the MARBIS, ul. Kombatantów 60, 05-070 Sulejówek, Poland

Acta Protozool. (2001) 40: 83 - 97

ACTA
PROTOZOOLOGICA

Biogeographical Differences in a Common Soil Ciliate, *Gonostomum affine* (Stein), as Revealed by Morphological and RAPD-Fingerprint Analysis

Wilhelm FOISSNER[1], Thorsten STOECK[2], Helmut SCHMIDT[2] and Helmut BERGER[3]

[1]Universität Salzburg, Institut für Zoologie, Salzburg, Austria; [2]Universität Kaiserslautern, Abteilung Ökologie, Kaiserslautern, Germany; [3]Technisches Büro für Ökologie, Salzburg, Austria

Summary. *Gonostomum affine* is a common, hypotrichous soil ciliate showing a wide variety of more or less distinct morphologies which, depending on the view, can be considered as taxonomic entities or variations of a single morphotype. Thus, we chose it as a model to investigate some main questions in ciliate alpha-taxonomy and biodiversity, viz., (i) the power of morphological methods and RAPD-fingerprints to separate two distinct morphospecies of *Gonostomum*; (ii) whether morphology and RAPD agree in separating the most dissimilar morphotypes; and (iii) whether *G. affine* has a biogeographical population structure. Accordingly, we investigated one *G. strenuum* population from Australia and compared it with six *G. affine* populations from Europe, Africa, and South America. Data were analysed with classical similarity trees and two new methods combining morphological features and RAPD-fingerprints in single similarity trees. The main results of this study were: (i) Morphology could separate the two morphospecies very clearly, while RAPD could not, irrespective of the indices and clustering algorithms used; (ii) Morphotrees did not agree with RAPD-trees and not show a distinct biogeographical pattern. However, a rather distinct biogeographical population structure became recognisable when morphological features and RAPD-fingerprints were combined in a single similarity tree, indicating (iii) a certain degree of geographical uniqueness of various genotypes. Generally, however, separation was rather weak and highly dependent on the indices and clustering algorithms used, indicating that, at the present state of knowledge, most *Gonostomum affine*-like morphotypes fall into the range of natural variability of a single species.

Key words: biodiversity, biogeography, Ciliophora, Protozoa, similarity trees, soil ciliates.

INTRODUCTION

Gonostomum affine is a very common ciliate in limnetic and terrestrial habitats, usually preferring the latter, where it may gain high abundances. Apparently, *G. affine* has a cosmopolitan distribution, although many more or less distinct morphotypes exist, several of which have Linnean names (for reviews, see Foissner 1998 and Berger 1999). Most of the variability concerns body size (length 50-160 μm), and number (6-22) and pattern of the fronto-ventral-transverse cirri. Recent authors tend to interpret these differences as part of the natural variability of this species and thus synonymise most of the named populations (Buitkamp 1977, Foissner 1982, Berger 1999), although different opinions exist (Maeda and Carey 1984) and gene sequence data and ecological specialisations indicate that, in general, mor-

Address for correspondence: Wilhelm Foissner, Universität Salzburg, Institut für Zoologie, Hellbrunnerstrasse 34, A-5020 Salzburg, Austria (Europe); Fax +43 (0) 662 8044-5698

phologists heavily under-split ciliates (Nanney *et al.* 1998, Dini and Nyberg 1999).

It has not yet been investigated whether variability follows a biogeographical pattern in *G. affine*. Generally, such studies are rare in ciliates. The best studied examples are the sibling species of *Tetrahymena pyriformis*, *Paramecium aurelia*, and *Stylonychia mytilus*, some of which are very likely restricted to certain geographic regions (Nanney and McCoy 1976, Ammermann 1985, Wichtermann 1986, Nanney *et al.* 1998). On the other hand, several reproductively isolated *Euplotes* strains obviously lack a geographic pattern (Dini and Gianni 1985) and a morphological analysis of four *Mesanophrys* species, all described from different hosts, strongly suggests that all belong to a single, facultatively histophagous morphospecies (Wiąckowski *et al.* 1999).

RAPD-fingerprinting and riboprinting are new tools for investigating population structures and have been successfully used also in ciliates (Kusch and Heckmann 1996; Kusch 1998; Stoeck and Schmidt 1998; Stoeck *et al.* 1998, 2000a). And even three common soil ciliate species of the genus *Colpoda* have been investigated (Bowers and Pratt 1995, Xu *et al.* 1997, Bowers *et al.* 1998). The riboprints and some main morphometrics did not show a biogeographical population structure in these species. However, the conclusion is not definitive because the rRNA gene region used was probably not informative enough (Bowers *et al.* 1998). Furthermore, molecular and morphological data were not combined in the similarity trees, so a common failure that often makes it difficult to know the extent results are influenced by incomplete data analysis. Others abandon morphology altogether, ascribing an unfounded power to molecular methods (Malpartida *et al*. 1995, Martin *et al.* 1997).

Our study is designed to overcome some of these shortcomings and specifically addresses the following matters: (i) to develop methods combining morphological data with RAPD-fingerprints in a single similarity (dissimilarity) tree; (ii) to compare the power of morphological methods and RAPD-fingerprints in separating two morphospecies of *Gonostomum*; (iii) to investigate whether morphology and RAPD agree in separating the most dissimilar morphotypes; and (iv) to investigate whether *G. affine* has a biogeographical population structure. Such questions address biodiversity and conservation matters, both very controversially discussed in ciliates (Finlay and Fenchel 1999, Foissner 2000a).

MATERIALS AND METHODS

Material. We investigated seven *Gonostomum* populations belonging to two morphospecies, viz., *Gonostomum affine* (Stein, 1859) Sterki, 1878 and *G. strenuum* (Engelmann, 1862) Sterki, 1878. Identification followed the review by Berger (1999). Although *G. affine* is a very common ciliate in soils worldwide (Foissner 1998), we could establish pure cultures (on Eau de Volvic enriched with some crashed wheat grains or baker's yeast) only from the *G. affine* population of Namibian site (31) and from the *G. strenuum* population of Australia. Raw cultures were set up from air-dried soil with the non-flooded Petri dish method, as described in Foissner (1987).

Population 1: *Gonostomum affine* from a beech forest brown earth soil in the surroundings of Salzburg, Austria, Europe (E 13°40' N 47°47').

Population 2: *Gonostomum affine* from a very sandy pasture soil near the village of Alqasab, about 130 km northeast of Riyadh, Saudi Arabia, Africa (E 47°30' N 25°).

Population 3: *Gonostomum affine* from Namibian site (26), that is, from organic debris and sand collected in the Sossus Vlei of the Namib Desert, Southwest Africa (E 15°20' S 24°40').

Population 4: *Gonostomum affine* from Namibian site (31), that is, from very sandy soil around a *Welwitschia* plant near Swakopmund, Namibia, Southwest Africa (E 15°30' S 22°40').

Population 5: *Gonostomum affine* from a cloud rain forest in the Henry Pittier National Park, Venezuela, South America (W 77° N 12°).

Population 6: *Gonostomum affine* from soil of the gallery forest at the bank of the Rio Negro (Amazon floodplain), Manaus, Brazil, South America (W 60° S 3°).

Population 7: *Gonostomum strenuum* from soil of the River Murray floodplain near Albury, Australia (E 147° S 37°).

Morphological analysis. Specimens from the raw or pure cultures were protargol-impregnated following the protocol A as described in Foissner (1991). This method provides permanent slides and shows the structures measured or counted very clearly (Fig. 4). Measurements and counts were performed at a magnification of X1000 (oil immersion), where a measuring unit is 1 µm in the eye piece. Scanning electron microscopy was performed as described in Foissner (1991), using concentrated aqueous mercuric chloride and osmium tetroxide (10:1) as fixative. The features investigated and the terminology used are shown in Fig. 1.

RAPD-fingerprinting. Three to five specimens each were used for the fingerprints, either directly from the (raw) non-flooded Petri dish cultures or the pure cultures. Specimens from the raw cultures were identified in vivo at a magnification of X250 and in protargol preparations (Figs. 7-9, 11, 12). Pre-treatment of specimens (three washes in SMB medium etc.) and fingerprinting were performed as described by Stoeck and Schmidt (1998), using primer Ro 360-04, with the sequence: 5' CCCTCATCAC (Roth, Karlsruhe, Germany). Furthermore, a control without any DNA-template was run with each of the populations.

Data analysis. The morphological data (Table 1) were compared with the Coefficient of Racial Likeness (CRL) described by Pearson (1926). The coefficient is a scale-independent distance function, which considers both the mean and variance of the variables (Sneath and Sokal 1973). Invariable features (number of dorsal kineties,

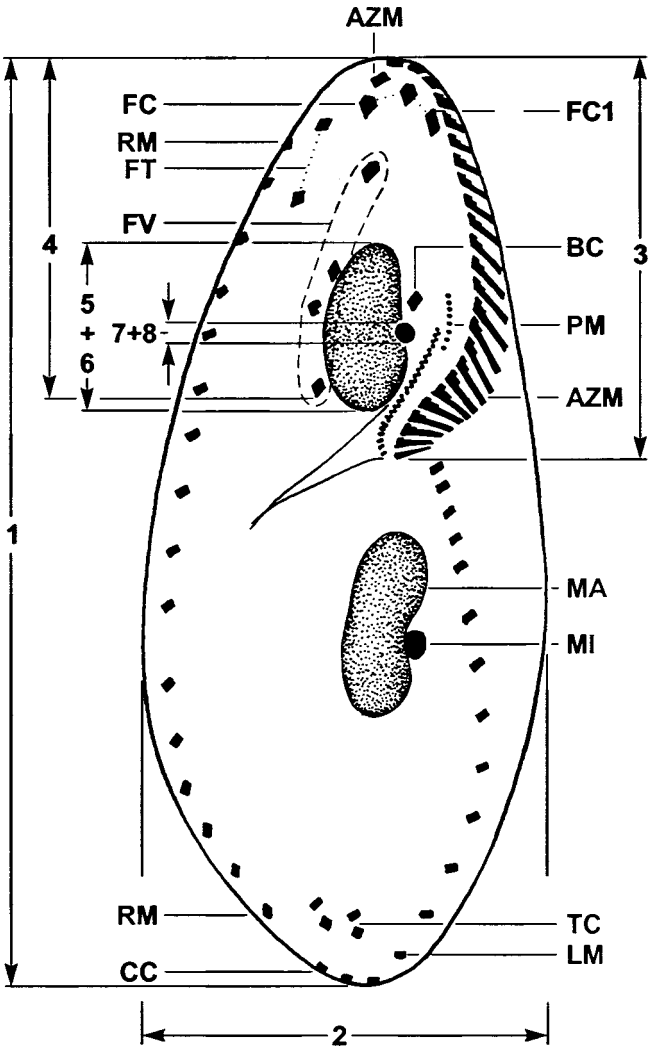

Fig. 1. Terminology used and features measured (numbers) or counted (labels) in *Gonostomum* populations. 1 - length of body; 2 - maximum width of body; 3 - length of adoral zone of membranelles, that is, distance between anterior body end and last adoral membranelle; 4 - distance between anterior body end and last frontoventral cirrus; 5 + 6 - length and width of anterior macronuclear nodule; 7 + 8 - length and width of anterior micronucleus; AZM - number of adoral membranelles; BC - number of buccal cirri; CC - number of caudal cirri; FC - number of frontal cirri; FC1 - first frontal cirrus; FT - number of frontoterminal cirri; FV - number of remaining frontoventral cirri; LM - number of cirri in left marginal row; MA - number of macronuclear nodules; MI - number of micronuclei; PM - number of cilia composing paroral membrane; RM - number of cirri in right marginal row; TC - number of pretransverse and transverse cirri

macronuclear nodules, frontal cirri and buccal cirri) have been omitted. Furthermore, features 7 and 8 were excluded because they are difficult to measure. Thus 16 characteristics remained (Table 1).

The fingerprints were aligned by eye (Fig. 16) and analysed with the association (band sharing) index of Simpson using the biodiversity program of Baev and Penev (1995). This index divides the number of species (= DNA bands) in common (= a) by (a) plus the number of species present in the shorter list only (b). The data were also analysed with the computer program HENNIG 86 (Farris 1988). In one trial, the Australian population (= *G. strenuum*) was defined as outgroup, in another trial we used an artificial outgroup in which all characteristics (= DNA bands) studied are absent (Lorenzen and Sieg 1991).

To analyse morphological and fingerprint data together two methods were developed. The first is a modification of the NNSDC (= Number of Not Significantly Different Characters) method proposed by Berger *et al.* (1985). The seven populations were compared by the nonparametric a posteriori testing procedure of Nemenyi, as described in Sachs (1984): There are k treatment groups (= populations) with equal sample size n; in the present study, k = 7 and n = 21 for each feature (Table 1). Rank all (k x n) observations from smallest to largest when pooled together into a single sample. In case of ties, compute the average ranks. Sum the ranks separately for each population and make all 21 possible absolute differences of these sums. If an observed difference between two treatments is as great as a critical value D (Table 180 in Sachs 1984) then a (real) difference exists. Only the 5% significance level was used. The fingerprint data of Table 2 were compared in pairs as follows: +/+ and -/- became - (= no difference); +/- and -/+ became + (= difference). Now both the 36 fingerprint bands and the 20 morphological features (Table 1; exclusive micronucleus measurements) are arranged in a table. Then the number of the not significantly different characteristics for each pair of the seven populations is added. These values are converted to percentages with 56 (36 + 20) equaling 100%, that is, "total similarity", and UPGMA (unweighted pair-group method using arithmetic averages) clustered.

The program of Baev and Penev (1995) was used for the second method to analyse RAPD-fingerprints and morphological data together. For this, the morphological values shown in Table 1 were transformed to simple presence/absence data, applying the following rule: if the arithmetic mean over all populations (n 7 x 21 = 147) was smaller than the mean of a single population (n = 21), then a minus was assigned and vice versa. For equal means a plus was assigned. We suggest naming the method "presence/absence transformation". Several indices were tried. Best results were obtained with the index of Sørensen (1948).

Dendrograms were constructed using various algorithms (Sneath and Sokal 1973, Pielou 1984, Baev and Penev 1995). The graphs presented were constructed by the UPGMA (unweighted pair-group method using arithmetic averages) and the complete linkage (farthest neighbour) method, which provided the most meaningful results. Furthermore, all methods used do not weigh individual features, that is, are unbiased, but the load of the fingerprints is greater in the combined trees, where 36 fingerprint bands (= features) are opposed to only 20 morphological features.

RESULTS

Brief description of the species investigated

Both species investigated were recently reviewed by Berger (1999). Thus, we provide only a brief description

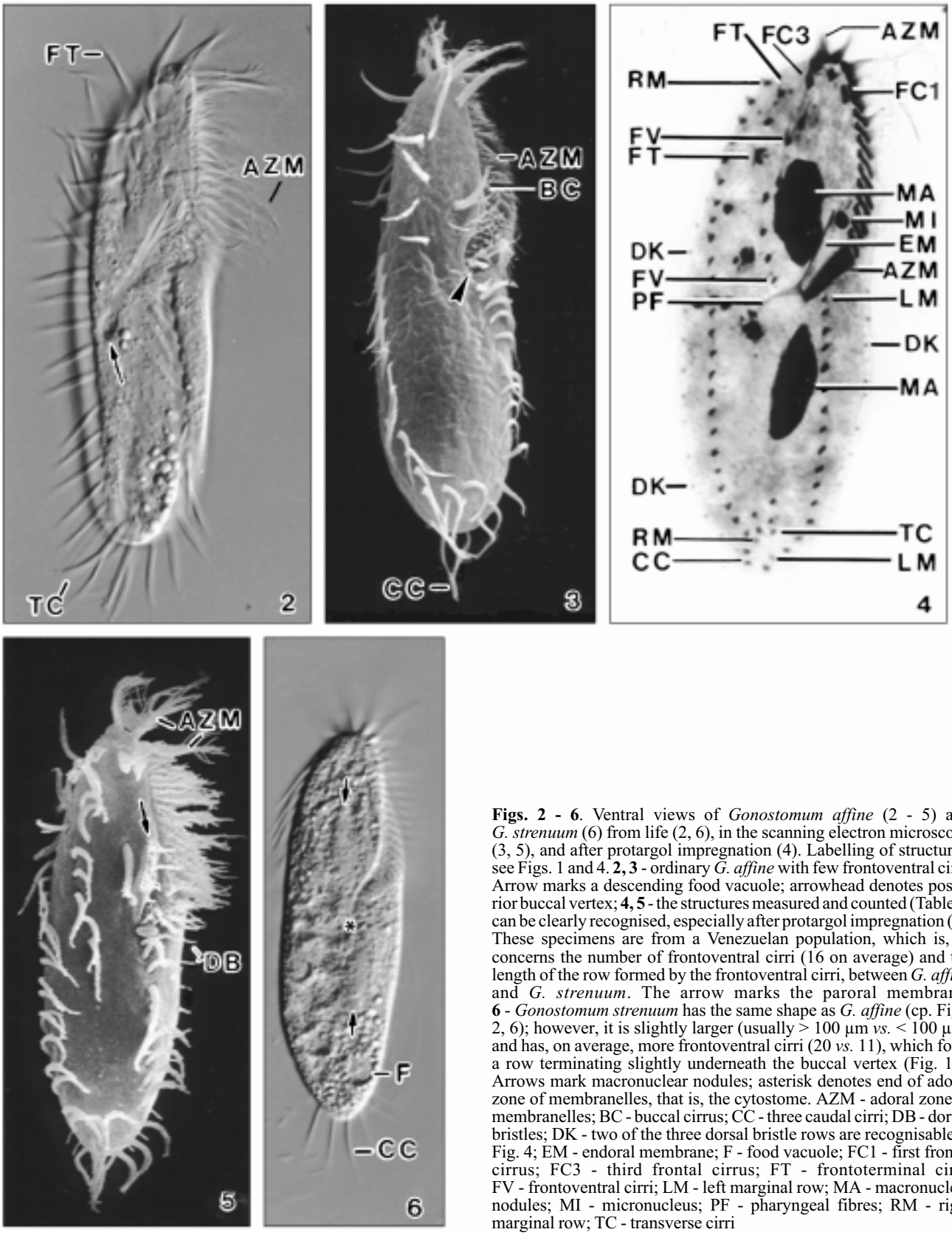

Figs. 2 - 6. Ventral views of *Gonostomum affine* (2 - 5) and *G. strenuum* (6) from life (2, 6), in the scanning electron microscope (3, 5), and after protargol impregnation (4). Labelling of structures, see Figs. 1 and 4. **2, 3** - ordinary *G. affine* with few frontoventral cirri. Arrow marks a descending food vacuole; arrowhead denotes posterior buccal vertex; **4, 5** - the structures measured and counted (Table 1) can be clearly recognised, especially after protargol impregnation (4). These specimens are from a Venezuelan population, which is, as concerns the number of frontoventral cirri (16 on average) and the length of the row formed by the frontoventral cirri, between *G. affine* and *G. strenuum*. The arrow marks the paroral membrane; **6** - *Gonostomum strenuum* has the same shape as *G. affine* (cp. Figs. 2, 6); however, it is slightly larger (usually > 100 µm *vs.* < 100 µm) and has, on average, more frontoventral cirri (20 *vs.* 11), which form a row terminating slightly underneath the buccal vertex (Fig. 14). Arrows mark macronuclear nodules; asterisk denotes end of adoral zone of membranelles, that is, the cytostome. AZM - adoral zone of membranelles; BC - buccal cirrus; CC - three caudal cirri; DB - dorsal bristles; DK - two of the three dorsal bristle rows are recognisable in Fig. 4; EM - endoral membrane; F - food vacuole; FC1 - first frontal cirrus; FC3 - third frontal cirrus; FT - frontoterminal cirri; FV - frontoventral cirri; LM - left marginal row; MA - macronuclear nodules; MI - micronucleus; PF - pharyngeal fibres; RM - right marginal row; TC - transverse cirri

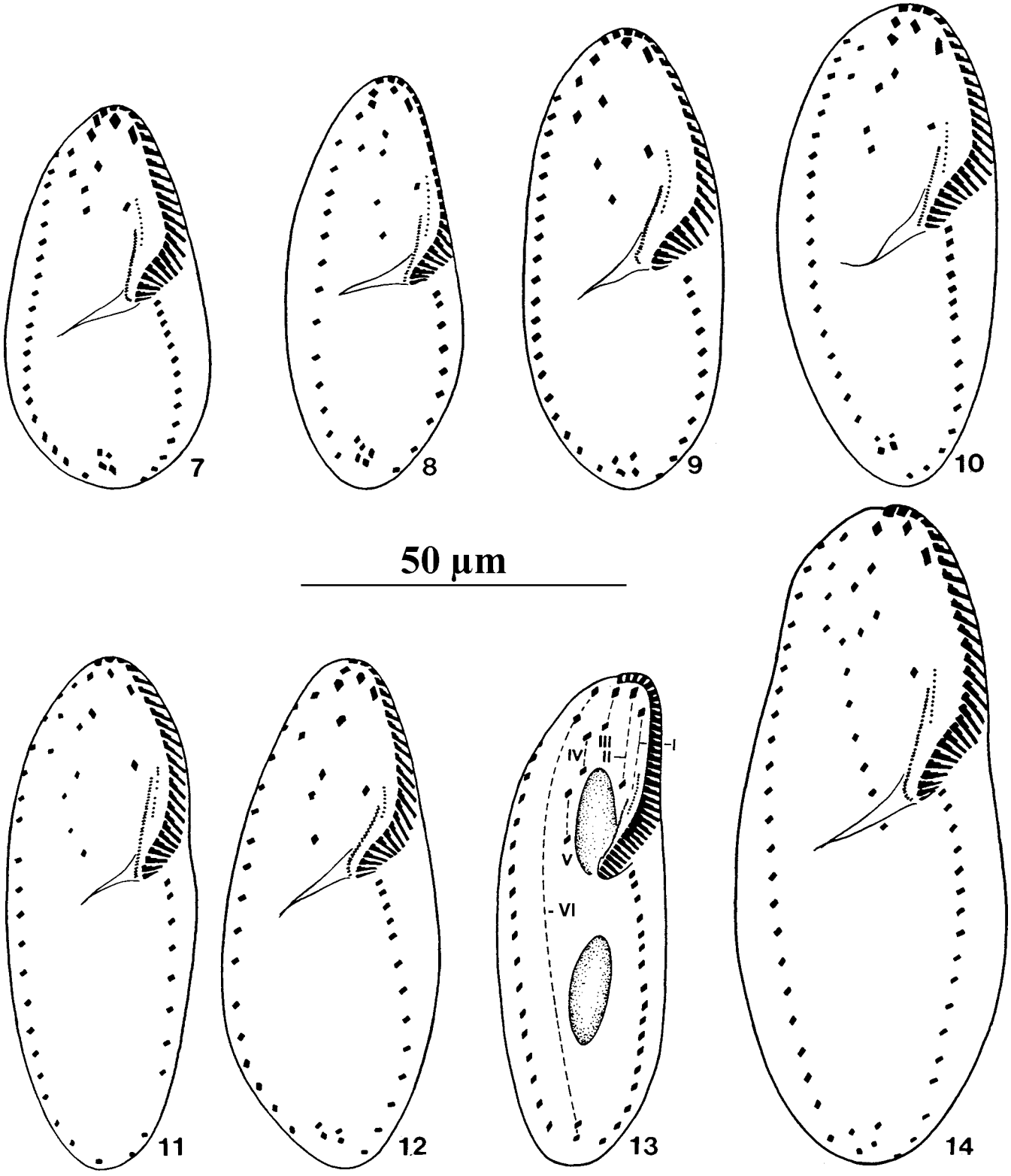

Figs. 7 - 14. Ventral infraciliature (~ cirral pattern) of the *Gonostomum affine* (7 - 12) and *G. strenuum* (14) populations investigated. All protargol-impregnated and drawn to scale. For labelling of structures, see Figs. 1 and 4. **7** - specimen from Namibian site 26, length 60 µm; **8** - specimen from Austria, length 65 µm; **9** - specimen from Brazil, length 71 µm; **10** - specimen from Namibian site 31, length 75 µm; **11** - specimen from Saudi Arabia, length 78 µm; **12** - specimen from Venezuela, length 79 µm; **13** - schema showing origin of the fronto-ventral-transverse cirri (from Berger 1999, modified). Cirri originating from the same anlage (Roman numbers) are connected by broken lines; **14** - specimen from Australia, length 93 µm

Table 1. Morphometric data on six populations of *Gonostomum affine* (Austria, Saudi Arabia, Namibian site 26, Namibian site 31, Venezuela, Brazil) and a population of *G. strenuum* from Australia. All - all *G. affine* populations combined. Numbers refer to Fig. 1

Characteristics[a]	Number	Populations	x	M	SD	SE	CV	Min	Max	n
Body, length	1	Austria	79.0	80.0	11.6	2.5	14.7	63	100	21
		Saudi Arabia	68.8	68.0	9.4	2.1	13.7	50	85	21
		Namibia 26	60.5	62.0	7.3	1.6	12.1	50	75	21
		Namibia 31	75.8	74.0	7.2	1.6	9.5	67	97	21
		Venezuela	72.5	71.0	6.0	1.3	8.3	60	82	21
		Brazil	81.0	82.0	8.7	1.9	10.8	70	93	21
		Australia	93.9	94.0	10.6	2.3	11.2	75	112	21
		All	72.9	71.0	10.9	1.0	14.9	50	100	126
Body, maximum width	2	Austria	34.7	33.0	5.3	1.2	15.4	28	44	21
		Saudi Arabia	28.6	30.0	4.1	0.9	14.2	21	35	21
		Namibia 26	29.2	29.0	4.5	1.0	15.6	21	37	21
		Namibia 31	31.8	31.0	3.8	0.8	12.0	26	40	21
		Venezuela	29.9	32.0	5.4	1.2	18.0	20	40	21
		Brazil	32.8	33.0	5.1	1.1	15.5	24	41	21
		Australia	38.3	37.0	4.8	1.0	12.4	32	48	21
		All	31.2	31.0	5.1	0.5	16.5	20	44	126
Anterior body end, distance to posterior end of adoral zone of membranelles (~ length of adoral zone)	3	Austria	41.9	43.0	7.6	1.7	18.0	29	55	21
		Saudi Arabia	33.2	34.0	4.1	0.9	12.4	26	40	21
		Namibia 26	29.2	29.0	3.7	0.8	12.5	25	42	21
		Namibia 31	36.6	37.0	1.5	0.3	4.1	34	40	21
		Venezuela	33.2	33.0	2.9	0.6	8.7	29	38	21
		Brazil	39.2	39.0	1.9	0.4	4.9	36	44	21
		Australia	44.5	44.0	2.7	0.6	6.0	40	50	21
		All	35.5	35.0	5.8	0.5	16.4	25	55	126
Anterior body end, distance to last ventral cirrus	4	Austria	33.6	33.0	7.3	1.6	21.6	22	49	21
		Saudi Arabia	25.9	26.0	3.2	0.7	12.3	21	32	21
		Namibia 26	17.6	17.0	3.3	0.7	18.6	13	28	21
		Namibia 31	21.7	22.0	2.1	0.5	9.7	18	25	21
		Venezuela	26.5	26.0	2.6	0.6	9.9	21	30	21
		Brazil	26.2	26.0	2.8	0.6	10.8	19	32	21
		Australia	49.5	49.0	6.3	1.4	12.7	41	65	21
		All	25.2	25.0	6.2	0.6	24.7	13	49	126
Macronucleus, length anterior nodule	5	Austria	17.1	18.0	3.3	0.7	19.2	11	22	21
		Saudi Arabia	14.0	13.0	3.2	0.7	23.1	10	20	21
		Namibia 26	11.4	12.0	1.7	0.4	14.5	9	15	21
		Namibia 31	14.1	14.0	2.3	0.5	16.0	10	18	21
		Venezuela	13.1	13.0	2.2	0.5	16.5	9	17	21
		Brazil	14.0	14.0	2.2	0.5	15.3	11	19	21
		Australia	16.7	17.0	2.9	0.6	17.5	13	25	21
		All	14.0	13.5	3.0	0.3	21.5	9	22	126
Macronucleus, width anterior nodule	6	Austria	7.9	8.0	0.9	0.2	11.2	6	10	21
		Saudi Arabia	7.1	7.0	1.1	0.2	14.9	5	9	21
		Namibia 26	6.6	6.0	0.7	0.1	10.3	6	8	21
		Namibia 31	6.8	7.0	0.9	0.2	13.1	5	9	21
		Venezuela	7.9	8.0	0.9	0.2	10.9	6	10	21
		Brazil	7.7	8.0	1.2	0.3	16.2	6	12	21
		Australia	6.9	7.0	0.9	0.2	12.9	5	9	21
		All	7.3	7.0	1.1	0.1	14.6	5	12	126
Micronucleus, length	7	Austria	3.1	3.0	0.8	0.2	25.4	2	4	21
		Saudi Arabia	2.3	2.5	0.3	0.1	15.0	2	3	21
		Namibia 26	2.2	2.0	0.5	0.1	20.9	2	3	21

Table 1 (contd.)

		Namibia 31	not measured							
		Venezuela	2.1	2.0	0.3	0.1	13.0	1	3	21
		Brazil	2.8	3.0	0.4	0.1	14.3	2	4	21
		Australia	3.0	3.0	0.3	0.1	10.5	3	4	21
		All	2.5	2.5	0.6	0.1	24.9	1	4	105
Micronucleus, width	8	Austria	2.3	2.5	0.5	0.1	21.9	2	3	21
		Saudi Arabia	1.9	2.0	0.2	0.1	12.4	2	3	21
		Namibia 26	1.4	1.5	0.3	0.1	21.6	1	2	21
		Namibia 31	not measured							
		Venezuela	1.9	2.0	0.2	0.1	12.7	1	2	21
		Brazil	2.0	2.0	0.2	0.0	11.2	2	3	21
		Australia	2.3	2.0	0.3	0.1	13.5	2	3	21
		All	1.9	2.0	0.4	0.0	22.5	1	3	105
Adoral membranelles, number	9	Austria	28.8	30.0	4.2	0.9	14.6	23	35	21
		Saudi Arabia	21.5	22.0	2.2	0.5	10.4	17	24	21
		Namibia 26	22.0	22.0	2.0	0.4	9.2	18	27	21
		Namibia 31	25.9	26.0	1.0	0.2	3.8	24	28	21
		Venezuela	24.7	25.0	1.6	0.4	6.6	21	27	21
		Brazil	27.1	27.0	0.9	0.2	3.3	25	29	21
		Australia	27.9	28.0	1.3	0.3	4.7	25	30	21
		All	25.0	25.0	3.4	0.3	13.7	17	35	126
Dorsal kineties, number	10	Austria	3.0	3.0	0.0	0.0	0.0	3	3	21
		Saudi Arabia	3.0	3.0	0.0	0.0	0.0	3	3	21
		Namibia 26	3.0	3.0	–	–	–	2	3	21
		Namibia 31	3.0	3.0	0.0	0.0	0.0	3	3	21
		Venezuela	3.0	3.0	0.0	0.0	0.0	3	3	21
		Brazil	3.0	3.0	0.0	0.0	0.0	3	3	21
		Australia	3.0	3.0	0.0	0.0	0.0	3	3	21
		All	3.0	3.0	–	–	–	2	3	126
Macronuclear nodules, number	11	Austria	2.0	2.0	0.0	0.0	0.0	2	2	21
		Saudi Arabia	2.0	2.0	0.0	0.0	0.0	2	2	21
		Namibia 26	2.0	2.0	0.0	0.0	0.0	2	2	21
		Namibia 31	2.1	2.0	–	–	–	2	3	21
		Venezuela	2.0	2.0	0.0	0.0	0.0	2	2	21
		Brazil	2.0	2.0	0.0	0.0	0.0	2	2	21
		Australia	2.0	2.0	0.0	0.0	0.0	2	2	21
		All	2.0	2.0	–	–	–	2	3	126
Micronuclei, number	12	Austria	1.9	2.0	0.6	0.1	30.9	0	3	21
		Saudi Arabia	2.3	2.0	1.0	0.2	44.1	0	4	21
		Namibia 26	1.9	2.0	0.4	0.1	22.9	1	3	21
		Namibia 31	0.0	0.0	0.0	0.0	0.0	0	0	21
		Venezuela	1.9	2.0	1.0	0.2	51.9	0	4	21
		Brazil	1.7	2.0	0.6	0.1	32.7	0	2	21
		Australia	3.1	3.0	1.3	0.3	40.6	0	6	21
		All	1.6	2.0	1.0	0.1	62.2	0	4	126
Right marginal row, number of cirri	13	Austria	16.6	17.0	2.9	0.6	17.2	10	21	21
		Saudi Arabia	17.8	18.0	2.9	0.6	16.0	12	23	21
		Namibia 26	16.5	16.0	2.3	0.5	13.7	11	20	21
		Namibia 31	19.5	19.0	2.3	0.5	12.0	16	26	21
		Venezuela	17.7	17.0	2.5	0.5	14.2	13	23	21
		Brazil	18.8	18.0	1.8	0.4	9.5	15	22	21
		Australia	25.4	24.0	4.2	0.9	16.5	21	33	21
		All	17.8	18.0	2.6	0.2	14.8	10	26	126

Table 1 (contd.)

Left marginal row, number of cirri	14	Austria	11.0	11.0	1.9	0.4	17.5	7	15	21
		Saudi Arabia	11.8	12.0	2.4	0.5	20.3	6	16	21
		Namibia 26	12.3	12.0	2.9	0.6	23.3	8	22	21
		Namibia 31	14.8	15.0	1.3	0.3	8.5	12	17	21
		Venezuela	12.6	12.0	1.6	0.3	12.6	10	16	21
		Brazil	12.3	12.0	1.1	0.2	8.6	11	15	21
		Australia	17.3	18.0	2.6	0.6	15.1	13	21	21
		All	12.4	12.0	2.2	0.2	18.0	6	22	126
Frontal cirri, number	15	Austria	3.0	3.0	0.0	0.0	0.0	3	3	21
		Saudi Arabia	3.0	3.0	0.0	0.0	0.0	3	3	21
		Namibia 26	3.0	3.0	0.0	0.0	0.0	3	3	21
		Namibia 31	3.0	3.0	0.0	0.0	0.0	3	3	21
		Venezuela	3.0	3.0	0.0	0.0	0.0	3	3	21
		Brazil	3.0	3.0	0.0	0.0	0.0	3	3	21
		Australia	3.0	3.0	0.0	0.0	0.0	3	3	21
		All	3.0	3.0	0.0	0.0	0.0	3	3	126
Frontoterminal cirri, number	16	Austria	2.0	2.0	0.0	0.0	0.0	2	2	21
		Saudi Arabia	2.9	3.0	–	–	–	2	3	21
		Namibia 26	2.0	2.0	–	–	–	2	3	21
		Namibia 31	2.0	2.0	0.0	0.0	0.0	2	2	21
		Venezuela	1.9	2.0	–	–	–	1	2	21
		Brazil	1.9	2.0	0.4	0.1	22.9	0	2	21
		Australia	4.1	4.0	0.6	0.1	13.8	3	6	21
		All	2.1	2.0	0.4	0.0	20.3	0	3	126
Remaining frontoventral ventral cirri, number	17	Austria	5.5	5.0	0.9	0.2	15.8	5	7	21
		Saudi Arabia	5.9	6.0	0.8	0.2	13.0	4	7	21
		Namibia 26	3.8	3.0	1.1	0.2	28.3	3	6	21
		Namibia 31	4.8	5.0	0.8	0.2	17.4	3	6	21
		Venezuela	5.0	5.0	0.4	0.1	7.8	4	6	21
		Brazil	3.1	3.0	0.5	0.1	15.2	3	5	21
		Australia	11.7	11.0	1.3	0.3	10.8	10	15	21
		All	4.7	5.0	1.2	0.1	26.0	3	7	126
Buccal cirri, number	18	Austria	1.0	1.0	0.0	0.0	0.0	1	1	21
		Saudi Arabia	1.0	1.0	0.0	0.0	0.0	1	1	21
		Namibia 26	1.0	1.0	0.0	0.0	0.0	1	1	21
		Namibia 31	1.0	1.0	0.0	0.0	0.0	1	1	21
		Venezuela	1.0	1.0	0.0	0.0	0.0	1	1	21
		Brazil	1.0	1.0	–	–	–	0	1	21
		Australia	1.0	1.0	0.0	0.0	0.0	1	1	21
		All	1.0	1.0	–	–	–	0	1	126
Transverse cirri, number	19	Austria	4.7	4.0	1.1	0.2	22.8	3	6	21
		Saudi Arabia	1.0	1.0	–	–	–	0	1	21
		Namibia 26	2.6	4.0	1.7	0.4	68.0	0	4	21
		Namibia 31	4.0	4.0	–	–	–	3	4	21
		Venezuela	4.0	4.0	0.7	0.1	16.9	3	6	21
		Brazil	3.9	4.0	0.5	0.1	12.4	2	4	21
		Australia	4.0	4.0	0.0	0.0	0.0	4	4	21
		All	3.3	4.0	1.5	0.1	45.8	0	6	126
Caudal cirri, number	20	Austria	3.0	3.0	0.0	0.0	0.0	3	3	21
		Saudi Arabia	3.0	3.0	–	–	–	2	3	21
		Namibia 26	2.8	3.0	0.7	0.2	25.4	0	3	21
		Namibia 31	2.5	3.0	0.7	0.2	29.7	1	3	21
		Venezuela	3.0	3.0	0.0	0.0	0.0	3	3	21
		Brazil	3.0	3.0	0.0	0.0	0.0	3	3	21

Table 1 (contd.)

		Australia	3.0	3.0	0.3	0.1	10.5	2	4	21
		All	2.9	3.0	0.5	0.0	15.9	0	3	126
Paroral, number of cilia	21	Austria	13.6	14.0	3.1	0.7	22.8	8	19	21
		Saudi Arabia	10.6	11.0	2.1	0.5	19.6	5	14	21
		Namibia 26	8.6	8.0	1.8	0.4	20.6	6	12	21
		Namibia 31	10.2	10.0	2.1	0.5	20.5	6	14	21
		Venezuela	9.0	9.0	1.7	0.4	19.3	6	11	21
		Brazil	12.5	13.0	1.9	0.4	14.9	6	16	21
		Australia	13.4	13.0	1.8	0.4	13.2	11	17	21
		All	10.8	11.0	2.8	0.2	25.7	5	19	126
Fronto-ventral-transverse cirri, total number	22	Austria	16.1	17.0	1.2	0.3	7.7	14	18	21
		Saudi Arabia	13.7	14.0	1.1	0.2	8.0	11	15	21
		Namibia 26	12.3	13.0	1.2	0.3	10.0	10	15	21
		Namibia 31	14.7	15.0	0.8	0.2	5.7	13	16	21
		Venezuela	14.8	15.0	0.7	0.2	4.7	14	17	21
		Brazil	12.9	13.0	0.9	0.2	7.1	10	15	21
		Australia	23.8	23.0	1.2	0.3	5.2	22	26	21
		All	14.1	14.0	1.6	0.1	11.6	10	18	126

[a]Data based on protargol-impregnated (Foissner 1991 method), mounted, randomly selected, morphostatic specimens. All measurements in µm. CV - coefficient of variation in %, M - median, Max - maximum, Min - minimum, n - number of individuals investigated, SD - standard deviation, SE - standard error of arithmetic mean, x - arithmetic mean

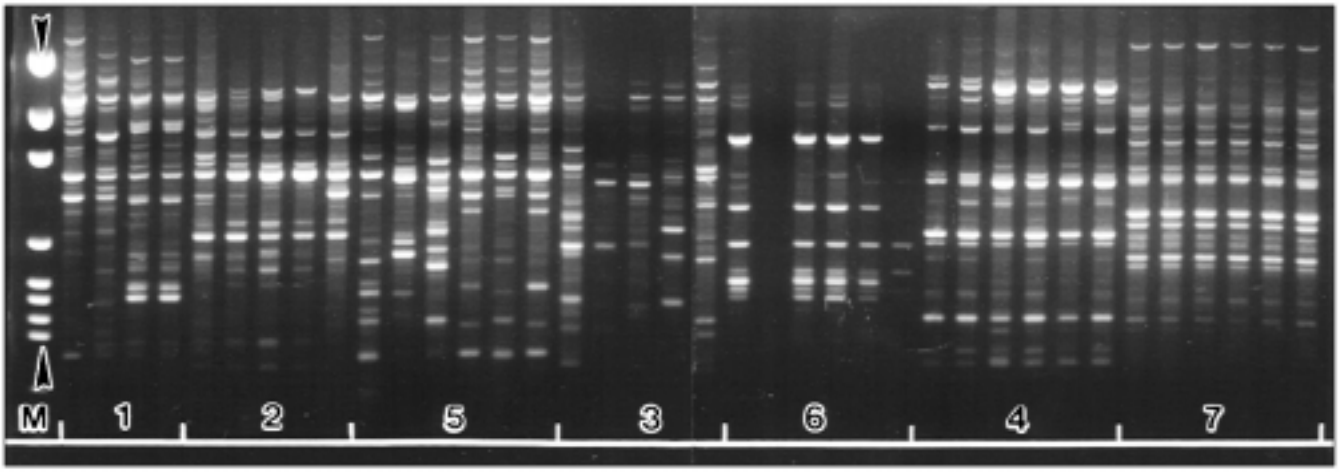

Fig. 15. RAPD-fingerprints from six *Gonostomum affine* populations (numbers 1- 6) and one *G. strenuum* population (number 7). M - pGEM-marker, arrowheads mark 222 and 1,605 bp

focusing on features important for the present paper. Furthermore, all relevant structures are shown in Figs. 1-6.

Gonostomum affine (Stein, 1859) Sterki, 1878 is a colourless, ellipsoidal, and laterally more or less distinctly flattened, oxytrichid ciliate having a size of about 90 x 30 µm, with length ranging from about 50 to 160 µm. As it is a hypotrich, the cilia are grouped into compound organelles, the cirri, which form a specific pattern. Usually, there are two ellipsoidal macronuclear nodules, each with a single micronucleus attached. The oral apparatus extends along the left margin of the anterior body half. It is composed of a conspicuous adoral zone of membranelles at the left margin of the oral field and two short, inconspicuous undulating membranes at the right. One of the undulating membranes, the paroral, is composed of few, comparatively widely spaced cilia, a specific feature of gonostomoid ciliates. The buccal cavity is small and inconspicuous. Only the right (ventral) side bears cirri, the dorsal surface is bare, except

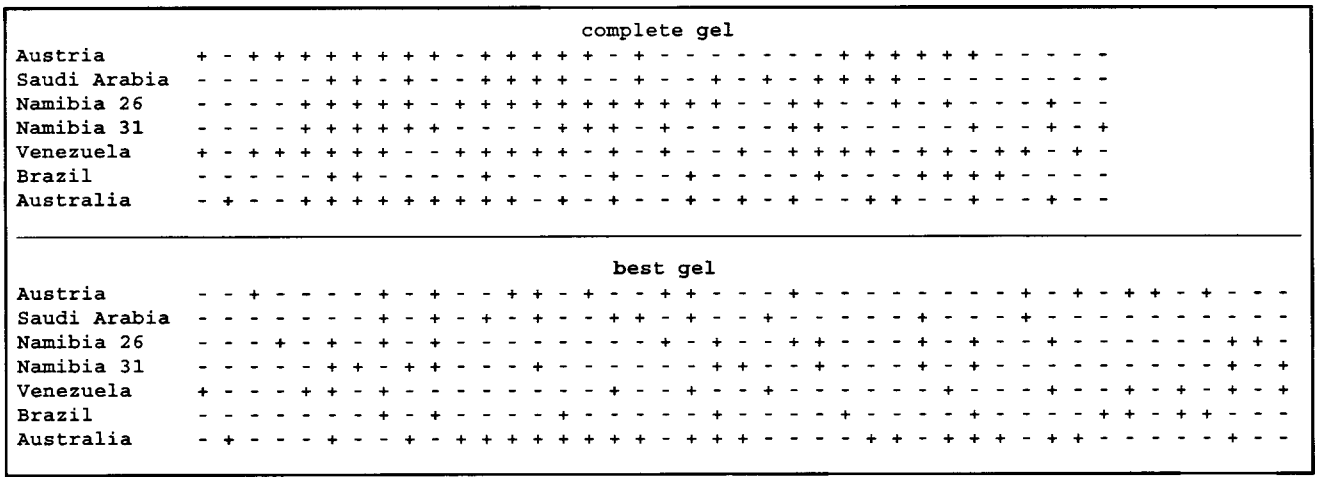

Fig. 16. Band pattern shown in Fig. 15 transformed to a presence/absence (+/-) matrix used for calculating band sharing indices. In the upper lane, all usable fingerprints were evaluated, in the lower lane only the "best looking" fingerprint from each population was used

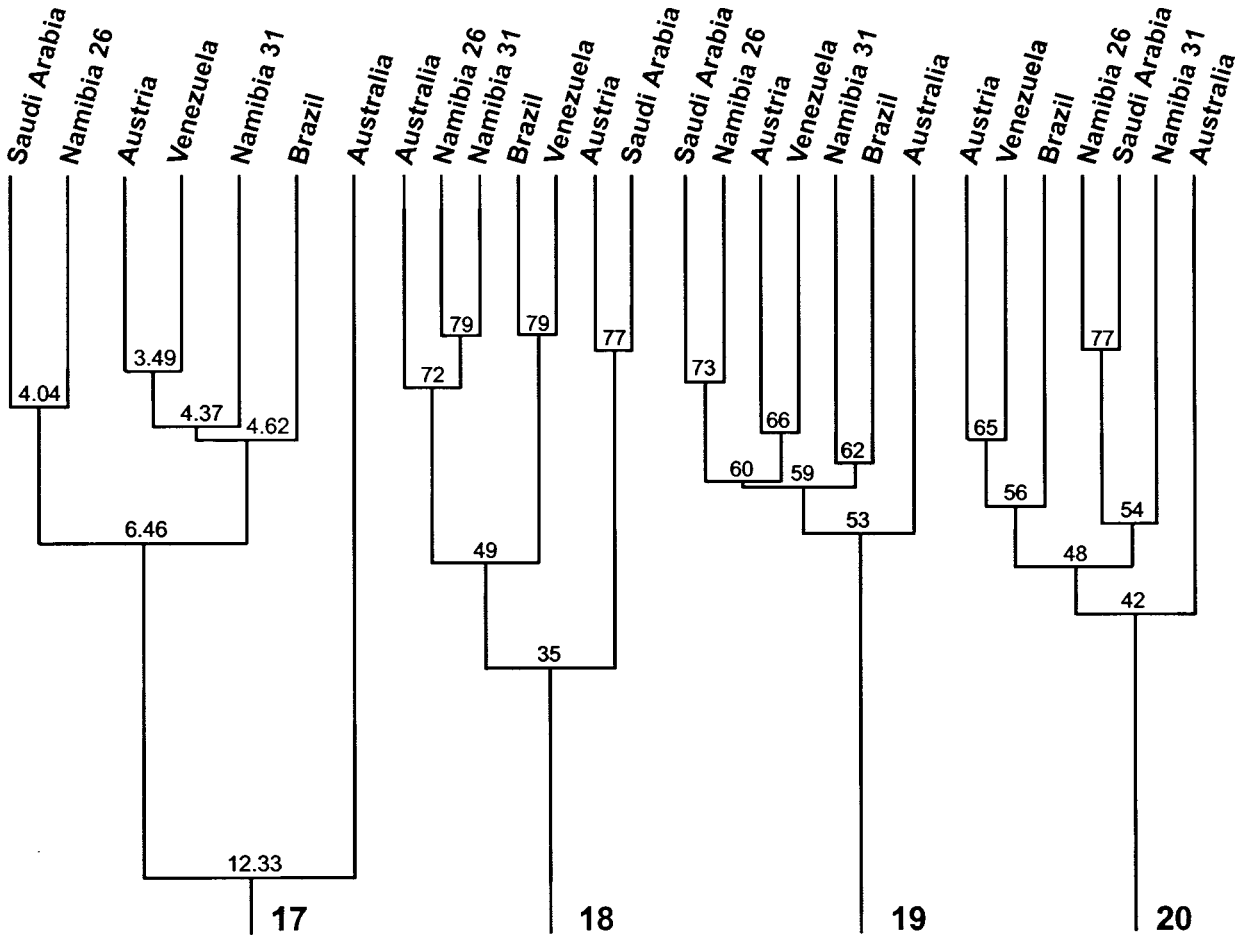

Figs. 17 - 20. Similarity trees. **17** - morphological tree with the coefficient of racial likeness UPGMA clustered; **18** - RAPD-fingerprint tree with the association (band sharing) index of Simpson complete-linkage clustered; **19** - combined morphological and RAPD-fingerprint tree based on the "number of not significantly different characters" UPGMA clustered; **20** - combined morphological and RAPD-fingerprint tree based on the "presence/absence transformation" data clustered with the complete-linkage method. For details on methods, see "data analysis" in the "Materials and Methods" section

for three rows of minute bristles associated with three caudal cirri at the posterior body end. The cirri form a row each at the right and left margin of the cell and several groups on the ventral surface, as shown in Figs.1and 4. Briefly, there are a highly variable number of fronto-ventral cirri (6-15) in the area between the anterior body end and the oral vertex, and an also highly variable number of transverse cirri (0-7) near the posterior body end. The fronto-ventral cirri are classified in frontal cirri (usually three at anterior body margin), buccal cirri (usually one near paroral membrane), frontoterminal cirri (usually two at right anterior body margin), and ventral cirri (all other cirri in the area mentioned above) forming a more or less distinct row never surpassing the oral vertex. *Gonostomum affine* usually feeds on bacteria, prefers terrestrial habitats, and has been recorded from all main biogeographical regions (Foissner 1998, Berger 1999).

Gonostomum strenuum (Engelmann, 1862) Sterki, 1878 (Figs. 6, 14) is rather similar to *G. affine*, but a distinct morphospecies, although Foissner (2000b) very recently described a population from Venezuela, which is intermediate in all main features (Figs. 4, 5). Usually, *G. strenuum* is slightly larger than *G. affine* (110 x 40 *vs.* 90 x 30 μm) and has more frontoterminal (4 *vs.* 2) and fronto-ventral cirri (20 *vs.* 11 on average). Thus, the row formed by the ventral cirri is much more conspicuous than in *G. affine* and extends beyond the level of the oral vertex. *Gonostomum strenuum* feeds mainly on bacteria and is a rare species preferring limnetic habitats (Berger 1999). Previously, it was known only from Eurasia, our record from the Murray River floodplain is the first from Australia.

Morphological investigations (Figs. 7-14, 17; Table 1)

The six populations of *G. affine* investigated are well within the range recorded in the literature (Berger 1999). Thus, identification is beyond reasonable doubt. Likewise, the Australian *G. strenuum* matches the literature data.

The smallest *G. affine* specimens are those from the most extreme environment, that is, Namibian site 26, the Namib Desert. This population is smaller also in all other features, such as the length of the adoral zone of membranelles, the width and length of the macronuclear nodules, the number of adoral membranelles, and the number of marginal and fronto-ventral-transverse cirri. The Saudi Arabian specimens are unique in having three frontoterminal cirri, thus bridging the gap between *G. affine* (usually 2) and *G. strenuum* (usually 4). Furthermore, they usually have only a single transverse cirrus, while all other populations have four on average (median). The Austrian specimens are unique in having most adoral membranelles, paroral cilia, and fronto-ventral-transverse cirri. Furthermore, this population has the highest average coefficient of variability. The average variation coefficient of the features 1-6, 9, 13, 14, 17, 21, 22 in Table 1 is distinctly higher in the Austrian (16.3%), Namibian site 26 (15.7%), and Saudi Arabian (14.8%) populations than in the Namibian site 31 (11%), Brazilian (11%), and Venezuelan (11.4%) populations.

The similarity tree (Fig. 17) shows two conspicuous attributes: (i) the two species, *G. affine* and *G. strenuum*, are very distinctly separated, while (ii) the *G. affine* populations do not show a consistent biogeographical pattern, although the resolution capacity of the coefficient is excellent, as shown by the two distinct *G. affine* subclusters. However, at least the South American populations are in the same subcluster. The Namibian site 26/Saudi Arabian subcluster matches the peculiarities mentioned above, but excludes the Austrian population although it is rather peculiar, too.

RAPD - fingerprints (Figs. 15, 16, 18)

Each of the seven populations has a distinct pattern (Fig. 15). Thus, the overall fingerprint similarity is only 64%. Within the parallel probes, those from populations 4 and 7 (both pure cultures started with one or two specimens), but also those from population 6, a raw culture, are very similar, indicating that each consists of only a single genotype. In contrast, the parallel probes from populations 1 and 3 each are very different, indicating that most belong to distinct genotypes. This matches the high average morphological variability coefficients of these populations (see above).

The similarity trees from the RAPD-fingerprints are all rather chaotic, irrespective of the indices and cluster methods used. None separates the two morphospecies as distinctly as the morphological trees do (Figs. 17, 18). However, at least the South American and Namibian populations each form a distinct subcluster. To improve the tree, we tried not only various indices and cluster methods, but also confined the analysis to the "best looking" fingerprint from each population (Fig. 16). Furthermore, we tried a matrix based only on the more conspicuous bands. However, trees could not be improved, that is, the two morphospecies were never clearly separated and the three African populations never in a single subcluster.

Combined similarity trees

Combining the morphological and fingerprint data should increase resolution because of the increased data set. This is indeed the case (Figs. 19, 20). Both methods applied can at least distinctly separate the two morphospecies, and the complete-linkage tree even provides a meaningful geographical population structure, that is, distributes the African and South American *G. affine* populations in distinct subclusters (Fig. 20). However, we emphasise that other indices and/or cluster algorithms (for instance, UPGM, average-linkage) provide much less "beautiful" trees, indicating that the differences are subtle.

DISCUSSION

Methodological problems

Methodological problems and constraints are often underestimated in investigations of the kind we performed. However, they greatly influence data interpretation and conclusions, and thus they are discussed in advance.

Correlated features: Basically, the quality of similarity trees increases with the number of **independent** features analysed. This is why we tried to combine morphological traits and RAPD-fingerprints in a single tree. However, not only the quantity but also the quality of the features influences the outcome. Features which depend on each other, that is, are correlated can produce artificial groupings simply by their numerical dominance (Remane 1952, Mayr 1975). In hypotrichous genera, for instance, body length is often correlated with body width and the number of adoral membranelles is usually correlated with the length of the adoral zone. Actually, two of the four features are redundant. Unfortunately, recognition of correlated features is impossible in fingerprints and also rather difficult for morphological traits. Thus, "uncleared" data were used. In combined trees, numerical character equivalence is an additional source of errors. In our trees, 20 morphological traits are somewhat outrivaled by 36 RAPD-bands.

Band-alignment: Fig.16 shows that RAPD-bands are subject to different interpretations because the intensity of the bands varies in parallel probes and some bands are so faint that it depends on the classifier whether they are used or not. Furthermore, if many probes are analysed they become distributed over several gels, and even the molecular marker cannot guarantee that different gels are entirely correctly aligned.

Probably, some variation of DNA band patterns is due to the problems with reproducibility, which are typical for RAPD patterns (Skroch and Nienhuis 1995, Woodburn *et al.* 1995). It is known, that the intensities of several amplified bands can vary between experiments with the template DNA (Stoeck and Schmidt 1998). Thus, it might be possible that DNA bands, which are relatively weak in one sample, could be missing in another sample from the same clone. Therefore, it is necessary to study different cells from a clone in several experiments to obtain a reliable and specific pattern. Differences in the patterns of populations 1 and 3 contribute to a large extent to the relatively low overall similarity of 64%; thus, this value is assumed to be an underestimation.

Indices and algorithms: it is well-known and confirmed by our experience that both the coefficient used for estimating similarity and the algorithm applied to the similarity matrix highly influence the similarity analysis. The coefficient of racial likeness, the Simpson index (and variations), and the Sørensen index have simple structures and are widely used. Thus, they are perhaps unproblematic. The two methods for combining morphological and fingerprint data are empirical and need a detailed mathematical investigation, which is beyond our possibilities. We developed them because no appropriate methods were available from the literature. In any case, both methods are simple and provide binary data, which can be clustered.

There is no "best" cluster algorithm because all have some disadvantages and the structure of the data influences clustering. Specialists recommend using several methods on the same data set (Pielou 1984, Birks 1987). If similar results emerge, one can have more confidence that the groups have some reality and are not simply artifacts of any one method. However, it is widely accepted that UPGM clustering is one of the best methods because it represents the original data matrix better than other algorithms (Sokal and Rohlf 1981). Thus, our farthest-neighbour clusters are more problematical than our UPGM clusters because the "representative point" is always "extreme" rather than "typical" of the cluster it represents (Pielou 1984).

Resolution power of RAPD-fingerprints and morphology

It is known that RAPD patterns are sometimes difficult to interpret when applied for taxonomical questions (Stoeck *et al.* 2000b). Nothing is known about the

DNA sequences amplified in RAPD fingerprints (Tingey and Tufo 1993); specific DNA bands cannot be associated with particular loci in the genome (Lynch 1991); and difficulties arise concerning the mathematical analysis of RAPD fingerprints (Backeljau *et al.* 1995, Skroch and Nienhuis 1995, Landry and Lapointe 1997). Consequently, RAPD data on their own are not sufficient to unambiguously answer taxonomical questions. However, Stoeck *et al.* (2000b) were successful in combining two molecular biological methods, RAPD and amplified ribosomal DNA restriction analyses (ARDRA), also known as riboprinting, to reject the hypothesis of sibling species in *Paramecium caudatum*.

As concerns the present study, we have three indicators that the investigations are technically correct: (i) two of the three *G. affine* populations with the highest average variability coefficients also have highly variable fingerprints; (ii) the combined similarity trees give a higher resolution than the individual trees; (iii) pattern variability within the pure cultures (sites/gels 4, 7 in Fig. 15) is much smaller than within the raw cultures, where it is likely that several genotypes occur (sites/gels 1, 2, 3, 5, 6 in Fig. 15). Thus, the failure of the RAPD method to distinguish between the two morphospecies of *Gonostomum* is very likely not a technical artifact but indicates high genotype variability in *G. affine* and/or a lower resolution power than morphology. Furthermore, we must not forget that other primers might have produced clearer results.

Are the morphotypes of *Gonostomum affine* distinct taxonomic entities?

Kusch and Heckmann (1996) investigated a hypotrichous ciliate genus with RAPD-fingerprints. They found that different *Euplotes* species shared 38-46% of their fingerprint bands, while sexually recombined strains of *E. octocarinatus* and *E. aediculatus* shared 60-70%. Within-population variability of *E. daidalos* was only 3% when originating from the same pond, but 40% in populations from different ponds. Similar results were obtained by Stoeck *et al.* (2000a) in *Paramecium novaurelia*, a sibling species of the *P. aurelia* complex: 14 strains showed 85.7-97.1%, on average 92.3% band pattern similarity. Several strains of *P. pentaurelia* showed no variability at all. Kusch (1998) investigated 721 individuals of *Stentor coeruleus* from seven sites up to 400 km apart. He observed four distinct genotypes, while about 15 genotypes were recognisable in the *G. affine* populations from the six sites and three continents. Comparing these similarity values with the 64% overall band sharing in the six *G. affine* populations, it becomes obvious that they are in the range of populations, and thus should not get Linnean names. This is emphasised by the overlapping morphologies (Table 1) and the possibility that the 64% overall band similarity is an underestimation caused by technical problems (see above).

Biogeographical patterns

Euplotes spp. (Kusch and Heckmann 1996), *Colpoda* spp. (Bowers *et al.* 1998), *Stentor coeruleus* (Kusch 1998), *Paramecium novaurelia* (Stoeck *et al.* 2000a), and *Gonostomum affine* (this paper) agree in having several distinct genotypes apparently lacking a geographic pattern. However, a rather distinct pattern becomes recognisable in *G. affine* when morphological and molecular data are combined in single similarity trees (Figs. 19, 20). Likewise, RAPD-fingerprints and strain crossing show a restricted geographical distribution of certain genotypes of *Paramecium sexaurelia*, another species of the *P. aurelia* complex (Stoeck *et al.* 1998). Unfortunately, strain crossing was impossible in *G. affine* because only one of the six populations could be grown in pure culture.

To sum up, it seems possible that further investigations will reveal a biogeographical population structure in *G. affine* and other ciliates, especially when several methods (morphology, gene sequences, mating reaction) are combined in **single** similarity trees. Such method not only increases the number of features considered, but possibly also reduces the bias caused by technical problems. This suggestion is supported by the molecular biological data which almost invariably show that morphological traits are much more conservative than DNA molecules (Nanney *et al.* 1998). The morphostasis of protists is still unexplained, but recognisable in the fossil record (Schönborn *et al.* 1999).

Acknowledgements. Supported by the Austrian Science Foundation (FWF project P 12367-BIO) and the Deutsche Forschungsgemeinschaft (DFG project IIB3 Schm 544/7-1). The technical assistance of Dr. B. Moser, Dr. E. Herzog and Mag. E. Strobl is gratefully acknowledged.

REFERENCES

Ammermann D. (1985) Species characterization and speciation in the *Stylonychia/Oxytricha* group (Ciliata, Hypotrichida, Oxytrichidae). *Memorie Soc. tosc. Sci. nat., Serie B* **92:** 15-27

Backeljau T., de Bruyn L., de Wolf H., Jordaens K., van Dongen S., Verhagen R., Winnepenninckx B. (1995) Random amplified poly-

morphic DNA (RAPD) and parsimony methods. *Cladistics* **11:** 119-130
Baev P. V., Penev L. D. (1995) BIODIV program for calculating biological diversity parameters, similarity, niche overlap, and cluster analysis. Version 5.1. Pensoft, Sofia, Moscow. ISBN: 0-925031-23-2
Berger H. (1999) Monograph of the Oxytrichidae (Ciliophora, Hypotrichia). Kluwer, Dordrecht
Berger H., Foissner W., Adam H. (1985) Morphological variation and comparative analysis of morphogenesis in *Parakahliella macrostoma* (Foissner, 1982) nov. gen. and *Histriculus muscorum* (Kahl, 1932), (Ciliophora, Hypotrichida). *Protistologica* **21:** 295-311
Birks H. J. B. (1987) Recent methodological developments in quantitative descriptive biogeography. *Ann. Zool. Fennici* **24:** 165-178
Bowers N. J., Pratt J. R. (1995) Estimation of genetic variation among soil isolates of *Colpoda inflata* (Stokes) (Protozoa: Ciliophora) using the polymerase chain reaction and restriction fragment length polymorphism analysis. *Arch. Protistenkd.* **145:** 29-36
Bowers N., Kroll T. T., Pratt J. R. (1998) Diversity and geographic distribution of riboprints from three cosmopolitan species of *Colpoda* Müller (Ciliophora: Colpodea). *Europ. J. Protistol.* **34:** 341-347
Buitkamp U. (1977) Über die Ciliatenfauna zweier mitteleuropäischer Bodenstandorte (Protozoa; Ciliata). *Decheniana* **130:** 114-126
Dini F., Gianni A. (1985) Breeding systems in the *Euplotes vannus-crassus-minuta* group. *Memorie Soc. tosc. Sci. nat., Serie B* **92:** 75-93
Dini F., Nyberg D. (1999) Growth rates of marine ciliates on diverse organisms reveal ecological specializations within morphospecies. *Microb. Ecol.* **37:** 13-22
Engelmann T. W. (1862) Zur Naturgeschichte der Infusionsthiere. *Z. wiss. Zool.* **11:** 347-393
Farris, J. S. (1988) Hennig 86, version 1.5. Port Jefferson Station, New York
Finlay B. J., Fenchel T. (1999) Divergent perspectives on protist species richness. *Protist* **150:** 229-233
Foissner W. (1982) Ökologie und Taxonomie der Hypotrichida (Protozoa: Ciliophora) einiger österreichischer Böden. *Arch. Protistenkd.* **126:** 19-143
Foissner W. (1987) Soil protozoa: fundamental problems, ecological significance, adaptations in ciliates and testaceans, bioindicators, and guide to the literature. *Progr. Protistol.* **2:** 69-212
Foissner W. (1991) Basic light and scanning electron microscopic methods for taxonomic studies of ciliated protozoa. *Europ. J. Protistol.* **27:** 313-330
Foissner W. (1998) An updated compilation of world soil ciliates (Protozoa, Ciliophora), with ecological notes, new records, and description of new species. *Europ. J. Protistol.* **34:** 195-235
Foissner W. (2000a) Protist diversity: estimates of the near-imponderable. *Protist* **150** (year 1999): 363-368
Foissner W. (2000b) Notes on ciliates (Protozoa, Ciliophora) from *Espeletia* trees and *Espeletia* soils of the Andean Páramo, with descriptions of *Sikorops espeletiae* nov. spec. and *Fragmocirrus espeletiae* nov. gen., nov. spec. *Stud. neotrop. Fauna Environm.* **35:** 52-79
Kusch J. (1998) Local and temporal distribution of different genotypes of pond-dwelling *Stentor coeruleus*. *Protist* **149:** 147-154
Kusch J., Heckmann K. (1996) Population structure of *Euplotes* ciliates revealed by RAPD fingerprinting. *Écoscience* **3:** 378-384
Landry P. A., Lapointe F. J. (1997) RAPD problems in phylogenetics. *Zool. Scr.* **25:** 283-290
Lorenzen S., Sieg J. (1991) Phylip, Paup, and Hennig 86 - how reliable are computer parsimony programs used in systematics? *Z. zool. Syst. Evolut.-forsch.* **29:** 466-472
Lynch M. (1991) Analysis of population genetic structure by DNA fingerprinting. In: DNA Fingerprinting: Approaches and Applications, (Eds. T. Burke, G. Dolf, A. J. Jeffreys and R. Wolffs). Birkhäuser, Basel, 113-126
Maeda M., Carey P. G. (1984) A revision of the genera *Trachelostyla* and *Gonostomum* (Ciliophora, Hypotrichida), including redescriptions of *T. pediculiformis* (Cohn, 1866) Kahl, 1932 and *T. caudata* Kahl, 1932. *Bull. Br. Mus. nat. Hist. (Zool.)* **47:** 1-17
Malpartida J. M., Martin-González A., Gutiérrez J. C. (1995) Comparison of PCR fingerprintings (RAPD method) and phylogenetic analysis of European, African and American colpodid species. *Second Europ. Congr. Protistol., Clérmont-Ferrand*, Abstract 155
Martín A., Palacios G., Olmo A., Martín-González A., Ruiz-Perez L. M., Gutiérrez J. C. (1997) Karyotypic variability in ribosomal DNA subchromosome size among colpodid ciliates, a possible tool to differentiate colpodid species. *Appl. Environ. Microbiol.* **63:** 1602-1605
Mayr E. (1975) Grundlagen der zoologischen Systematik. Parey, Hamburg
Nanney D. L., McCoy J. W. (1976) Characterization of the species of the *Tetrahymena pyriformis* complex. *Trans. Am. microsc. Soc.* **95:** 664-682
Nanney D. L., Park C., Preparata R., Simon E. M. (1998) Comparison of sequence differences in a variable 23S rRNA domain among sets of cryptic species of ciliated protozoa. *J. Euk. Microbiol.* **45:** 91-100
Pearson K. (1926) On the coefficient of racial likeness. *Biometrika* **18:** 105-117
Pielou E. C. (1984) The Interpretation of Ecological Data. Wiley & Sons, New York
Remane A. (1952) Die Grundlagen des natürlichen Systems, der vergleichenden Anatomie und der Phylogenetik. Akademische Verlagsgesellschaft, Leipzig
Sachs L. (1984) Angewandte Statistik. 6 ed. Springer, Berlin
Schönborn W., Dörfelt H., Foissner W., Krienitz L., Schäfer U. (1999) A fossilized microcenosis in triassic amber. *J. Euk. Microbiol.* **46:** 571-584
Skroch P., Nienhuis J. (1995) Impact of scoring error and reproducibility of RAPD data on RABD based estimates of genetic distance. *Theor. appl. Genet.* **91:** 1086-1091
Sneath P. H. A., Sokal R. R. (1973) Numerical Taxonomy. The Principles and Practice of Numerical Taxonomy. Freeman, San Francisco
Sørensen T. (1948) A method of establishing groups of equal amplitude in plant sociology based on similarity of species content and its application to analyses of the vegetation on Danish commons. *K. danske Vidensk. Selsk. Skr.* **5:** 1-35
Sokal R. R., Rohlf F. L. (1981) Biometry. 2 ed. Freeman, San Francisco
Stein F. (1859) Der Organismus der Infusionsthiere nach eigenen Forschungen in systematischer Reihenfolge bearbeitet. I. Abtheilung. Allgemeiner Theil und Naturgeschichte der hypotrichen Infusionsthiere. Engelmann, Leipzig
Sterki V. (1878) Beiträge zur Morphologie der Oxytrichinen. *Z. wiss. Zool.* **31:** 29-58
Stoeck T., Schmidt H. J. (1998) Fast and accurate identification of European species of the *Paramecium aurelia* complex by RAPD-fingerprints. *Microb. Ecol.* **35:** 311-317
Stoeck T., Przyboś E., Schmidt H. J. (1998) A combination of genetics with inter- and intra-strain crosses and RAPD-fingerprints reveals different population structures within the *Paramecium aurelia* species complex. *Europ. J. Protistol.* **34:** 348-355
Stoeck T., Przyboś E., Kusch J., Schmidt H. J. (2000a) Intra-species differentiation and level of inbreeding of different sibling species of the *Paramecium aurelia* complex. *Acta Protozool.* **39:** 15-22
Stoeck T., Welter H., Seitz-Bender D., Kusch J., Schmidt H. J. (2000b) ARDRA and RAPD-fingerprinting reject the sibling species concept for the ciliate *Paramecium caudatum* (Ciliophora, Protoctista). *Zool. Scr.* **29:** 75-82
Tingey S. V., Tufo J. P. (1993) Genetic analyses with random amplified polymorphic DNA markers. *Pl. Physiol.* **101:** 349-352
Wiąckowski K., Hryniewiecka-Szyfter Z., Babula A. (1999) How many species are in the genus *Mesanophrys* (Protista, Ciliophora,

facultative parasites of marine crustaceans)? *Europ. J. Protistol.* **35:** 379-389

Wichterman R. (1986) The Biology of *Paramecium*. 2 ed. Plenum Press, New York

Woodburn M. A., Youston A. A., Hilu K. H. (1995) Random amplified polymorphic DNA fingerprinting of mosquito-pathogenic and nonpathogenic strains of *Bacillus sphaericus*. *Int. J. Syst. Bact.* **45:** 212-217

Xu Z., Bowers N., Pratt J. R. (1997) Variation in morphology, ecology, and toxicological responses of *Colpoda inflata* (Stokes) collected from five biogeographic realms. *Europ. J. Protistol.* **33:** 136-144

Received on 25th August, 2000; accepted on 7th February, 2001

Acta Protozool. (2001) 40: 99 - 106

ACTA
PROTOZOOLOGICA

Murine Model of Drug-induced Reactivation of *Toxoplasma gondii*

Olgica DJURKOVIĆ-DJAKOVIĆ and Vladimir MILENKOVIĆ

Toxoplasmosis Research Laboratory, Institute for Medical Research, Belgrade, Yugoslavia

Summary. A murine model of recrudescence of chronic toxoplasmosis, mimicking this life-threatening condition in immunosuppressed humans, was developed in Swiss-Webster mice infected 6 weeks previously with 10 cysts of the Me49 strain of *Toxoplasma gondii,* by treatment with dexamethasone (DXM, 2.5 mg/kgBM/day in drinking water), alone or combined with cortisone-acetate (CA, 50 mg/kg by subcutaneous injection 3 times a week). Treatment was continued for 7 weeks. Both DXM and DXM+CA treatment significantly increased mortality, as compared to infected untreated mice (P=0.0002 and P<10^{-4}, respectively), and to uninfected DXM-treated mice (P=0.043 and P=0.001, respectively). In both treatment groups, mean cyst numbers were 2-9-fold increased compared with chronically infected untreated mice. Spleen/body mass ratios and numbers of splenocytes were significantly lower (P<10^{-4}) than in untreated both infected and uninfected mice, indicating decreased immune reactivity in treated animals. Acquired immunity too was impaired by corticoids, as shown by lower resistance to challenge infection with the mouse-virulent RH strain of *T. gondii* in mice with established chronic infection treated with DXM than in those left untreated (P=0.038). Most importantly, 8 of the 56 treated animals (14.2%) developed clinical signs of toxoplasmic encephalitis, which was verified histologically. In these, survival was significantly shorter (P=0.009) and cyst numbers 6-fold augmented (P<10^{-4}) as compared to treated animals, which did not develop neurological signs. This simple model of drug-induced recrudescence of chronic toxoplasmosis, in addition to its potential use for *in vivo* studies of the pathogenic mechanisms of *T. gondii* reactivation, may be particularly suitable for the evaluation of chemotherapeutics.

Key words: chronic infection, corticoid drugs, immunosuppression, *Mus musculus,* reactivation, *Toxoplasma gondii*, toxoplasmosis.

Abbreviations: AIDS - acquired immunodeficiency syndrome, BM - body mass, HIV- human immunodeficiency virus, i.p. - intraperitoneal, s.c. - subcutaneous, TE - toxoplasmic encephalitis.

INTRODUCTION

Toxoplasma gondii is a ubiquitous intracellular protozoan parasite capable of infecting all types of nucleated mammalian host cells. Following a brief acute stage characterized by the proliferative tachyzoite stage of the parasite, primary *T. gondii* infection of an immunocompetent host is converted into latency, characterized by slowly growing bradyzoites within tissue cysts mostly found in the brain and skeletal muscles. Tissue cysts remain viable presumably for the life of the host, controlled mainly by cellular immune mechanisms (Hunter *et al.* 1996). However, if the balance between the host immune defenses and the parasite is disrupted, cyst rupture and renewed parasite proliferation may occur leading to clinical reactivation. The advent of AIDS and use of intensive immunosuppressive therapies for the

Address for correspondence: Olgica Djurković-Djaković, Toxoplasmosis Research Laboratory, Institute for Medical Research, Dr. Subotića 4, PO Box 102, 11129 Belgrade, Yugoslavia; Fax: +381(11)643691; E-mail: olgicadj@imi.bg.ac.yu

treatment of malign and systemic diseases, or pre/post organ and tissue transplantation, have established a population of immunocompromised individuals prone to reactivation of opportunistic pathogens, including *T. gondii*, particularly in geographic areas with a high exposure to this protozoan. Interestingly, death due to toxoplasmosis following renal transplantation has recently been reported in pet animals as well (Bernsteen *et al.* 1999).

In patients with AIDS, *T. gondii* has emerged as the leading cause of focal cerebral lesions most commonly presenting as life-threatening TE (Luft and Remington 1992). Since current therapies are unable to eliminate the parasite from the infected host, treatment of a TE episode must be followed by life-long maintenance therapy. However, standard treatment is associated with considerable toxicity (Haverkos *et al.* 1987, Katlama 1996). Consequently, there is an urgent need for new therapeutics. We have shown in a murine model of acute toxoplasmosis that the combination of clindamycin and atovaquone may be promising (Djurković-Djaković *et al.* 1999); to further these studies an appropriate animal model is required, resembling the natural course of recrudescence of chronic toxoplasmosis in man.

While existing murine models have been invaluable for studying various aspects of the host-parasite relationship, many do not follow the natural history of *T. gondii* infection. A model of TE has been developed by direct intracerebral injection of *T. gondii* into mice immunosuppressed with cortisone acetate (Hofflin *et al.* 1987), in which TE is thus not a consequence of recrudescence of previously established infection. Dual infection models with *T. gondii* and a viral infection such as CMV (Pomeroy *et al.* 1989) and LP-BM5 MULv (Gazzinelli *et al.* 1992, Watanabe *et al.* 1993, Lacroix *et al.* 1994), have not had pharmacological applications due to their complexity and potential lack of reproducibility (Lacroix *et al.* 1996). In a SCID mouse model, rather than suppressing the host, sulfadiazine treatment suppressed infection thus allowing chronicity to develop, and its withdrawal led to relapse (Johnson 1992). Reactivation of the parasite was also attempted by administration of drugs with known immunosuppressive effect. Although Frenkel *et al.* (1975) have long ago induced reactivation of latent toxoplasmosis by cortisone in hamsters infected with the RH strain of *T. gondii,* in mice, however, Sumyuen *et al.* (1996) observed little reactivation following administration of drugs frequently used in organ transplantation, suggesting a mild immunosuppressive potential for cortisol acetate and azathioprine. On the other hand, Nicoll *et al.* (1997) obtained recrudescence with dexamethasone, but it is unclear why they failed to histologically demonstrate brain cysts in 60-70% of mice inoculated with *T. gondii*. Since corticosteroid drugs are often used in human therapy, we considered of interest to develop a murine model resembling the natural course of *T. gondii* reactivation in humans, in which consistently chronically infected immunocompetent mice are subsequently immunosuppressed with corticoid drugs.

MATERIALS AND METHODS

Mice. Female Swiss Webster mice (Medical Military Academy Animal Research Facility, Belgrade), 5-6 weeks old, weighing 18-22 g at the beginning of experiments were used. Mice were housed 6 per cage, and offered drinking water and regular mouse feed *ad libitum*, unless specified otherwise.

Parasites. Brain cysts of the Me49 strain of *T. gondii* (kindly provided by Dr. J. P. Dubey, Beltsville, MD), regularly maintained by passage through Swiss Webster mice twice a year, were used to establish chronic infection. The Me49 strain was used since it belongs to the type-2 strains, which account for 65% of cases of clinical toxoplasmosis in AIDS (Howe and Sibley 1995). To obtain brain cysts for experimental infections, mice infected at least 8 weeks previously were killed, brains removed and homogenized in a tissue homogenizer with 1 ml saline each. For cyst enumeration, 25 µl of the brain suspensions were placed on slides and microscopically counted. The number of cysts per brain was calculated by multiplying the number counted in 2 drops by 2 different investigators by 20, giving a threshold sensitivity of 20 cysts per brain. For experimental infections, mice were inoculated by intraoesophageal gavage with 250 µl brain suspensions assessed to contain 10 cysts. An inoculum of 10 cysts was chosen since in our experience an inoculum of this size regularly produces consistent infection without mortality, while larger inocula (>20) result in mortality unless treated with sulfadiazine.

For challenge experiments, tachyzoites of the virulent RH strain maintained through serial i.p. passages were used. For experimental infections, tachyzoites were harvested from mouse peritoneal fluids 72 h post-infection and purified by filtration through 3µm polycarbonate filters (Nuclepore ®, Maidstone, UK, lot 1050308). The parasites were counted in a haemocytometer and their numbers were adjusted to 2×10^6 / ml with saline. Suspensions were serially 10-fold diluted, and 0.5 ml aliquots of 2×10^2 / ml dilutions were inoculated i.p.

Drugs. Dexamethasone (DXM, dexamethasone sodium phosphate, ICN Galenika, Belgrade, Yugoslavia) was given at a dose of 2.5 mg/kgBM/day per mouse, obtained by dissolving 5 mg DXM per 1-liter drinking water. Treated as well as untreated water was changed 3 times a week.

Cortisone acetate (CA, hydrocortisone-21-acetate, lot 87494, ICN Biomedicals Inc., Aurora, OH) was administered by s.c. injection 3 times a week at 50 mg/kg BM.

Amoxicillin and clavulanic acid (Panklav®, Panfarma, Belgrade, Yugoslavia) was given in drinking water at 1g/l throughout the experiment to prevent bacterial superinfection.

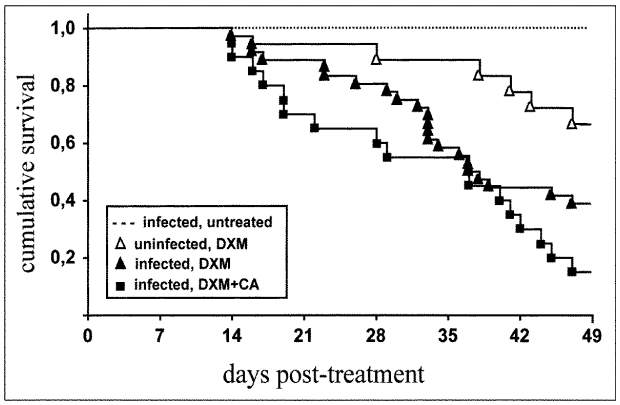

Fig. 1. Effect of DXM (2.5 mg/kg/day) alone or combined with CA (50 mg/kg/ 3 x week) on survival (Kaplan-Meier estimates) of mice with chronic *T. gondii* infection established by peroral inoculation of 10 Me49 cysts 6 weeks prior to treatment. Survival was significantly lower in infected DXM-treated mice than in infected untreated (P=0.0002) and uninfected DXM-treated mice (P=0.043), and in infected DXM+CA-treated mice than in infected untreated ($P<10^{-4}$) and uninfected DXM-treated mice (P=0.001)

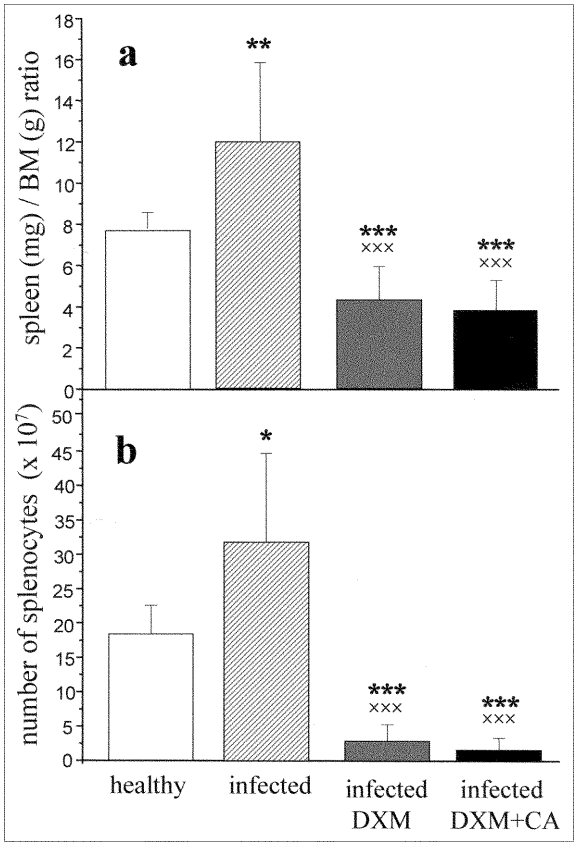

Fig. 2. a - effect of corticoid drug treatment of mice with established chronic *T. gondii* infection on spleen (mg) / BM (g) ratios; **b -** numbers of splenocytes. Data are presented as mean ± SD. Relative spleen size (** P=0.0004) and splenocyte numbers (* P=0.0072) were significantly greater in chronically infected untreated controls than in healthy control mice. In contrast, relative spleen size and number of splenocytes were significantly lower in both DXM and DXM+CA treated mice than in healthy (***$P<10^{-4}$) and chronically infected untreated (*** $P<10^{-4}$) controls

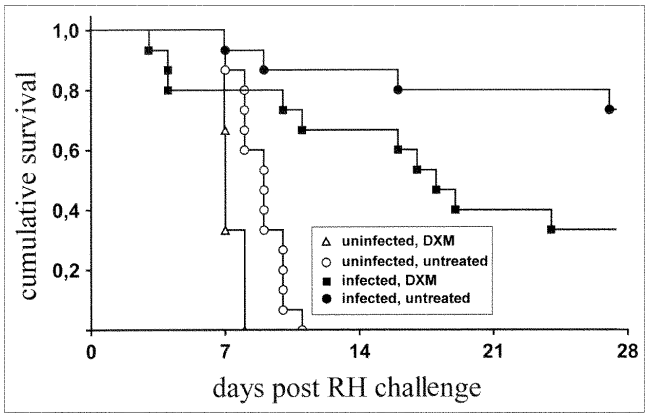

Fig. 3. Effect of i.p. challenge with 10^2 RH tachyzoites on survival of mice with previously established chronic *T. gondii* infection treated with DXM during 7 weeks. Survival times were calculated from day of RH challenge. Significantly lower survival is obvious in chronically infected DXM-treated mice than in chronically infected untreated mice (P=0.038), but longer than in uninfected untreated control mice (P=0.008)

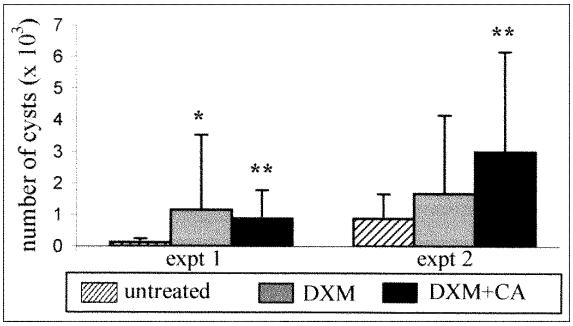

Fig. 4. Numbers of brain cysts (mean ± SD) in mice with established chronic toxoplasmosis after treatment with DXM alone or combined with CA. Compared to untreated chronically infected controls, cyst burdens were significantly higher in DXM-treated mice (* P=0.05) in experiment 1 and in DXM+CA-treated mice (** P=0.01) in either experiment

The immunosuppressive drug regimens were selected on the basis of preliminary experiments performed to assess the dosages of these drugs resulting in the highest degree of immunosuppression without causing lethality. For DXM, the assayed doses were 2.5 and 5 mg/kgBM/day (5 and 10 mg/l drinking water, respectively), similar to those used by Nicoll *et al.* (1997). Since in contrast to their study, the latter dose was toxic as shown by 80% mortality over a period of 6 weeks, the dose selected for this study was 2.5 mg/kg. For CA, the dose of 50 mg/kg was selected as well tolerated in both a similar study (Sumyuen *et al.* 1996) and our preliminary experiments. Since these had also revealed that CA did not cause sufficient reactivation as demonstrated by both little clinical signs and no mortality, the present study was designed on the basis of administration of DXM alone or combined with CA.

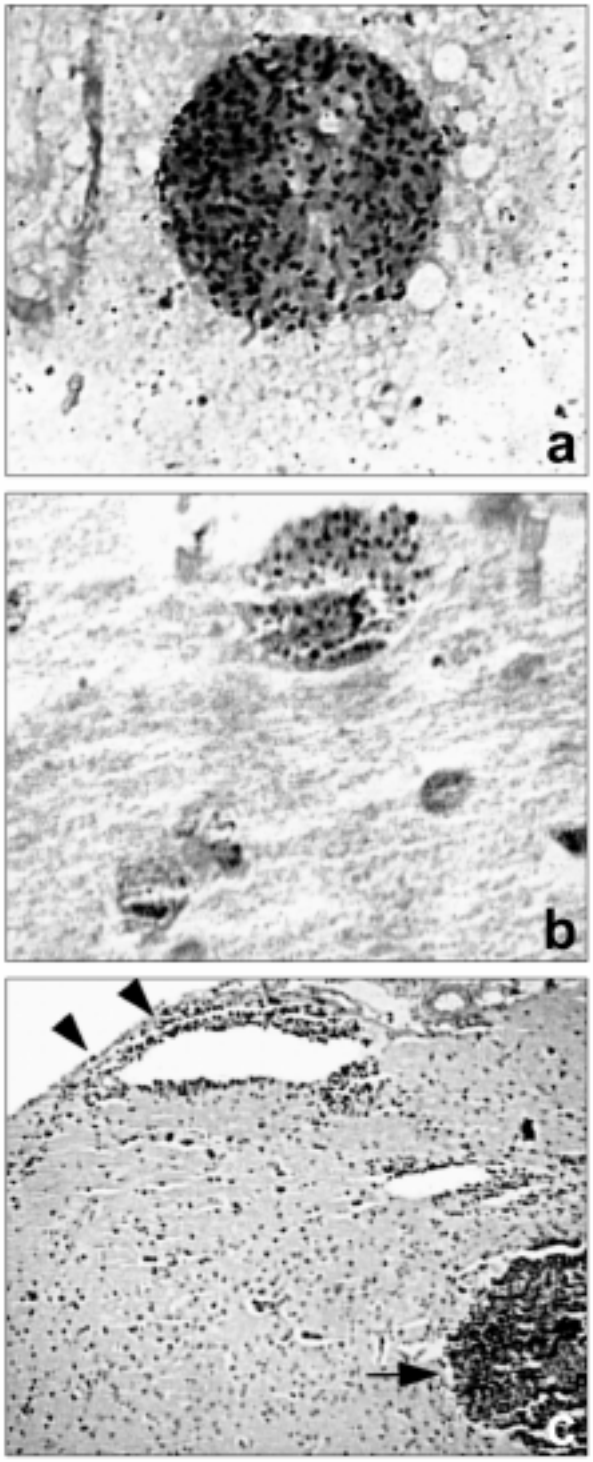

Fig. 5. Brain of mouse infected with 10 cysts of the Me49 strain of *T. gondii* 6 weeks prior to beginning of treatment with DXM (2.5mg/kg/day), which died with clinical signs of toxoplasmic encephalitis at day 32 day of treatment. Haematoxylin-eosin stain. **a** - squash smear of typical *T. gondii* tissue cyst. Magnification x 1000. **b -** brain section showing *T. gondii* tissue cyst with no inflammatory reaction in surrounding tissue. Magnification x 1000. **c -** brain section showing inflammatory infiltrate in meningeae and surrounding small blood vessels (arrowheads), and a large area of necrosis (arrow). Magnification x 200

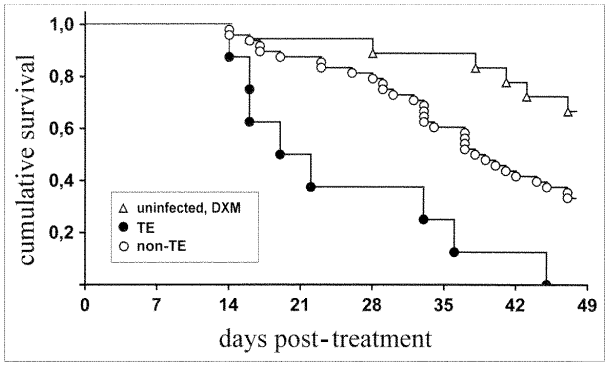

Fig. 6. Survival (Kaplan-Meier estimates) in mice with established chronic toxoplasmosis treated with corticoid drugs (both regimens) with respect to the occurrence of clinical TE. Survival was significantly lower in mice which developed TE than in those, which did not (P=0.009), but also lower in mice, which did not exhibit TE than in uninfected DXM-treated mice (P=0.01)

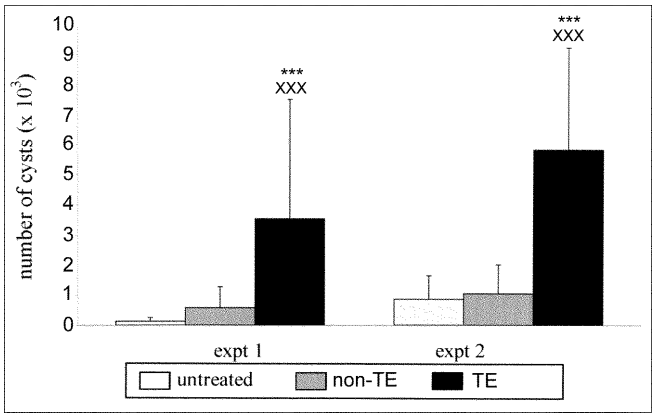

Fig. 7. Numbers of brain cysts (mean ± SD) in mice with established chronic toxoplasmosis treated with corticoid drugs with respect to the occurrence of clinical TE. Significantly higher cyst burdens were noted in mice which developed TE than in treated mice which did not exhibit neurological signs (***$P<10^{-4}$), and also than in chronically infected untreated mice (*** $P<10^{-4}$) in either experiment

Experimental Design. Groups of mice infected 6 weeks previously with cysts of the *T. gondii* Me49 strain were arbitrarily assigned to treatment with DXM alone or combined with CA over a period of 7 weeks, or left untreated as controls. Treatment groups comprised 6-12 animals each, depending on the experiment. Survival was monitored daily, and any clinical alterations (ruffled fur, hunchback appearance, locomotor alterations, paralysis) and deaths were recorded. Animals were weighed weekly. Mice dying during treatment were examined as described below. At the end of the 7-week treatment period, some survivors were challenged with RH strain parasites to examine the effect of corticoids on acquired immunity, and the remaining mice were killed by asphyxiation in chloroform for further examination. Each animal was weighed and brain and spleen

removed. Brain tissue homogenates were prepared for cyst enumeration. If histology was to be performed, brains were divided in halves; one half was homogenized, while the other was fixed in 9% formalin and paraffin-embedded, and 5 μm sections stained with haematoxylin-eosin. The relative spleen size determined as the spleen mass (mg)/ BM (g) ratio and total splenocyte numbers were both taken as parameters of immune activation / suppression. Thus, the spleens were weighed, and single cell suspensions made for enumeration of nucleated cells. The experiments were performed at least twice, and the results shown represent their cumulative results, unless specified otherwise.

Statistics

Survival of mice on different drug regimens was evaluated by the Kaplan-Meier product limit method. The difference between the curves obtained was analysed by the Peto and Peto Wilcoxon test. Differences in the cyst numbers, relative spleen sizes and total spleen cell counts between groups were examined by Student's t test. The level of statistical significance was 0.05.

RESULTS

Mice with established chronic toxoplasmosis were treated with DXM alone or combined with CA over a period of 7 weeks. Two control groups were included, comprising chronically infected untreated mice, and uninfected mice treated with DXM. All infected untreated mice survived. Treated animals, irrespective of whether infected or not, began exhibiting signs of general weakness and loss of subcutaneous adipose tissue as early as in the second week of treatment. In addition to general signs, some infected animals developed neurological signs compatible with the clinical presentation of TE. Mortality began after 2 weeks of treatment and continued throughout the treatment period. DXM and DXM+CA treatment resulted in 61.1% and 85% mortality, respectively. However, there was a 33% mortality in the control group of uninfected mice treated with DXM. Analysis of the estimated probabilities of survival is shown in Fig. 1. Both DXM and DXM+CA treatment significantly increased mortality, as compared to infected untreated mice ($P=0.0002$ and $P<10^{-4}$, respectively), and to uninfected DXM-treated mice ($P=0.043$ and $P=0.001$, respectively). Between the treatment groups, although DXM+CA treatment resulted in higher mortality, the difference in survival was not significant ($P>0.05$).

Evidence that corticoid drug treatment was actually immunosuppressive for treated mice was obtained by calculation of the spleen/BM ratios (Fig. 2a) and enumeration of spleen cells (Fig. 2b) at the time of death or at the end of the 7-week treatment period. Chronic infection was associated with significant spleen enlargement ($P=0.0004$) and marked increase in the number of splenocytes ($P=0.0072$) as compared to healthy controls. In contrast, in infected mice which received corticoids, both parameters were dramatically lower than in infected untreated mice ($P<10^{-4}$) and also than in healthy mice ($P<10^{-4}$). Between treatment groups, relative spleen size and cellularity were both lower, although insignificantly ($P>0.05$), in mice on the combined drugs than in mice treated with DXM alone.

To examine the effect of corticoid treatment on established protective immunity to *T. gondii*, groups of DXM-treated 7-week survivors were challenged with 10^2 tachyzoites of the RH strain of *T. gondii.* Infection with this strain, irrespective of the inoculum size, is invariably lethal for non-immunized mice. Groups of uninfected untreated mice, uninfected DXM-treated mice, and chronically infected untreated mice, were all included as controls. Uninfected untreated animals all succumbed to acute infection by day 11, as expected, and survival of uninfected treated mice was slightly lower ($P=0.052$) (Fig. 3). In contrast, mice with established chronic infection which received immunosuppressive treatment survived better than uninfected untreated controls ($P=0.008$), but less well than chronically infected untreated mice ($P=0.038$) of which, expectedly, most were protected against challenge. Evidence that these mice died of toxoplasmosis was provided by demonstration of masses of extracellular *T. gondii* tachyzoites in their peritoneal fluids.

In treated mice, the mean brain cysts counts were 2-9-fold increased as compared to those in chronically infected untreated mice killed at the end of the experiment (Fig. 4). However, the numbers of cysts in these chronically infected untreated controls varied greatly between different experiments (130 ± 122 in Expt 1 and 884 ± 748 in Expt 2). Thus, the results were analysed for each experiment separately. Compared to the cyst counts in untreated mice, despite the broad ranges in the numbers of cysts within each group, the increase was significant in mice on DXM treatment in the first ($P=0.05$), as well as in mice on DXM+CA treatment in either experiment ($P=0.013$ and $P=0.016$, respectively). It should be noted that in corticoid drug-treated mice, the cysts varied in size and quality; thus, there were large cysts containing numerous bradyzoites, as well as many small

cysts; some appeared normal while others were partly destroyed and/or degenerate. Similar as with other parameters, the numbers of cysts did not vary significantly between the treatment groups ($P>0.05$).

Most importantly, clinical reactivation manifested by decreased activity and tottering walk followed within days by chemiparesis and paralysis, developed, as mentioned above, in 8 of 56 (14.2%) mice on both treatment regimens. Evidence for these clinical observations was obtained by pathohistological analysis of brain sections of representative mice, which, in addition to brain cysts, showed perivascular and meningeal infiltration consistent with the diagnosis of meningoencephalitis (Fig. 5), despite the anti-inflammatory activity of corticoids. All animals which developed TE, died within days after the appearance of clinical signs, and their survival was significantly ($P=0.009$) shorter than that of treated mice without clinically evident TE (Fig. 6). On the other hand, treated mice not exhibiting neurological signs died more rapidly than uninfected DXM-treated mice ($P=0.01$). Furthermore, both spleen / BM ratios and splenocyte numbers in the TE mice (3.65 and $1.52x10^7$, respectively) were lower, although insignificantly ($P=0.32$ and $P=0.21$, respectively), than in mice which did not exhibit neurological signs (3.98 and $2.08x10^7$, respectively). Brain cyst burdens, both per experiment (Fig. 7) and cumulatively, were greatly (6-fold) increased compared with treated mice, which did not develop TE ($P<10^{-4}$), and (up to 27-fold) compared with chronically infected untreated mice ($P<10^{-4}$). The effect of the combined corticoid treatment was more rapid since mice on DXM+CA treatment exhibited clinical reactivation earlier during the course of treatment and died after a mean period of 18.3 days as compared to the mean survival of 29.2 days of mice treated with DXM alone.

DISCUSSION

The results presented demonstrate reactivation of previously latent murine *T. gondii* infection induced by 7-week-long administration of corticosteroid drugs DXM and CA. High mortality of treated animals was associated with increased brain cyst burdens and markedly lowered spleen size and cellularity, as compared to both healthy and infected untreated mice. Furthermore, clinical disease with typical locomotor signs of cerebral toxoplasmosis was demonstrated in 14.2% of the treated animals, associated with slightly deeper immunosuppression but significantly shorter survival and greatly increased (by 6-fold) brain cyst burdens compared with treated animals which did not exhibit TE. Since our work did not include a detailed histological study and histological sections were used merely for demonstration of encephalitis in evidently ill animals, it is possible that histologically demonstrable encephalitis existed in more treated animals. However, infected treated mice not displaying TE survived significantly shorter than uninfected treated mice, which suggests that neurological signs do not necessarily accompany death due to *T. gondii* reactivation. A parallel may be made with immunosuppressed humans, in which subclinical reactivation is more frequent than overt disease in transplant patients (Dérouin *et al.* 1987, Gallino *et al.* 1996).

The effect of corticoid drugs on acquired immunity in infected treated animals was shown by challenge with the RH strain of *T. gondii.* Between groups of mice with established chronic infection, a more detrimental effect of challenge infection in corticoid-treated mice than in those untreated, indicates impairment of protective immunity by corticoids. These findings are similar to those of Johnson *et al.* (1995), who showed that among mice immunized with a vaccine (ts-4) strain, RH challenge was less well tolerated by mice which received sublethal irradiation than by those which did not. Although we did not analyse the immunological mechanisms underlying impairment of acquired immunity by corticoids, the decrease in the numbers of CD4+ and CD8+ T cells shown to be induced by irradiation is plausible in our model too since general cellularity was greatly diminished.

The described model imitates the natural course of reactivation of *T. gondii* infection in man in that mice were infected with cysts of a type-2 strain responsible for most cases of human TE (Howe and Sibley 1995), using the peroral route which is the major route of human infection (Dubey and Beattie 1988). After the chronic infection was established, corticosteroid drugs often used in human therapy induced immunosuppression. Mice belong to a steroid sensitive species, and corticosteroids have long been known to cause destruction of murine lymphoid tissues, resulting in lymphocytopenia, monocytopenia, and shrinkage of the spleen (Antopol 1950). In addition, immunosuppression of mice by DXM has been reported to induce release of parasites from preexisting cysts and new cyst formation as early as after 6-12 days of administration (Odaert *et al.* 1996). Both regimens we used, DXM alone and combined with CA, induced significant immunosuppression and subse-

quent reactivation of the parasite in infected animals, but the effect of the combined treatment was greater, although not significantly, than the effect of DXM alone. While CA alone had just a mild effect, as shown by Sumuyen *et al.* (1996) and in our preliminary experiments, this study shows it potentiates the effect of DXM when the 2 are combined. However, it should be noted that a prolonged course of DXM itself causes considerable toxicity, since administration during 7 weeks resulted in death of one third of healthy control mice. These animals were progressively loosing weight and died with signs of general weakness. The discrepancy between our findings and those of Nicoll *et al.* (1997), who did not observe mortality with a prolonged administration of DXM even at a dose as high as 8 mg/L, is difficult to explain unless Swiss Webster mice are more susceptible to negative effects of DXM than the Porton mice used in their study.

The reproducibility of our model has been examined in repeated experiments yielding similar results. While parameters of immune activation varied little between experiments, the major difference was the baseline level of cysts formed in mouse brains following inoculation of cysts, obviously reflecting variations in the initial cyst content; this may vary between a few and several hundreds (Dubey 1997). However, such broad ranges are common in Swiss Webster mice after inoculation of even a controlled number of bradyzoites (Dubey 1997). On the other hand, the broad range of the numbers of cysts induced by treatment (wide standard deviations in Fig. 4) is easily explained since the data shown included all treated animals of which those that developed TE harbored dramatically greater cyst burdens. Hence, we chose to work with intact tissue cysts as the source of natural infection.

The presented model is simple to perform and to interpret since it does not include as many variables as coinfection models (Lacroix *et al.* 1996), and is not as requiring in terms of precautionary measures nor as costly as work with nude or SCID mice. In addition to the potential use of this model in studies of the pathogenic mechanisms of recrudescence of chronic toxoplasmosis, its simplicity and reproducibility recommend it particularly for the evaluation of chemotherapeutics, for which it is currently being used in our laboratory.

Acknowledgements. The results presented in this paper were reported at the 10th European Congress of Clinical Microbiology and Infectious Diseases (ECCMID) in Stockholm, Sweden, May 28-31, 2000. Vladimir Milenković, BSc., was an ECCMID Travel Award recipient. We thank Drs. Slavica Ušaj-Knežević and Vesna Čemerikić-Martinović for help with the histological studies, Dr. Nevenka Stojanovič for useful suggestions, and Mrs. Jordanka Djurović for expert technical assistance.

REFERENCES

Antopol W. (1950) Anatomic changes produced in mice treated with excessive doses of cortisone. *Proc. Soc. Exp. Med.* **73:** 262-265

Bernsteen L., Gregory C. R., Aronson L. R., Lirtzman R. A., Brummer D. G. (1999) Acute toxoplasmosis following renal transplantation in three cats and a dog. *J. Am. Vet. Med. Ass.* **215:** 1123-1126

Dérouin F., Debure A., Godeault E., Larivière M., Kreis H. (1987) *Toxoplasma* antibody titers in renal transplant recipients: pre and post transplant follow up of 73 patients. *Transplantation* **44:** 515-518

Djurković-Djaković O., Nikolić T., Robert-Gangneux F., Bobić B., Nikolić A. (1999) Synergistic effect of clindamycin and atovaquone in acute murine toxoplasmosis. *Antimicrob. Agents Chemother.* **43:** 2240-2244

Dubey J. P., Beattie C. P. (1988) Toxoplasmosis of Animals and Man. CRC Press, Boca Raton, FL

Dubey J. P. (1997) Bradyzoite-induced murine toxoplasmosis: stage conversion, pathogenesis, and tissue cyst formation in mice fed bradyzoites of different strains of *Toxoplasma gondii*. *J. Euk. Microbiol.* **44:** 592-602

Frenkel J. K., Nelson B. M., Arias-Stella J. (1975) Immunosuppression and toxoplasmic encephalitis. *Human Pathol.* **6:** 97-111

Gallino A., Maggiorini M., Kiowski W., Martin X., Wunderli W., Schneider J., Turina M., Follath F. (1996) Toxoplasmosis in heart transplant recipients. *Eur. J. Clin. Microbiol. Inf . Dis.* **15:** 389-393

Gazzinelli R. T., Hartley J. W., Fredrickson T. N., Chattopadhyay S. K., Sher A., Morse H. C. (1992) Opportunistic infections and retrovirus-induced immunodeficiency: studies of acute and chronic infections with *Toxoplasma gondii* in mice infected with LP-BM5 murine leukemia viruses. *Infect. Immun.* **60:** 4394-4401

Haverkos H. W., the TE Study Group (1987) Assessment of therapy for toxoplasma encephalitis. *Amer. J. Med.* **82:** 907-914

Hofflin J. M., Conley F. K., Remington J. S. (1987) Murine model of intracerebral toxoplasmosis. *J. Infect. Dis.* **155:** 550-557

Howe D. K., Sibley L. D. (1995) *Toxoplasma gondii* is comprised of three clonal lineages: correlation of parasite genotype with human disease. *J. Infect. Dis.* **172:** 1561-1566

Hunter C. A., Suzuki Y., Subauste C. S., Remington J. S. (1996) Cells and cytokines in resistance to *Toxoplasma gondii*. *Curr. Topics Microbiol. Immunol.* **219:** 113-125

Johnson L. L. (1992) SCID mouse models of acute and relapsing chronic *Toxoplasma gondii* infections. *Infect. Immun.* **60:** 3719-3724

Johnson L. L., Gibson G. W., Sayles P. C. (1995) *Toxoplasma gondii:* Effect of sublethal irradiation on host resistance in mice. *Expl Parasitol.* **81:** 172-181

Katlama C. (1996) Diagnosis and treatment of toxoplasmosis of the CNS in patients with AIDS. *CNS Drugs* **5:** 331-343

Lacroix C., Levacher-Clergeot M., Chau F., Sumyuen M. H., Sinet M., Pocidalo J.J., Dérouin F. (1994) Interactions between murine AIDS (MAIDS) and toxoplasmosis in co-infected mice. *Clin. Exp. Immunol.* **98:** 190-195

Lacroix C., Brun-Pascaud M., Maslo C., Chau F., Romand S., Dérouin F. (1996) Co-infection of *Toxoplasma gondii* with other pathogens: pathogenicity and chemotherapy in animal models. In: Current Topics in Microbiology and Immunology. *Toxoplasma gondii* (Ed. U. Gross). Springer-Verlag, Berlin, Heidelberg **219:** 223-233

Luft B. J., Remington J. S. (1992) Toxoplasmic encephalitis in AIDS. *Clin. Infect. Dis.* **15:** 211-222

Nicoll S., Wright S., Malay W., Burns S., Buxton D. (1997) A mouse model of recrudescence of *Toxoplasma gondii* infection. *J. Med. Microbiol.* **46:** 263-266

Odaert H., Soete M., Fortier B., Camus D., Dubremetz J. F. (1996) Stage conversion of *Toxoplasma gondii* in mouse brain during infection and immunodepression. *Parasitol. Res.* **82:** 28-31

Pomeroy C., Kline S., Jordan M. C., Filice G. A. (1989) Reactivation of *Toxoplasma gondii* by cytomegalovirus disease in mice: antimicrobial activities of macrophages. *J. Infect. Dis.* **160:** 305-311

Sumyuen M. H., Garin Y. J. F., Dérouin F. (1996) Effect of immunosuppressive drug regimens on acute and chronic murine toxoplasmosis. *Parasitol. Res.* **82:** 681-686

Watanabe H., Suzuki Y., Makino M., Fujiwara M. (1993) *Toxoplasma gondii*: Introduction of toxoplasmic encephalitis in mice with chronic infection by inoculation of a murine leukemia virus inducing immunodeficiency. *Expl Parasitol.* **76:** 39-45

Received on 29th September, 2000; accepted on 3rd January, 2001

Acta Protozool. (2001) 40: 107 - 115

ACTA
PROTOZOOLOGICA

Morphological Redescription and Morphogenesis of the Marine Ciliate, *Pseudokeronopsis rubra* (Ciliophora: Hypotrichida)

Xiaozhong HU and Weibo SONG

Laboratory of Protozoology, Ocean University of Qingdao, Qingdao, P. R. China

Summary. The morphology and morphogenesis of the marine ciliate, *Pseudokeronopsis rubra* (Ehrenberg, 1838) isolated from shrimp culturing water of Qingdao (Tsingtao, China), are investigated using protargol silver impregnation. The Qingdao population presents the following characteristics: body slim and reddish, size in vivo 160-200 x 24-40 μm, with longitudinal furrow on the ventral side; brick-red pigments constituting rosettes on dorsal side and ventral arrays along the base of cirri; blood cell-like cortical granules throughout the endoplasm. AZM consisting of 46-60 membranelles; long midventral row with 30 pairs of cirri on average; 2-4 transverse cirri and 4-6 dorsal kineties. The overall pattern of the morphogenetic events resembles the other populations described previously: in the opisthe new basal bodies originate close to intact left midventral cirri; the adoral membranelles primordia (AMP), undulating membranes anlagen (UMA) and fronto-midventral-cirral anlagen (FMA) develop from the growing anarchic primordium. In the proter, the AMP and UMA generate de novo on the surface of the buccal cavity. The FMA originate apokinetally to the right of the parental paroral membrane. The UMA generate the first frontal cirrus, PM and EM in both daughter cells as in other hypotrichs. The AMP, UMA and FMA develop in a usual way as in other urostylids. Marginal cirral rows and dorsal kineties occur within the parental structures. The numerous macronuclear segments divide without prior fusion. Reorganization corresponds to the divisional processes in the opisthe. The most remarkable feature is that the old structures do not participate in the formation of the new organelles.

Key words: Hypotrichida, marine ciliate, morphology, morphogenesis, *Pseudokeronopsis rubra.*

INTRODUCTION

The genus *Pseudokeronopsis* is commonly found in all different habitats with mostly overlapping characters (cell color, size and infraciliature), which gives rise to great confusion for species identification. Among this genus, the marine form, *P. rubra* is likely one of the most debatable species though many studies using modern methods have been carried out (Ehrenberg 1835 a, b; Borror 1972, 1979; Borror and Wicklow 1983; Foissner 1984; Wirnsberger *et al.* 1987). Moreover, according to the data obtained, all known *Pseudokeronopsis* studied share similar morphogenetic characters (Wallengren 1901, Morgan 1926, Rühmekorf 1935, Borror 1972, Ruthmann 1972, Wirnsberger 1987, Mihailowitsch and Wilbert 1990). However, the complete morphogenetic process including the development of new ciliature in daughters and the evolution of macronuclear segments is still lacking.

Address for correspondence: Weibo Song, Laboratory of Protozoology, Ocean University of Qingdao, Qingdao 266003, P. R. China; Fax: +86 532 203 2283; E-mail: wsong@ouqd.edu.cn

The present study gives the results based on the Qingdao population of *P. rubra*, in order to provide some new characters for a solid redefinition of these "well-known" ciliates at morphological and morphogenetic level.

MATERIALS AND METHODS

Samples were isolated from a shrimp culturing water in Qingdao (Tsingtao, 36°08'N; 120°43'E), China. Water salinity was about 12‰, water temperature about 20°C and pH *ca* 8.0. Specimens were cultured in boiled seawater to which squeezed rice grains were added.

The infraciliature was revealed with the protargol staining method according to Wilbert (1975). All drawings were made at a magnification of x125 with the help of camera Lucida. For clarity, in the morphogenetic stages, the parental structures were showed by outline, whereas the new ones were shaded. The terminology was according to Hemberger (1982) and Wirnsberger (1987).

RESULTS

Morphological redescription of the Qingdao population of *Pseudokeronopsis rubra* (Figs.1a-i, 4-10; Table 1)

Body slender, intensively contractile and highly flexible, size *in vivo* about 160-200 x 24-40 μm. Right and left edges are slightly convex, anterior end bluntly round, while posterior end often spoon-like. One conspicuous longitudinal furrow present along the middle of the cell at the ventral side. Dorsoventrally flattened (Fig.1c). Cortex reddish (under low magnification), with underlying brick-red pigment (<0.5 μm in diameter), which are grouped along the cirral rows (Fig. 1b) and dorsal kineties (about 6-10 granules comprise one rosette around the cilia) (Figs. 4-6); cortical granules about 1-2 μm in diameter, blood cell shaped (Fig. 1d, arrowheads). Numerous macronuclear segments, spherical to ovoid, distributed throughout the whole cell. Cytoplasm relatively transparent, containing several food vacuoles. Movement slowly. Conjugation was frequently observed under cultural condition.

Adoral zone of membranelles (AZM) consisting of 46-60 membranelles, usually like a question mark extending onto right-ventral side, about 1/3-1/4 of body length, apical membranelles *ca* 15 μm long. Buccal field narrowed and strongly deepened; pharyngeal fibers conspicuous; paroral membrane rather shorter than endoral one. Bicorona consists of about 7 anterior, slightly enlarged frontal cirri and 5-6 posterior ones. Constantly one buccal and two frontoterminal cirri (Fig.1e, arrowhead); midventral rows consisting of 49-77 cirri, located at ventral concaved furrow (Fig. 1c), cirri about 7-8 μm long; 2-4 transverse cirri about 15 μm in length each, protruding out of posterior edge.

Marginal rows posteriorly unconfluent, cirri 8 μm long, bases composed of 2 basal body rows; 4-6 dorsal kineties, each as long as the body; dorsal cilia about 3 μm long.

Divisional morphogenesis of *Pseudokeronopsis rubra* (Figs.1j-l; 2a-h; 3a, b; 11; 14-16)

Marginal cirri and dorsal kineties develop in a usual way, of which the anlagen appear within old structures and stretch toward both sides to replace the old structures (Figs. 2b-h; 3a, b)

1. Stomatogenesis and development of the somatic ciliature in the opisthe

Stomatogenesis commences with the forming of small groups of basal bodies very close to several left midventral cirri. With the proliferation of basal bodies, these groups join to make a longish field, which is the anarchic primordium (AP) of the opisthe (Fig.1j). During the process, the left midventral cirri remain intact. When the adoral membranelles of the opisthe organize in a posteriad direction in adoral membranelles primordia (AMP, as shown in Figs.1k, l), several oblique streaks appear at the right-anterior position of AP, which is fronto-midventral cirral anlagen (FMA, arrows; Figs. 1k, l; 2a); later, undulating membranes anlagen (UMA) separate to the right of the remaining primordia (Fig. 2a, arrow). At the present three parts join together at the posterior portion (Figs. 2a, b). Soon, they depart one another and develop into new structures. With the number of adoral membranelles increasing in AMP, a single frontal cirrus derives from UMA and the remaining of UMA splits longitudinally to make undulating membranes (PM, EM) (Figs. 2b, d; arrows); meanwhile, each streak of FMA divides into 2 segments (cirri) except for the posterior 4 streaks (3 or 4 segments/cirri) (Figs. 2d, e): the posterior cirrus from the first streak move to PM to be buccal cirrus (Figs. 2e, g; long arrows); the anterior two cirri from the last streak will migrate anteriad to be FTC (Figs. 2g, arrowheads; 3a, arrow); each of the posterior 2-4 streak contributes one cirrus (TC) to the daughter cell; the remaining new cirri are to be FC and MVC.

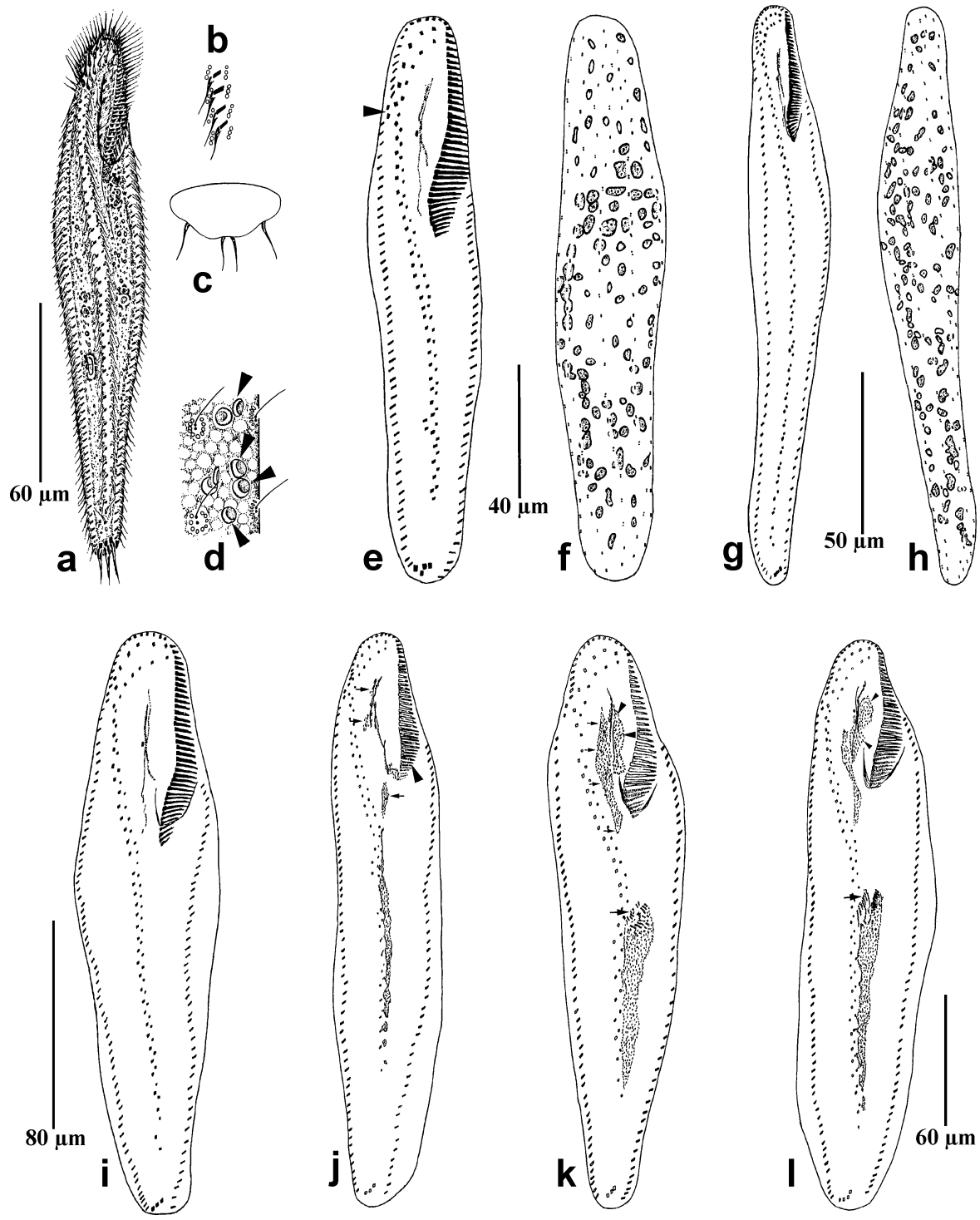

Figs. 1 a-l. Morphology and early stages of morphogenesis in *Pseudokeronopsis rubra* from living observation (a-d) and after protargol impregnated specimens (e-l); **a** -ventral view *in vivo*; **b** - showing the arrangement of pigments near cirri; **c** - transverse section; **d** - portion of dorsal view, indicating dorsal cilia, pigments and cortical granules (arrowheads); **e, f** - ventral and dorsal views of the same individual, arrowhead showing FTC; **g, h** - ventral and dorsal views of the same cell; **i** - ventral view; **j** - ventral view; arrowhead indicating dedifferentiating of old AZM, short arrows marking FMA in the proter; **k** - ventral view, long arrow showing FMA in the opisthe, short arrows marking FMA in the proter, arrowheads indicating AMP in the proter; **l** - ventral view, long arrow showing FMA in the opisthe, arrowheads indicating AMP in the proter, AM - adoral membranelles, AMP - adoral membranelles primordium, AP - anarchic primordium, AZM - adoral zone of membranelles, FMA - frontomidventral cirral anlagen, FTC - frontoterminal cirri

Table 1. Morphometrical data of *Pseudokeronopsis rubra*. Three populations are respectively according to author (first line) and Wirnsberger *et. al.* (1986) (second and third line). Data are based on protargol-impregnated specimens. Measurements in μm. CV - coefficient of variation in %; Max - maximum; Min - minimum; n - number of individuals examined; SD - standard deviation; SE - standard error of mean; Mean - arithmetic mean

Character	Min	Max	Mean	SD	SE	CV	n
Body length	124	264	180.7	37.51	8.19	20.8	21
	140	189	171.8	12.50	3.20	7.3	15
	159	220	189.5	17.10	4.40	9.4	15
Body width	32	64	50.8	8.15	1.86	16.0	19
	24	41	30.5	4.40	1.10	14.4	15
	37	63	50.4	8.40	2.20	16.7	15
Buccal field length	51	76	62.2	7.23	1.62	11.6	20
	48	57	52.0	2.90	0.70	5.6	15
	57	80	62.7	6.20	1.60	9.9	15
Adoral membranelles, No.	46	60	51.6	3.72	0.83	7.2	20
	50	65	58.0	3.90	1.00	6.7	15
	66	92	78.1	7.10	1.80	9.1	15
Anterior frontal cirri, No.	11*	14*	12.6*	1.07*	0.24*	8.4*	19*
	6	10	8.1	1.00	0.30	12.8	15
	5	12	8.5	2.60	0.70	31.2	15
Posterior frontal cirri, No.	-	-	-	-	-	-	-
	4	7	5.6	1.00	0.20	17.5	15
	5	13	7.7	2.10	0.60	27.9	15
Frontoterminal cirri, No.	2	2	2	0	0	0	20
	-	-	-	-	-	-	-
	-	-	-	-	-	-	-
Midventral cirri, No.	49**	77**	61.6**	8.28**	2.07**	13.4**	16**
	30***	43***	38.0***	3.50***	0.90***	9.2***	15***
	28***	47***	36.7***	5.20***	1.30***	14.2***	15***
Buccal cirrus, No.	1	1	1	0	0	0	21
	-	-	-	-	-	-	-
	-	-	-	-	-	-	-
Left marginal cirri, No.	45	62	52.7	5.19	1.26	9.9	17
	57	82	72.0	7.10	1.80	9.8	15
	48	71	62.0	6.40	1.60	10.2	15
Right marginal cirri, No.	48	67	57.9	4.64	1.13	8.0	17
	59	95	79.0	9.10	2.30	11.5	15
	45	73	63.6	7.80	2.00	12.2	15
Transverse cirri, No.	2	4	3.1	0.62	0.15	19.8	16
	6	9	7.2	0.90	0.20	13.0	15
	4	9	7.1	1.50	0.40	21.7	15
Dorsal kineties, No.	4	7	5.1	0.72	0.18	14.0	16
	5	8	6.3	-	-	-	15
	5	8	6.4	-	-	-	15

* including posterior frontal cirri
** including right midventral cirri
*** referring to number of pairs of midventral cirri
- not available

2. Stomatogenesis and development of the somatic ciliature in the proter

Just as appearing of AP in the opisthe, groups of basal bodies developed independently on the surface and to the right of the buccal cavity and behind buccal fields (Figs. 1j, k; short arrows); meanwhile, the posterior adoral membranelles begin to dedifferentiate in an anteriad direction (Fig. 1j, arrowhead). Lately, with the proliferation of basal bodies, a longish field forms, which will develop into FMA (Fig. 2a); at the same time, an anarchic field occur on the surface of buccal cavity and to the left of the endoral membrane (Figs.1k, l, arrowheads; 2a). With the joining of new basal bodies in the

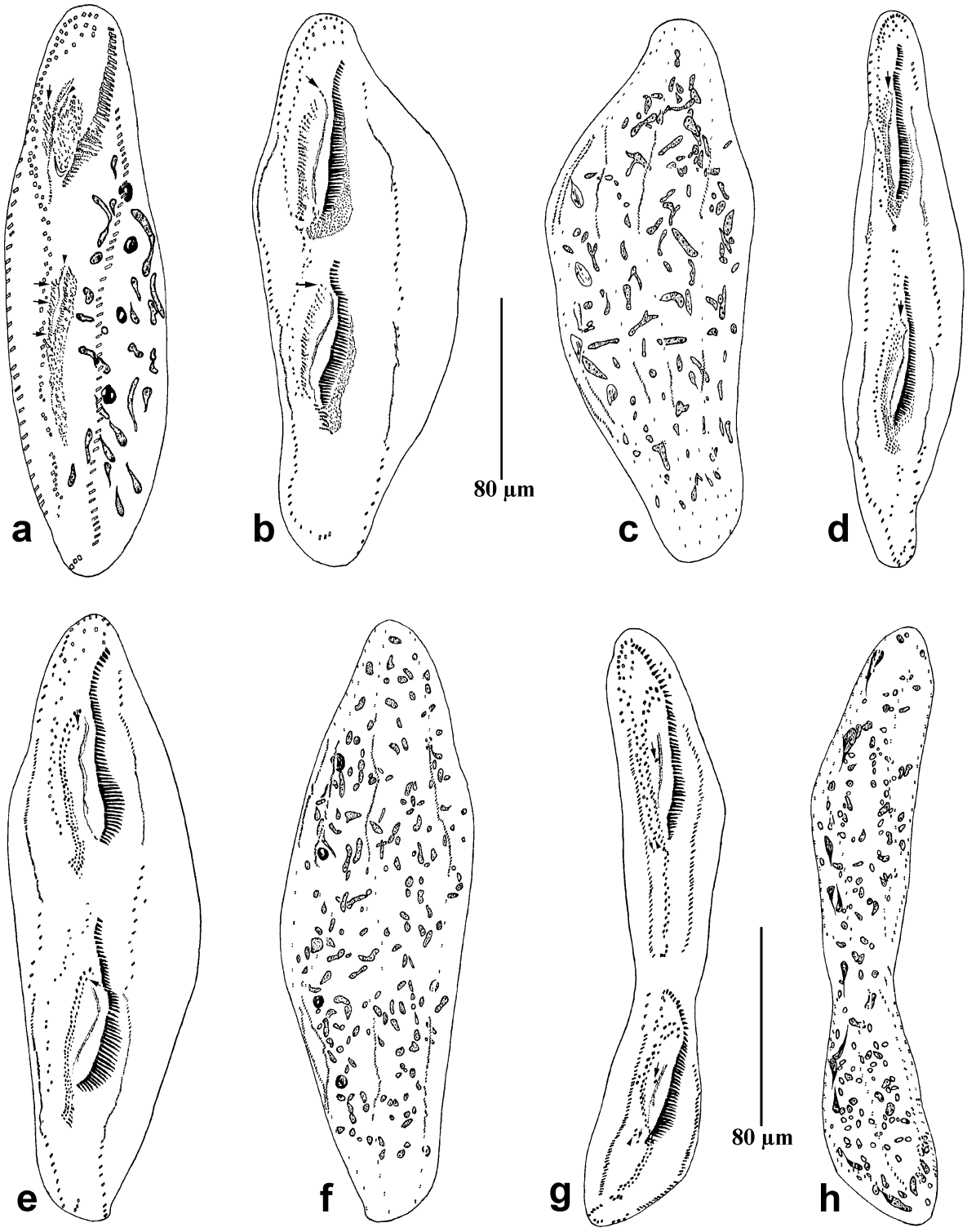

Figs. 2a-h. Middle and late stages of morphogenesis in *Pseudokeronopsis rubra* from protargol impregnated specimens; **a** - ventral view with partial macronuclear segments, arrows showing FMA, arrowheads indicating UMA; **b, c** - ventral and dorsal views of the same individual, arrows showing the first frontal cirrus from UMA; **d** - ventral view, arrows showing the first frontal cirrus from UMA; **e, f** - ventral and dorsal views of the same cell, arrows showing buccal cirri in both dividers; **g, h** - ventral and dorsal views of the same individual, long arrows indicating buccal cirrus, arrowheads showing the migration of cirri, short arrows marking additional cirri (probably to be absorbed lately). FMA - frontoterminal cirral anlagen, UMA - undulating membranes anlagen

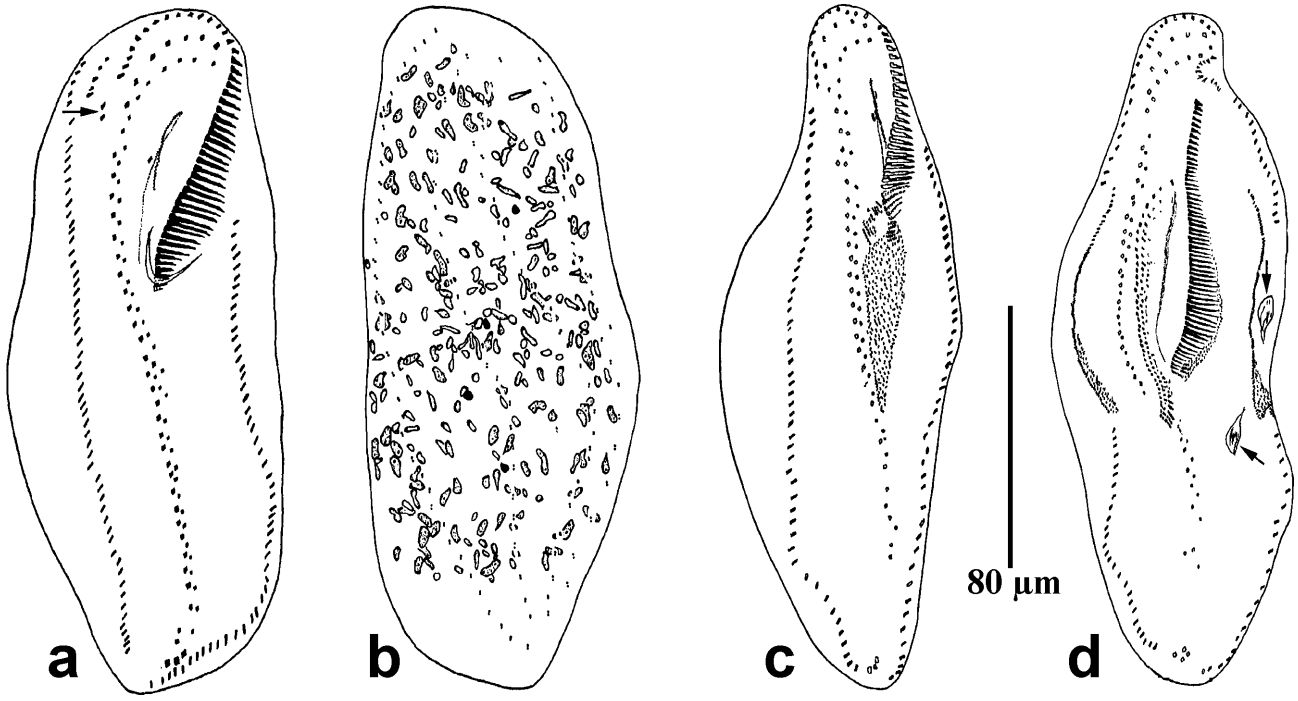

Figs. 3a-d. The daughter cell and regenerative stages of *Pseudokeronopsis rubra*. **a, b** - ventral and dorsal views of the same daughter cell, arrow showing FTC; **c, d** - different regenerative stages, arrows showing micronuclei. FTC - frontoterminal cirri

anarchic field, the new adoral membranelles gradually organize in a posteriad direction (Figs. 2b, d); simultaneously, UMA detaches and generates frontal cirrus at its anterior end (Figs. 2b, d; short arrow). As in the opisthe, FMA develop into FC, BC, MVC and TC (Figs. 2b, d, e, g).

3. Evolution of nuclear apparatus

In the process of evolution of macronuclei, a striking feature was apparently observed that the numerous (more than 100) macronuclear segments divide without prior fusion as in the description of Wirnsberger (1987). The micronuclei behave like those of other hypotrichs.

Reorganization morphogenesis (Figs. 3c, d)

Physiological regeneration normally takes place in well-fed cultures. Regenerator possesses only one set of primordium, which develops in the same way as in the opisthe, as showing in Figs. 3c, d and Figs. 12, 13. However, the old adoral membranelles dedifferentiate and the old undulating membranes are reabsorbed. Now, it is uncertain that the basal bodies from the old AZM join in the forming of new adoral membranelles in reorganization, but the new adoral membranelles replace the old AZM completely.

DISCUSSION AND CONCLUSION

Pseudokeronopsis remains one of the most compound taxa because of the overlapping of many morphological characters, including body form, cell color and the wide range of variation of the dorsal kineties (Foissner 1982, Wirnsberger *et al.* 1987).

According to the descriptions by Foissner (1984), Borror and Wicklow (1983) and Wirnsberger *et al.* (1987), we identified our form mainly because of slender body form, brick-red pigment and long midventral row. But Qingdao-population differs from other populations described previously in the presence of blood cell-like cortical granules and the low number of TC and DK (Table 1).

The color of the cell is still an arguable feature: e.g., at low magnification, cells seem dark red (or red-brown?), but the cortical granules at high magnification are only reddish. So it is evidently a character which is

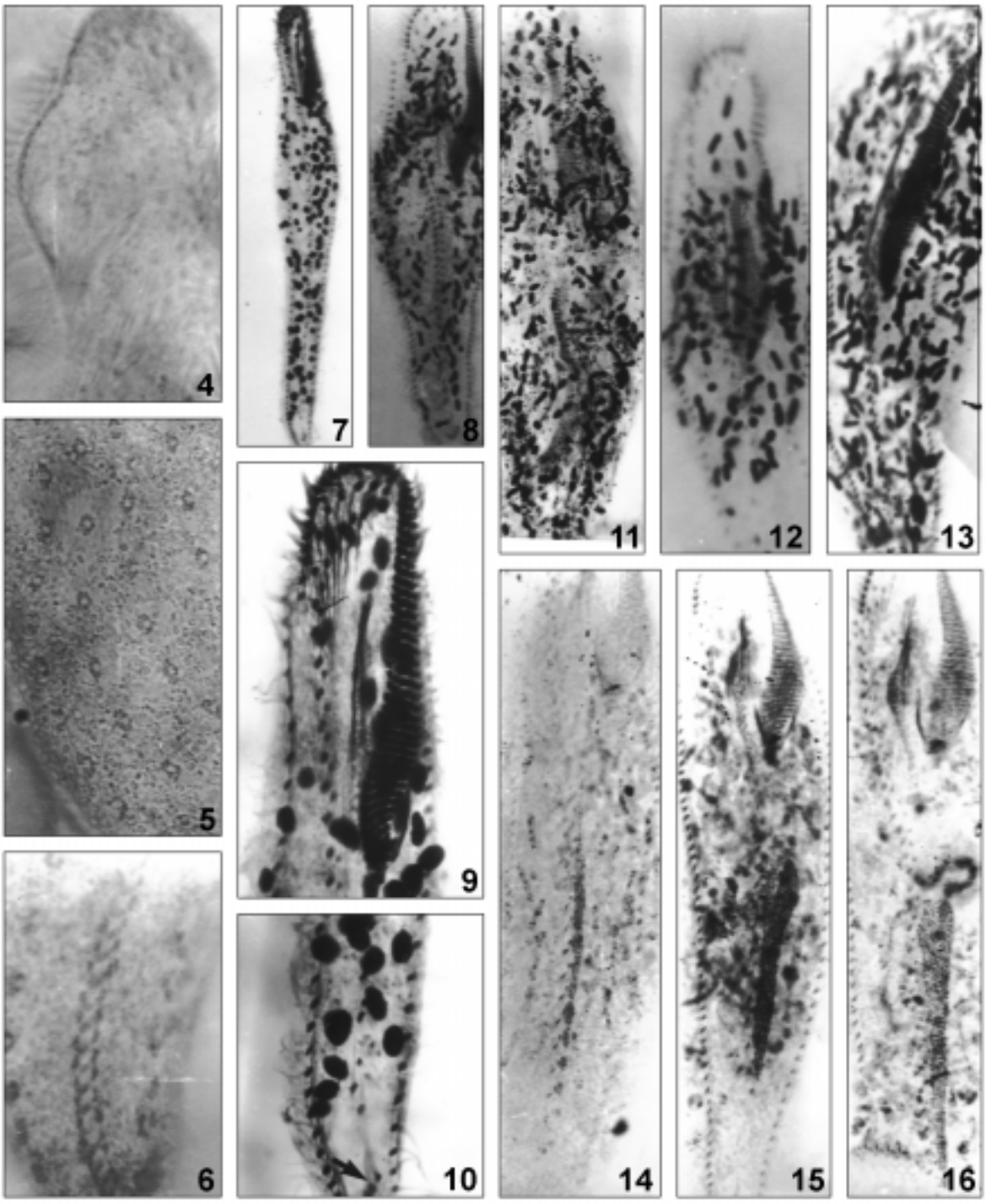

Figs. 4-16. Micrographs of morphology, morphogenesis and reorganization in *Pseudokeronopsis rubra*. **4** - anterior view, showing undulating membranes; **5** - portion of dorsal view, marking rosettes and cortical granules; **6** - posterior view, indicating pigments arrays along the base of cirri; **7, 8** - ventral views of different cells, showing infraciliature; **9** - ventral view in the anterior area of the same individual as in Fig. 7, showing oral apparatus; **10** - ventral view in the posterior region of the same individual as in Fig. 7, arrow marking transverse cirri; **11** - ventral view of a middle stage in morphogenesis, showing the forming of both AZM and new cirri; **12, 13** - showing ventral views of two reorganization stages; **14-16** - early stages of morphogenesis, indicating the development of AP and the dedifferentiating of the old AZM

highly dependent on the author's observations and description, i.e. it is likely less reliable than respected for species identifications.

Another thing resulting in confusion is the number of DK. In most hypotrichs, the number of DK is rather constant but *Pseudokeronopsis* seems to be very variable even within the same population (Table 1), which probably indicates a strong generic and ecological radiation of this taxon (Wirnsberger *et al*. 1987). We agree with Wirnsberger *et al.* (1987) that the population studied by Foissner (1984) could be *P. carnea* rather than *P. rubra* because of low number of midventral cirri and orange-red color.

While in divisional morphogenesis, the Qingdao population of *P. rubra* exhibits the following characteristics:

(1) Complete replacement of the old AZM in the proter by newly-built structures, as described in *P. carnea*, *P. rubra*, *P. ignea* by Wallengren (1901), Wirnsberger (1987) and Mihailowitsch and Wilbert (1990) respectively.

(2) Independent occurring of FMA and AMP (Wirnsberger 1987), unlike that in *P. carnea*, *P. pulchra* and *P. ignea*, in which FMA and AMP join together posteriorly.

(3) The joined sets of primordia in the opisthe, which is in accordance with observation in the opisthe of *P. rubra* by Wirnsberger (1987).

(4) A peculiar dividing behavior of the macronuclei, like in other congeners, a few haptorids, a scuticociliate and the heterotrich genus *Protocruzia* (Raikov 1982), in which the macronuclear segments will not confuse into a spherical macronucleus before asexual division. According to Raikov (1982), this character is probably very important in evolution (Wirnsberger 1987). However, the whole morphogenetic process distinctly shows the partial confusion of macronuclear segments before cytogenesis, which seems to signify some kind of phylogenetic relationship among urostylid genus.

(5) The parental basal bodies do not participate in the forming of ciliary structures of daughter cells, which is confirmed by Wirnsberger (1987) and different from other urostylids, in which fronto-ventral-transverse cirri originate from left or right midventral cirri or from buccal and/or frontal cirri (Jerka-Dziadosz 1972, Jerka-Dziadosz and Janus 1972, Borror 1972, Wicklow 1981, Martin *et al*. 1981, Hemberger 1982, Wiąckowski 1985, Hu *et al*. 2000). The phenomenon of the non-involvement of the buccal cirrus is also known in the *Stylonychia mytilus* complex and *Kerona polymorphum* (Hemberger 1982, Hemberger and Wilbert 1982, Wirnsberger *et al*. 1986).

Acknowledgements This work was supported by the "National Science Foundation of China (project number 39770093) and the Cheung Kong Scholars Program". We wish to extend our thanks to Dr. Zhang Daobo for collecting the sample. Many thanks are also due to Mr. Ma Hongwei for his kindly help in microphotographing.

REFERENCES

Borror A. C. (1972) Revision of the order Hypotrichida (Ciliophora, Protozoa). *J. Protozool.* **19:** 1-23

Borror A. C. (1979) Redefinition of the Urostylidae (Ciliophora, Hypotrichida) on the basis of morphogenetic characters. *J. Protozool.* **26:** 544-550

Borror A. C., Wicklow B. J. (1983) The suborder Urostylina Jankowski (Ciliophora, Hypotrichida): morphology, systematics and identification of species. *Acta Protozool.* **22:** 97-126

Ehrenberg C. G. (1835a) Bericht an die Versammlung am 19. 1. 1835. *Mittheilungen der Gesellschaft naturforschender Freunde zu Berlin, Jahr.* **1836:** 1-5

Ehrenberg C. G. (1835b) Zusätze zur Erkenntnis großer organischer Ausbildung in den kleinsten thierischen Organismen. *Abh. Königl Akad Wiss. Berlin Jahr*. **1937**: 151-180

Foissner W. (1982) Ökologie und Taxonomie der Hypotrichida (Protozoa: Ciliophora) einiger österreichischer Böden. *Arch. Protistenkd*. **126:** 19-143

Foissner W (1984) Infraciliatur, Silberliniensystem und Biometrie einiger neuer und wenig bekannter terrestrischer, limnischer und mariner Ciliaten (Protozoa: Ciliophora) aus den Klassen Kinetofragminophora, Colpodea und Polyhymenophora. *Stapfia* **12:** 1-165

Hemberger H. (1982) Revision der Ordnung Hypotrichida Stein (Ciliophora, Protozoa) an Hand von Protargolpräparaten und Morphogenesedarstellungen. Diss. Univ. Bonn

Hemberger H., Wilbert N. (1982) Revision der Familie Keronidae Dujadin 1840 (Ciliophora, Hypotrichida) mit einer Beschreibung der Morphogenese von *Kerona polymorphum* Ehrenberg, 1835. *Arch. Protistenkd.* **125:** 261-270

Hu X., Wang M., Song W. (2000) Morphogenetic studies on *Holosticha diademata* during asexual reproduction cycle. *J. Zibo Univ.* **2:** 78-81 (in Chinese with English summary)

Jerka-Dziadosz M. (1972) Cortical development in *Urostyla.* I. Comparative study on morphogenesis in *U. cristata* and *U. grandis*. *Acta Protozool.* **10:** 73-100

Jerka-Dziadosz M., Janus I. (1972) Localization of primordia during cortical development in *Keronopsis rubra* (Ehrenberg, 1838) (Hypotrichida). *Acta Protozool*. **10:** 249-262

Martin J., Fedriani C., Nieto J. (1981) Étude comparée des processus morphogénétiques d'*Uroleptus* sp. (Kahl, 1932) et de *Holosticha* (*Paruroleptus*) *musculus* (Kahl, 1932) (Ciliés, Hypotriches). *Protistologica* **17:** 215-224

Mihailowitsch B., Wilbert N. (1990) *Bakuella salinarum* nov. sp. und *Pseudokeronopsis ignea* nov. sp. (Ciliata, Hypotrichida) aus einem solebelasteten Fließgewaser des ostlichen Münsterlandes, BRD. *Arch. Protistenkd.* **138:** 207-219

Morgan W. D. (1926) Further observation on marine ciliate living in the laboratory tanks of Plymouth. *J. mar. boil. Ass. UK* **14:** 23-53

Raikov I. B. (1982) The Protozoan Nucleus. Morphology and Evolution. Cell Biol Monogr 9. Springer Verlag-Vienne et New York

Rühmekorf T. (1935) Morphologie, Teilung und Hungerformen von *Keronopsis*. *Arch. Protistenkd*. **85:** 255-288

Ruthmann A. (1972) Division and formation of the macronuclei of *Keronopsis rubra*. *J. Protozool.* **19:** 661-666

Wallengren H. (1901) Zur Kenntniss des Neubildungs-und Resorptionsprocesses bei der Theilung der hypotrichen Infusorien. *Zool. Jb. Anat*. **15:** 1-58

Wiąckowski K. (1985) The morphology and morphogenesis of *Keronella gracilis* n. gen., n. spec. (Hypotrichida, Ciliophora). *Protistologica* **21:** 81-91

Wicklow B. J. (1981) Evolution within the order Hypotrichida (Ciliophora, Protozoa): ultrastructure and morphogenesis of *Thigmokeronopsis jahodai* (n. gen., n. sp.), phylogeny in the Urostylina (Jankowski, 1979). *Protistologica* **17:** 331-351

Wilbert N. (1975): Eine verbesserte Technik der Protargolimpragnation für Ciliaten. *Mikrokosmos* **64:** 171-179

Wirnsberger E. (1987) Division and reorganization in the genus *Pseudokeronopsis* and relationships between urostylids and oxytrichida (Ciliophora, Hypotrichida). *Arch. Protistenkd*. **134:** 149-160

Wirnsberger E., Foissner W., Adam H. (1986) Biometric and morphogenetic comparison of the sibling species *Stylonychia mytilus* and *S. lemnae*, including a phylogenetic system for the oxytrichds (Ciliophora, Hypotrichida). *Arch. Protistenkd*. **132:** 167-185

Wirnsberger E., Larsen H. F., Uhlig G. (1987) Rediagnoses of closely related pigmented marine species of the genus *Pseudokeronopsis* (Ciliophora, Hypotrichida). *Europ. J. Protistol*. **23:** 76-88

Received on 28th September, 2000; accepted on 18th January, 2001

Acta Protozool. (2001) 40: 117 - 123

ACTA
PROTOZOOLOGICA

Presence of Myxosporidea (Myxozoa: Myxosporea) of the Genus *Henneguya* Thelohan, 1892 in Freshwater Fishes from Chad (Central Africa)

Boguyana KOSTOÏNGUE, Cheikhna DIEBAKATE, Ngor FAYE and Bhen Sikina TOGUEBAYE

Laboratory of Parasitology, Department of Animal Biology, Faculty of Sciences and Technologies, University C. A. DIOP of Dakar, Dakar, Senegal

Summary. Examination of some freshwater fishes from Chari and Logone rivers of Chad (Central Africa) revealed the presence of Myxosporidea species of the genus *Henneguya* Thelohan, 1892. They are: *H. auchenoglanii* sp. n. in *Auchenoglanis occidentalis* (Valenciennes, 1840) (Bagridae), *H. logonensis* sp. n. in *Citharinus citharus* (Geoffroy Saint-Hilaire, 1809) (Citharinidae), *H. mailaoensis* sp. n. in *Mormyrus cashive* (Linné, 1784) (Mormyridae), *H. massii* sp. n. in *Lates niloticus* (Linné, 1762) (Centropomidae), *H. mormyri* sp. n. in *Mormyrus cashive* (Linné, 1784) (Mormyridae) and *H. branchialis* Ashmawy, Abu-Elwafa, Imam and El-Otifi, 1989 in *Clarias anguilaris* (Linné, 1758) (Clariidae). All these species infected the gill filaments of their hosts and formed cysts.

Key words: Central Africa, Chad, freshwater fishes, *Henneguya auchenoglanii* sp. n., *Henneguya logonensis* sp. n., *Henneguya mailaoensis* sp. n., *Henneguya massii* sp. n., *Henneguya mormyri* sp. n., *Henneguya* species, Myxosporidea.

INTRODUCTION

Myxosporidea are frequently described in fish and have an importance in ichtyopathology (Sakiti *et al*. 1990, 1996; Diamant 1992; Lom and Dyková 1992; Fomena *et al*. 1993; Voronin and Chernysheva 1993; Eiras 1994). In Africa, about 135 species of these parasites are currently known to infect freshwater, brackish and marine fishes (Bahri and Marques 1996; Kpatcha *et al*. 1996a, 1996b, 1997, 1999; Fomena and Bouix 1997; Fall *et al*. 1997; Kabre *et al*. 1997; Kostoïngue *et al*. 1998, 1999; Diebakate *et al*. 1999; Faye *et al*. 1999; Sakiti *et al*. 1999). Up to date, amongst these species, only 13 *Henneguya* Thelohan, 1892 are described in freshwater fishes. In the present paper, we described new *Henneguya* species found during our investigations in freshwater fishes from Chad (Central Africa).

MATERIALS AND METHODS

The fishes studied were collected from Logone and Chari rivers near Ndjamena (Chad). These fishes belong to the genera *Auchenoglanis*, *Citharinus*, *Lates*, *Mormyrus* and *Clarias*. All measurements based on more twenty fresh spores, were made with an

Address for correspondence: Bhen S. Toguebaye, Department of Animal Biology, Faculty of Sciences and Technologies, University C. A. DIOP of Dakar, Dakar, Senegal; Fax: (221) 825 25 29 or 824 63 18; E-mail: parasito@ucad.refer.sn

eyepiece micrometer. Permanent preparations were fixed with methanol and stained with Giemsa. For scanning electron microscopy, spores were fixed with glutaraldehyde, dehydrated in ethanol, critical point dried and examined with a JEOL 35 CF scanning electron microscope.

RESULTS

The characteristics of *Henneguya* species found in freshwater fishes are as follows:

Henneguya auchenoglanii sp. n.

Type host: *Auchenoglanis occidentalis* (Valenciennes, 1840) (Bagridae).

Site of infection: primary gill lamellae.

Type locality: Chari River.

Prevalence: 36,8 % (21/57).

Type specimen: one slide deposited in the parasitological collection (N° Myxo-093), Department of Animal Biology, Faculty of Sciences and Technologies, University C.A. DIOP of Dakar, Senegal.

Etymology: the specific name is given after the generic name of the host.

Description: cysts were ovoid, and their length was 1 to 1.5 mm. They were located at the base of primary gill lamellae. The spore body (Figs. 1, 8) was lanceolate, elongated and measured 12.0 ± 0.40 (11-13) x 3.2 ± 0.14 (3-4) µm. The two tails were always fused and their length was 39.42 ± 0.8 (37-40). The total length of the spore was 56.4 ± 0.9 (52-58) µm. The two polar capsules were pyriform, elongated and of equal size: 6.3 ± 0.1 (6-7) x 2.1 ± 0.1 (2-3) µm. Their polar filament was not apparent. The sporoplasm was finely granular.

Discussion: up to date, 13 species of *Henneguya* have been previously described in freshwater fishes from Africa (Fomena and Bouix 1997, Kabre *et al*. 1997, Kostoïngue *et al*. 1999). These species are mentioned in the Table 1. It appeared that by the length of its spore, the present species is only similar to *H. fusiformis;* but it is distinct from this species by the length and shape of its spore body. Therefore, we consider it as a new species and name it *Henneguya auchenoglanii* sp. n. to remember the generic name of its type host.

Henneguya logonensis sp. n.

Type host: *Citharinus citharus* (Geoffroy) (Saint-Hilaire, 1809) (Citharinidae).

Site of infection: primary gill lamellae.

Type locality: Logone River.

Prevalence: 25.8 % (16/32).

Type specimen: one slide deposited in the parasitological collection (N° Myxo-094), Department of Animal Biology, Faculty of Sciences and Technologies, University C.A. Diop of Dakar, Senegal.

Etymology: the specific name relates to its type locality.

Description: cysts were ovoid, located on primary gill lamellae and their length was 0.5 to 1.5 mm. Spore body (Figs. 2, 7, 9) was oval with attenuated anterior end; its length and width was 12.03 ± 0.1 (11-13) x 3.2 ± 0,09 (3-4) µm. The length of caudal appendages was 22.5 ± 0.4 (20-25) µm and the total length of the spore was 34.6 ± 0.9 (33-37) µm. The polar capsules were pyriform and of unequal size. The big polar capsule measured 3.7 ± 0.09 (3-4) x 1.6 ± 0.09 (1-2) µm and the smaller measured 2.2 ± 0.08 (2-3) x 1.4 ± 0.09(1-2) µm. The polar filaments were not apparent and the sporoplasm was finely granular.

Discussion: amongst the *Henneguya* described in freshwater fishes from Africa, only spores of *H. nyongensis* and *H. clariae* resemble those of the present species by their morphology. However, *H. nyongensis* is distinct by the length of its polar capsule and *H. clariae* by the total length of its spores (Table 1). For these reasons, we think that the present species is new and we name it *Henneguya logonensis* sp. n. to remember the river where it was first found.

Henneguya mailaoensis sp. n.

Type host: *Mormyrus cashive* (Linné, 1784) (Mormyridae).

Site of infection: primary gill lamellae.

Type locality: Chari River.

Prevalence: 13.3 % (12/90).

Type specimen: one slide deposited in the Parasitological collection (N° Myxo-095), Department of Animal Biology, Faculty of Sciences and Technologies, University C.A. DIOP of Dakar, Senegal.

Etymology: the specific name is given after one village of Chad.

Description: cysts where ovoid, fixed on the primary gill lamellae and measured 0.5 to 1.5 mm. The spore body (Figs. 3, 10) was lanceolate, elongated and measured 17.6 ± 0.4 (15-18) x 5.7 ± 0.1 (5-6) µm. The two polar capsules were pyriform and equal size: 5.9 ± 0.33 (5-7) x 2.2 ± 0.09 (2-3) µm. Their polar filament was not apparent. The two caudal appendages were equal, separated from their base and had 44.5 ± 1.07 (41-46) µm in length. The total length of the spore was 61.7 ± 1.3 (58-63) µm.

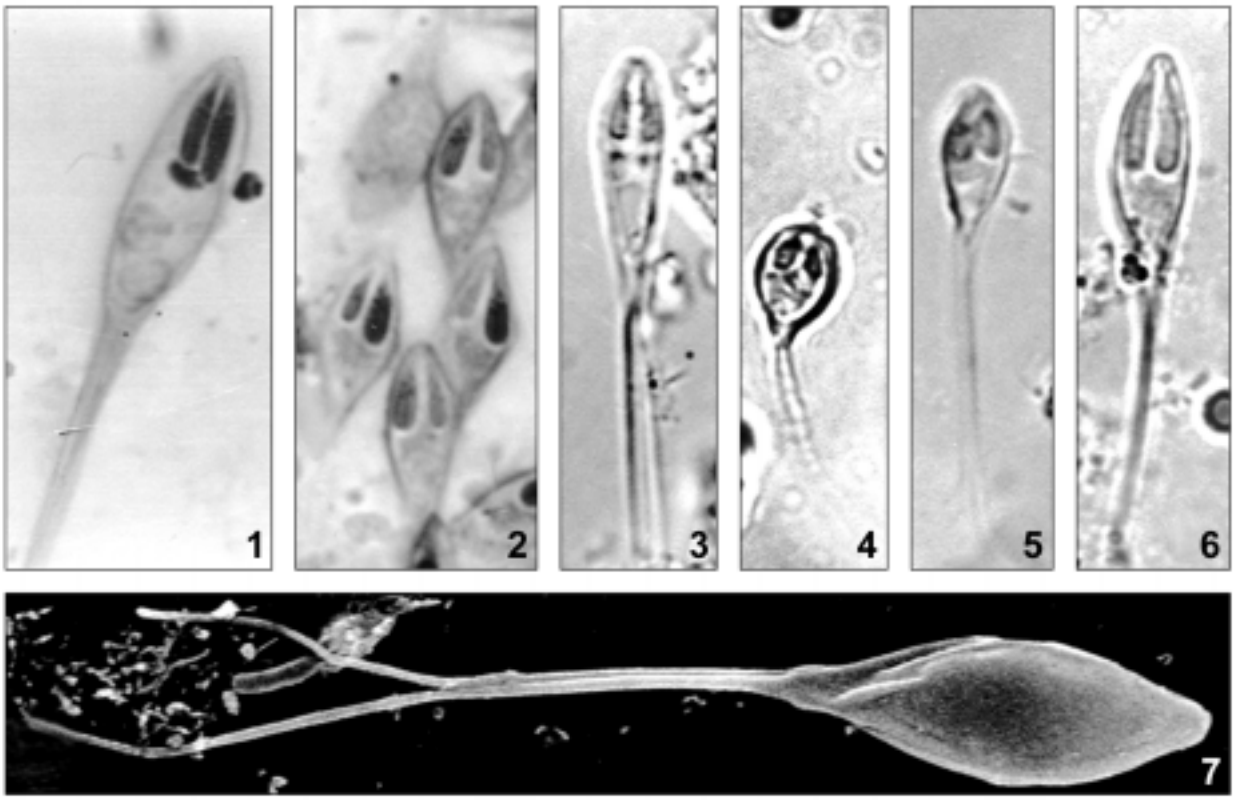

Figs. 1-7. Mature spores: **1** - *Henneguya auchenoglanii* sp. n. stained with Giemsa (x 1800); **2** - *Henneguya logonensis* sp. n. stained with Giemsa (x 1800); **3** - living *Henneguya mailaoensis* sp. n. (x 1800); **4** - living *Henneguya massii* sp. n. (x 1800); **5** - living *Henneguya mormyri* sp. n. (x 1800); **6** - living *Henneguya branchialis* (x 1800); **7** - *Henneguya logonensis* sp. n. in scanning electron microscope (x 5500)

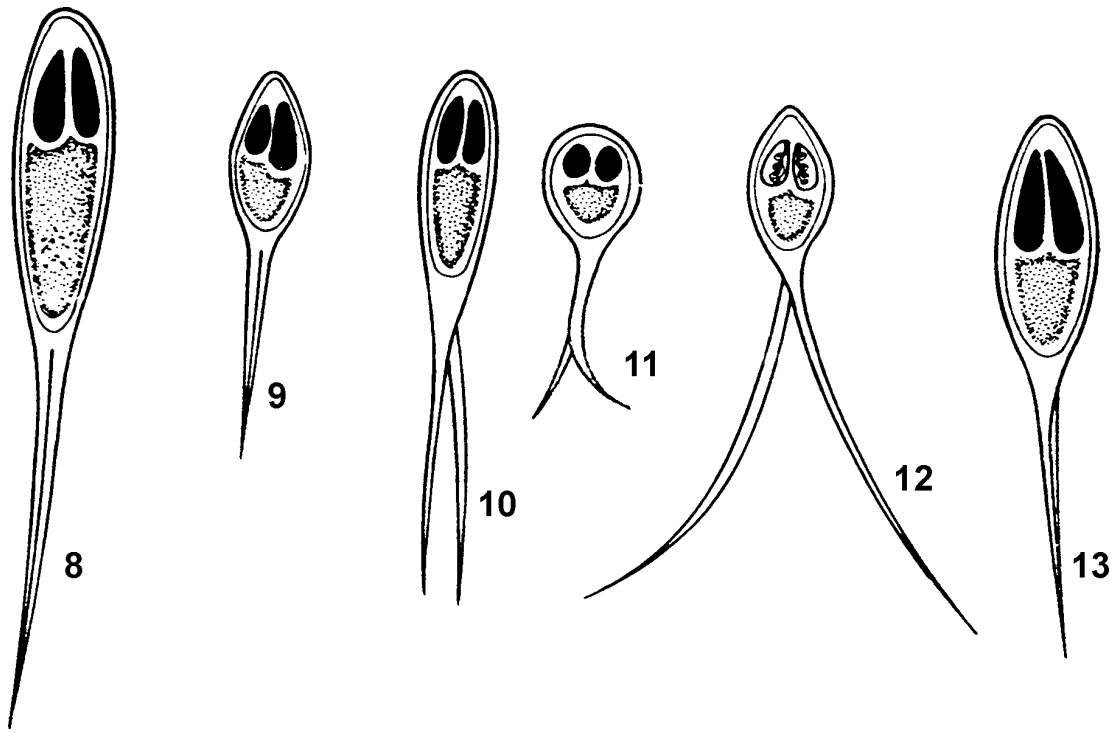

Figs. 8-13. Line drawing of mature spores: **8** - *Henneguya auchenoglanii* sp. n.; **9** - *Henneguya logonensis* sp. n.; **10** - *Henneguya mailaoensis* sp. n.; **11** - *Henneguya massii* sp. n., **12** - *Henneguya mormyri* sp. n.; **13** - *Henneguya branchialis.* Scale bar - 5 μm

Table 1. *Henneguya* species previously described in freshwater fishes from Africa. All measures in µm

Species	Hosts	Characteristics of spores	Sites of infections
H. bopeleti Fomena & Bouix, 1987	*Chrysichthys nigrodogitatus*	Spore body: ovoid, 15-19 x 5.5-7; polar capsules: pyriform, 7-9 x 1.5-2.5; caudal appendages: fused, 22.5-32; total length: 41-48	Gills
H. branchialis Ashmawy, Abu-Elwafa, Imam & El-Otifi, 1989	*Clarias lazera*	Spore body: anterior end pointed, 12.5-17.5 x 4.5-6.5; polar capsules: pyriform; 6-8.5 x 1.5-3; caudal appendages: separated, 15.5-23.5; total length: 28-41	Gills, intestine
H. camerounensis Fomena & Bouix, 1987	*Synondontis batesii, Utropius multitoeniatus*	Spore body: ovoid, 9-11 x 4-5.5µm; polar capsules: pyriform, 4.5-6.5 x 1-2; caudal appendages: fused, 4-11.5; total length: 13.5-21.5µm	Gills
H. chrysichthyi Obiekezie & Enyenihi, 1988	*Chrysichthys nigrodigitatus*	Spore body: fusiform, 13.5-16 x 4.5-6.5; polar capsules: unequal, pyriform, 4.5 –5.5 x 1-1.5 and 4-4.5 x 1.5-2; caudal appendages: unequal; total length: 27-32	Gills
H. clariae Abolarin, 1971	*Clarias lazera*	Spore body: ovoid, 17.5-28.5 x 5.5-8.5; polar capsules: pyriform, 5–13.5 x 2.5- 3.5; caudal appendages: fused; total length: 45-107	Gills
H. ctenopomae Fomena & Bouix, 1997	*Ctenopoma manum*	Spore body: ovoid, anterior end rounded, 13-17 x 8-10.5; polar capsules: pyriform, 5-5.5 x 2-3; caudal appendages: separated from their base, 2-10; total length: 17-25 µm	Gills
H. dini Kabre, Sakiti, Marques & Sawadogo, 1997	*Heterotis niloticus*	Spore body: elongated, 11-12 x 3-5; polar capsules: pyriform, 3-4 x 1-1.5; caudal appendages: separated from their base, 16-20; total length: 27-32 µm	Gills

Table 1. (contd.)

H. fusiformis Kostoïngue, Fall, Faye & Toguebaye, 1999	*Clarias anguilaris*	Spore body: fusiform, 29-33 x 5-7; polar capsules: pyriform, one located behind the other, 5-6 x 3-4; caudal appendages: separated, curved, 28-31; total length: 59-61 µm	Gills
H. laterocapsulata Obiekezie & Schmahl, 1993	*Clarias lazera* and *Heterobranchus bidorsalis* hybrid	Spore body: fusiform, 13.8-16 x 3.7-5.3; polar capsules: pyriform to flask-shaped, one displaced laterally, 4.1-5.3 x 2.2-3.0; caudal appendages: separated, curved, 15.2-20.2 total length: 29.0-36.2	Body
H. malapteruri Fomena & Bouix, 1997	*Malapterurus electricus*	Spore body: ovoid, anterior end rounded, 14-18 x 8.3-11; polar capsules: pyriform, 5-7.3 x 2.8-4; caudal appendages: separated, presence of bulge at the base, 24-36.5; total length: 42-53	Muscles and skin
H. ntemensis Fomena & Bouix, 1996	*Brienomyrus brachyistus*	Spore body: ovoid, 9-12 x 7-9; polar capsules: pyriform, 5-7 x 3-4; caudal appendages: sometimes fused, 3-10; total length: 12.5-17.5 µm	Kidney, spleen, gall-bladder wall
H. nyongensis Fomena & Bouix, 1996	*Marcusenius moorii*	Spore body: ovoid, anterior end pointed, 10-14 x 4.5-6.5; polar capsules: pyriform, with neck-like structure, 5.5-7 x 2-3; caudal appendages: filiform, separated from their base, 20-23.5; total length: 30.5-36.5	Gills, muscles
H. odzai Fomena & Bouix, 1996	*Marcusenius moorii*	Spore body: elongate, anterior end rounded, 13-16 x 3.5-4.5; polar capsules: pyriform, 3-5 x 1-1.5; caudal appendages: filiform, separated from their base, 15-21.5; total length: 29-36.5	Gills

Discussion: the morphology of some *Henneguya* species described in freshwater fishes from Africa resemble to that of the present species. It concerns: *H. auchenoglanii* sp. n., *H. branchialis*, *H. dini* and *H. bopeleti* (Table 1). However, all these four species are too small. For this reason, we think that the species described here is new and we name it *Henneguya mailaoensis* sp. n. to remember one village of Chad.

***Henneguya massii* sp. n.**

Type host: *Lates niloticus* (Linné, 1762) (Centhropomidae).

Site of infection: primary gill lamellae.

Type locality: Chari River.

Prevalence: 4.4 % (3/67).

Type specimen: one slide deposited in the Parasitological collection (N° Myxo-096), Department of Animal Biology, Faculty of Sciences and Technologies, University C.A. DIOP of Dakar, Senegal.

Etymology: the name is given after the Professor MASSI from the University of NDjamena (Chad).

Description: cysts were spherical, small (0,5-1 mm in diameter) and numerous on the primary gill lamellae. The spore body (Figs. 4, 11) was oval with rounded anterior and attenuated posterior ends. It measured 8.3 ± 0.1 (8-9) x 5.6 ± 0.1 (5-6) µm. The two caudal appendages were short, equal and well separated. They measured 13.6 ± 0.3 (12-14) µm. The two polar capsules were pyriform, small and measured 2.8 ± 0.09 (2-3) x 1.6 ± 0.05 (1-2) µm. The polar filaments were not apparent. The sporoplasm, finely granular, contained two typical nuclei when stained. The total length of spores was 22.2 ± 0.4 (20-23) µm.

Discussion: by its size, the present species is similar to *Henneguya ctenopomae* (Table 1). But it differs from this species by the length of its spore body and caudal appendages (Table 1). Paperna (1973) has reported *Henneguya latesi* in *Lates albertianus* from Ouganda without data on this species. Thus, we cannot compare it with our finding.

For all these reasons, we think that the present species is new and name it *Henneguya massii* sp. n. in honor to the Professor MASSI from University of Chad.

***Henneguya mormyri* sp. n.**

Type host: *Mormyrus cashive* (Linné, 1784) (Mormyridae).

Site of infection: primary gill lamellae.

Type locality: Chari River.

Prevalence: 10 % (6/60).

Type specimen: one slide deposited in the Parasitological collection (N° Myxo-097), Department of Animal Biology, Faculty of Sciences and Technologies, University C.A. DIOP of Dakar, Senegal.

Etymology: the name is given after the generic name of the type host.

Description: this species formed in primary gill lamellae numerous small and spherical cysts measuring 0.4 to 0.8 mm in diameter. The spore body (Figs. 5, 12) was oval with a pointed anterior end and measured 8.4 ± 0.09 (8-9) x 4.5 ± 0.09 (4-5) µm. The two polar capsules were pyriform, of equal size and measured 3.3 ± 0.09 (3-4) x 1.9 ± 0.08 (1-3) µm and had 3 to 4 filament coils. The sporoplasm was small. The two caudal appendages were equal, measured 23.1 ± 0.6 (23-25) µm and separated from their base. The total length of the spore was 32.2 ± 0.7 (30-34) µm.

Discussion: the present species is dissimilar to all species previously described in freshwater fishes from Africa (Table 1) because its small spore body. Taking into account this difference, the present species is considered as a new species and designated as *Henneguya mormyri* sp. n. after the name of its type host.

***Henneguya branchialis* Ashmawy, Abu-Elwafa, Imam and El-Otifi, 1989**

Host: *Clarias anguilaris* (Linné, 1958) (Clariidae).

Site of infection: primary gill lamellae.

Locality: Chari River.

Prevalence: 9,1 % (4/44).

Specimen: one slide deposited in the Parasitological collection (N° Myxo-098), Department of Animal Biology, Faculty of Sciences and Technologies, University C.A. DIOP of Dakar, Senegal.

Description: oocysts were ovoid, whitish and measured 1 to 2 mm. The spore body (Figs. 6, 13) was lanceolate, elongated with anterior end more or less blunt and measured 14.3 ± 0.5 (12-16) x 5.1 ± 0.2 (4-7) µm. The two polar capsules were equal, pyriform and measured 5.7 ± 0.6 (4-6) x 1.4 ± 0.2 (1-2) µm. The polar filaments were not apparent. The sporoplasm was finely granular. The length of the two caudal appendages, which are of equal size was 19.1 ± 0.9 (18-20) µm. The total length of the spore was 33.7 ± 0.8 (30-36) µm.

Discussion: amongst the *Henneguya* species described in freshwater fishes in Africa, only *Henneguya branchialis* presented characteristics resembling those of the present species (Table 1). Indeed, according to Kabre *et al*. (1997) which have also mentioned

H. branchialis in *Clarias anguilaris* from Burkina Faso, the morphometric characteristics of the spore of this species are: total length 34.4 ±1.34 (31-39); spore body length and width 13.45 ± 0.51 (12-16) x 5.01 ± 0.5 (4-7) µm; polar capsules length and width 5.7 ± 0.47 (4-6) x 1.35 ± 0.27 (16-20) µm; caudal appendages length 18.37 ± 1.27 (16-20). The sporal body is elongated, the polar capsules and the caudal appendages are equal in size. For all these reasons, we think that the present species is *H. branchialis*.

Acknowledgments. The investigation was supported by research grand from Third World Network of Scientific Organizations (TWNSO).

REFERENCES

Bahri S., Marques A. (1996) Myxosporean parasites of the genus *Myxobolus* from *Mugil cephalus* in Ichkeul lagoon, Tunisia: description of two new species. *Dis. Aquat. Org.* **27:** 115-122

Diamant A. (1992) A new pathogenic histozoic *Myxidium* (Myxosporea) in cultured gilt head sea bream *(Sparus aurata*). *Bull. Eur. Ass. Fish Pathol*. **12:** 64-66

Diebakate C., Fall M., Faye N., Toguebaye B.S. (1999) *Unicapsula marquesi* n. sp. (Myxosporea, Multivalvulida) parasite des branchies de *Polydactylus quadrifilis* (Cuvier, 1829) (Poisson, Polynemidae) des côtes sénégalaises (Afrique de l'Ouest). *Parasite* **6:** 231-235

Eiras J.C. (1994) Elementos de ictioparasitologia. Fundaçao Eng. Antonio de Almeida, Porto

Fall M., Kpatcha T. K., Diebakate C., Faye N., Toguebaye B. S. (1997) Observations sur des Myxosporidies (Myxozoa) du genre *Myxobolus* parasites de *Mugil cephalus* (Poisson, Téleostéen) du Sénégal. *Parasite* **2:** 173-180

Faye N., Kpatcha T. K., Diebakate C., Fall M., Toguebaye B. S. (1999) Gill infections due to myxosporean (Myxozoa) parasites in fishes from Senegal with description of *Myxobolus hani* sp. n. *Bull. Eur. Ass. Fish Pathol*. **19:** 14-10

Fomena A., Bouix G. (1997) Myxosporea (Protozoa: Myxozoa) of freshwater fishes in Africa: keys to genera and species. *Syst. Parasitol*. **37:** 161-178

Fomena A., Marques A., Bouix G. (1993) Myxosporidea (Myxozoa) of *Oreochromis niloticus* (Linnaeus, 1757) (Teleost, Cichlidae) in fish-farming pools at Melen (Yaoundé, Cameroon, Central Africa). *J. Afr. Zool*. **107:** 45-56

Kabre B. G., Sakiti N. G., Marques A., Sawadogo L. (1997) Presence of Myxosporeans (Myxozoa, Myxosporea) of the genus *Henneguya* (Thelohan, 1892) parasites of fishes caught in fisheries of Burkina Faso. *Bull. Eur. Ass. Fish Pathol*. **17:** 43-46

Kostoïngue B., Faye N., Toguebaye B. S. (1998) Nouvelles espèces de Myxosporidies des genres *Myxidium* Bütschli, 1882 et Myxobolus Bütschli, 1882 (Myxozoa, Myxosporea) chez des poissons d'eau douce du Tchad (Afrique Centrale). *J. Afr. Zool*. **112:** 249-259

Kostoïngue B., Fall M., Faye N., Toguebaye B. S. (1999) Three new myxosporidian (Myxozoa: Myxosporea) parasites of freshwater fishes from Chad (Central Africa). *Acta Protozool*. **38:** 323-326

Kpatcha T. K., Diebakate C., Toguebaye B. S. (1996a) Myxosporidies (Myxozoa, Myxosporea) des genres *Sphaeromyxa* Thelohan, 1892. *Myxidium* Bütschli, 1882, *Zschokkella* Aueubach, 1910, *Bipteria* Kovaljova, Zubtchenko & Krasin, 1983 et *Leptotheca* Thelohan, 1895 parasites des poissons des côtes sénégalaises (Afrique de l'Ouest). *J. Afr. Zool*. **110:** 309-317

Kpatcha T. K., Diebakate C., Faye N., Toguebaye B. S. (1996b) Quelques nouvelles espèces de Myxosporidies du genre *Ceratomyxa* Thelohan, 1895 parasites des poissons marins du Sénégal (Afrique de l'Ouest). *Parasite* **3:** 223-228

Kpatcha T. K., Faye N., Diebakate C., Fall M., Toguebaye B. S. (1997) Nouvelles espèces d'*Henneguya* Thelohan, 1895 (Myxozoa, Myxosporea) parasites des poissons marins du Sénégal: étude en microscopie photonique et électronique. *Ann. Sci. Nat. Zoologie, Paris* **18:** 81-91

Kpatcha T. K., Diebakate C., Faye N., Toguebaye B. S. (1999) Light and electron microscopic observations on *Kudoa boopsi* sp. n. (Myxosporea: Kudoidae), a gill parasite of *Boops boops* (Pisces: Teleostei: Sparidae) from Coasts of Senegal (West Africa). *Acta Protozool*. **38:** 317-321

Lom J., Dyková I. (1992) Protozoan Parasites of Fishes. *Development in aquaculture and fisheries science* **26**, Elsevier, Amsterdam

Obiekezie A. I., Schmahl G. (1993) *Henneguya laterocapsulata* Landsberg, 1987 (Myxosporea, Myxozoa) in cultured hybrid African catfish: ultrastructure of the parasite host interface. *Europ. J. Protistol*. **29:** 38-41

Paperna I. (1973) Occurrence of Cnidospora infections in freshwater fishes in Africa*. Bull. Instit. Fond. Afr. Noire, sér. A* **35:** 509-521

Sakiti G. N., Blanc E., Marques A., Bouix G. (1990) Pathology of protozoan parasites on the gill arches of cichlid fish in Benin (West Africa). *Bull. Eur. Assoc. Fish Pathol*. **10:** 81-83

Sakiti N., Tarer V., Jacquemin D., Marques A. (1996) Présence en Méditerranée occidentale d'une Myxosporidie histozoïque pathogène dans les élevages de la Daurade. *Sparus aurata* L. *Ann. Sci. Nat., Zool., Paris* **17:** 123-127

Sakiti N., Kabre G., Marques A., Dossou C. (1999) Gill diseases caused by Myxozoa in fishes of Inland waters of the south of Benin. *J. Euk. Microbiol*. **46:** 15A

Voronin V. N., Chernysheva N. B. (1993) An intracellular gill parasite as possible causative agent of mortality during swim-bladder inflammation in common carp, *Cyprinus carpio* L. *J. Fish Dis.* **16:** 609-611

Received on 6th June, 2000; accepted on 2nd January, 2001

Acta Protozool. (2001) 40: 125 - 130

ACTA
PROTOZOOLOGICA

Myxoproteus cheni sp. n. and *Sinuolinea mai* sp. n. (Myxosporea: Sinuolineidae) Parasitic in the Urinary Bladder of Marine Fish (*Thamnaconus septentrionalis* Gunther, 1877) from the Yellow Sea, off the Qingdao Coast of China

Yuanjun ZHAO[1,2] and Weibo SONG[1]

[1]Aquaculture Research Laboratory, Ocean University of Qingdao, Qingdao; [2]Animal Biology Research Laboratory, Chongqing Normal College, Chongqing, China

Summary. Two new species of myxosporeans (Myxosporea: Sinuolineidae), *Myxoproteus cheni* sp. n. and *Sinuolinea mai* sp. n., parasitized in marine fishes collected from the Yellow Sea, off the Qingdao coast of China, are described. Both species, including spores and plasmodia were found in the urinary bladder of the host, *Thamnaconus septentrionalis* Gunther, 1877. The diagnostic features of *Myxoproteus cheni* sp. n.: trophozoites monosporous or disporous; spore inversely pyramidal or triangular to subspherical with smooth surface, fine sutural line straight or slightly sinuous, 14.0 ± 0.8 (12.8-15.3) x 12.8 ± 1.3 (11.2-15.0) x 12.5 ± 1.5 (11.2-15.0) µm in size; two spherical polar capsules located anteriorly and conspicuously separated from each other, 3.6 ± 0.4 (3.2 - 4.2) µm in diameter; coelozic. *Sinuolinea mai* sp. n.: trophozoites disporous; spore body inversely pyramidal to spherical with smooth surface, sutural line highly sinuous, 22.4 ± 0.5 (21.7-23.0) x 19.5 ± 0.5 (18.8-20.2) µm in size; two spherical polar capsules located anteriorly and conspicuously separated from each other, 5.8 ± 0.4 (5.0-6.3) µm in diameter; coelozic.

Key words: marine fishes, *Myxoproteus cheni* sp. n., Myxozoa, *Sinuolinea mai* sp. n., Sinuolineidae, *Thamnaconus septentrionalis*, urinary bladder.

INTRODIUCTION

Protozoan parasites from the Yellow Sea have never been paid attention until recently, although enormous development of commercial fish farming has been taking place in this region in last decades (Meng Qingxian 1996, Zhao and Song 1999, Zhao *et al.* 2000). In view of the recognized pathogenicity inflicted by many protozoan fish parasites on commercial and aquarium fish, it is desirable to obtain data on protozoa infecting fish in this region.

During the recent investigations on the fauna of protozoan parasites from marine fishes off the coast of the Yellow Sea, some myxosporean parasites were found. Among those, compared with their known congeners, some organisms obtained are believed to be new members of the family Sinuolineidae. This communication brings description of two new myxosporean species of the genera *Sinuolinea* and *Myxoproteus* from a

Address for correspondence: Yuanjun Zhao, Laboratory of Protozoology, College of Fisheries, Ocean University of Qingdao, 266003 Qingdao, P. R. China; Fax: +86 532 203 2283; E-mail: protozoa@ouqd.edu.cn

marine fish, *Thamnaconus septentrionalis* Gunther, 1877.

MATERIALS AND METHODS

The host fish *Thamnaconus septentrionalis* Gunther, 1877 was obtained on two occasions in March to July, 1998 and April to June, 1999 in coastal water of the Yellow Sea off the Qingdao (Tsingtao), China. All body organs were examined in fresh mounts, and myxosporeans were observed and measured in fresh state. Preparations of parasites were studied from air-dried smears stained with Giemsa (1:20) after fixation in absolute methanol. The mixture of glycerin - ethyl alcohol 70% - formalin (G. : A. : F. = 12 : 108 : 5) was used to show the morphological structure of mature spores and immature spores as well as the plasmodia. All specimens were observed and measured at magnification of x 1250. Illustrations were drawn with the aid of camera Lucida and computer program Photoshop 5.0.

RESULTS AND DISCUSSION

Myxoproteus cheni sp. n. (Figs. 1-7)

Diagnosis: Trophozoites monosporous or disporous; spore inversely pyramidal or triangular to subspherical with smooth surface, sutural line fine straight or slightly sinuous, 14.0 ± 0.8 (12.8-15.3) × 12.8 ± 1.3 (11.2-15.0) x 12.5 ± 1.5 (11.2-15.0) μm in size; two spherical polar capsules located anteriorly and conspicuously separated from each other, 3.6 ± 0.4 (3.2 - 4.2) μm in diameter; coelozic.

Dedication: this species is named after Professor Chen Qiliu (Chen Chihleu), who kindly instructed the first author and who is Protozoologist and Myxosporologist of Institute of Hydrobiology, Academy of Sciences, to express our respects.

Trophozoites: early stage of sporogonic pseudo- plasmodia small and irregular in shape, with hyaline ectoplasmic layer, about 16.5 x 13.5 μm in size (Fig. 1); late stage of plasmodia with developing mono- and di-spore, which measure 25.9-86.7 x 15.9-56.7 μm in size; *in vivo* cells usually possessing two or three filament-shaped pseudopodia at both poles like amoeba (Figs. 1, 7).

Spore: inversely pyramidal or triangular to subspherical with smooth surface and straight or slightly curved sutural line; two spherical polar capsules set well apart; one binucleated sporoplasm in the spore cavity. Neither iodinophilous vacuole in sporoplasm nor mucous envelope around spore observed.

Host: *Thamnaconus septentrionalis* Gunther, 1877.

Site of infection: urinary bladder cavity.

Locality: coastal waters of Qingdao (36° 08' N, 120° 43' E) of the Yellow Sea, China.

Prevalence: one of 10 fish examined was infected (10%).

Ecological features: salinity about 32‰, water temperature 11-12°C.

Date of sampling: 1998. 5. 25, 1999. 5. 23.

Pathogenicity: unknown.

Type-specimens: syntypes on slide No. qd-19980525, deposited to the Laboratory of Protozoology, College of Fisheries, Ocean University of Qingdao, Qingdao, China.

Taxonomic affinities

Class: Myxosporea Bütschli, 1881

Order: Bivalvulida Schulman, 1959

Family: Sinuolineidae Schulman, 1959

Genus: *Myxoproteus* Doflein, 1898

Doflein (1898) established *Myxoproteus* firstly, then Davis (1917) emended its diagnostic characterization. Up to now, 18 species were described (Thelohan, 1895; Doflein, 1898; Davis, 1917; Fantham *et al*., 1940; Schulman, 1953, 1966; Kabata, 1962; Yoshino and Noble, 1973; Yoshino and Moser, 1974; Evdokimova, 1977; Moser and Noble, 1977; Sankurathri, 1977; Kovaleva and Gayevskaya, 1979, 1982; Kovaleva, 1989; Wierzbicka, 1986; Sarkar, 1996), and majority of them always live in the urinary bladder and urinary system of marine fishes, except *M. ambiguum* (Thelohan, 1895) Doflein, 1898 and *M. myoxocephali* Fantham *et al.,* 1940 in the gall bladder of marine fishes. Species of this genus share the following characters: spore inversely pyramidal, triangular to spherical in sutural view with rounded outline; anterior end broad and more or less truncated; straight or slightly sinuous sutural line; thick-walled shell with or without projections; two spherical polar capsules well apart; binucleated sporoplasm; trophozoites mono- and disporic (Kudo 1920, Schulman 1966, Lom and Dyková 1992).

In the light of the morphologically similar forms, following species should be compared with our species: *Myxoproteus elongatus* Schulman, 1953, *M. meridionalis* Evdokimova, 1977, and *M. cujaeus* Sarkar, 1996. *M. elongatus* differs from our form in having elongated inversely pyramidal spore, smaller size in width (6.0-7.0) and in thickness (7.0-8.5) of spores as well as relatively smaller diameter of polar capsules (2.0-3.5). *M. meridionalis* appears distinctly different

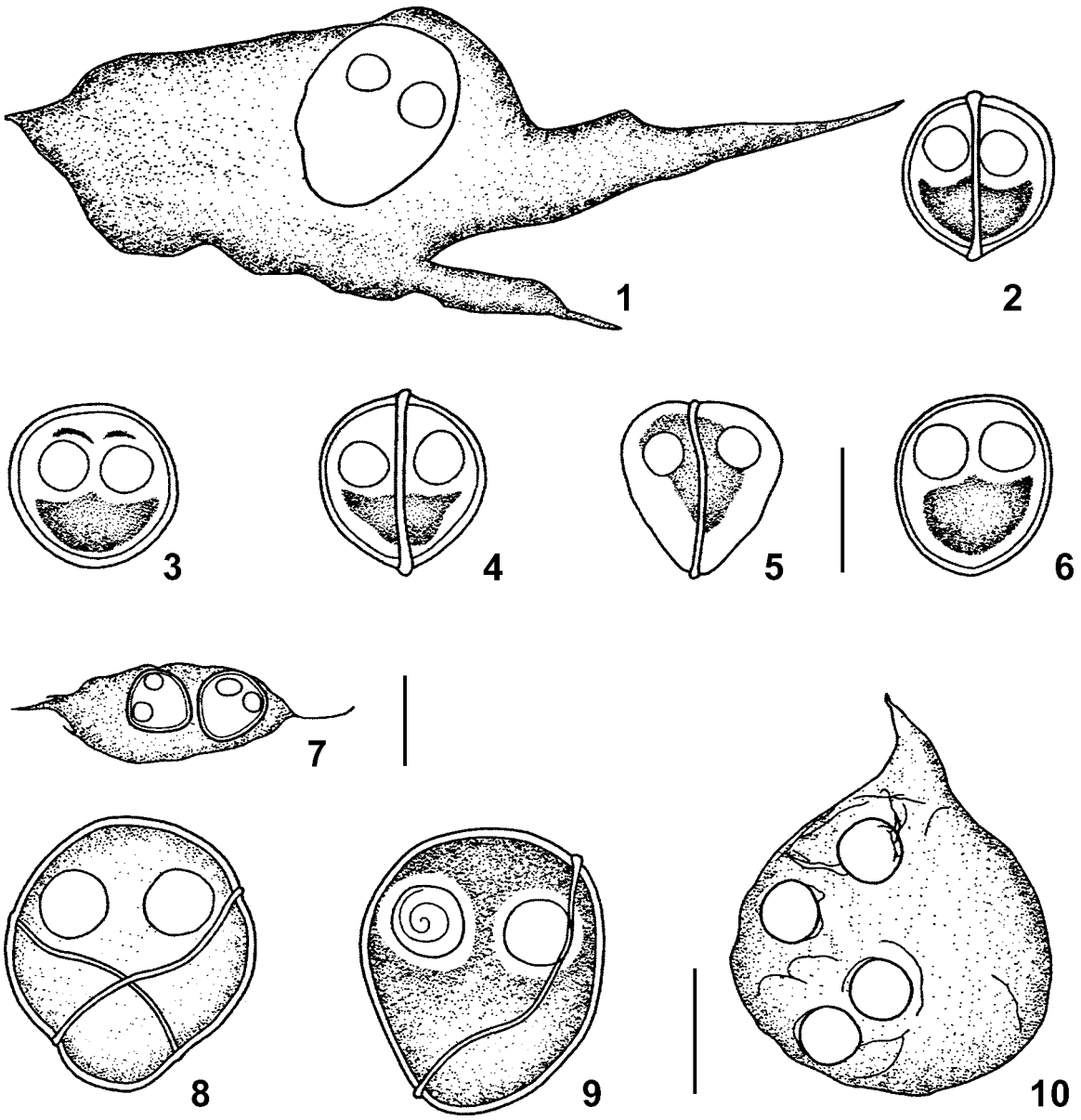

Figs. 1-10. Illustrations of *Myxoproteus cheni* sp. n. and *Sinuolinea mai* sp. n. **1-7**- *Myxoproteus cheni* sp. n. **1**- plasmodium with one developing spore; **2, 4, 5** - mature spore from lateral view; **3, 6** - mature spore from oblique view. **7** - plasmodium with two developing spores. **8-10** - *Sinuolinea mai* sp. n. **8, 9** - mature spore from lateral view; **10** - plasmodium with two early-stage spore. Scale bars - 10 μm (**1-6, 8-10**), 20 μm (**7**)

from our species in bearing ellipsoidal spores and smaller width of spore (8.0-9.3). *M. cujaeus* can be distinguished by possessing strongly sinuous sutural line and smaller spores (9.0-12.0 x 8.0-10.0). Our new species is distinguished by the following combined features: A) larger dimension of spore (12.8-15.3 x 11.2-15.0); B) inversely pyramidal or triangular to spherical and C) straight or slightly sinuous sutural line. Furthermore, all these 4 species are from different hosts and regions: *M. elongatus* from *Anarhichas lupus* Linnaeus, 1758 and *Licichthys deuyiculatus* of Barents Sea, White Sea; *M. meridionalis* in *Merluccius hubbsi* Marini,

Table 1. Comparison of the related species of *Myxoproteus* Doflein, 1898 with *Myxoproteus cheni* sp. n. L - length; W - width; T - thickness; D - diaminter (all in μm)

Species	Host	Locality	Localization	Shape of spore	Size of spore	Size of PC[a]	Data resource
Myxoproteus cheni sp. n.	*Thamnaconus septentrionalis*	The Yellow Sea, China	Urinary bladder	Inversely pyramidal or triangular to spherical	L: 14.0 ± 0.8 (12.8-15.3)[b] W: 12.8 ± 1.3 (11.2-15.0) T: 12.5 ± 1.5 (11.2-15.0)	D: 3.6 ± 0.4 (3.2 - 4.2)	This study
M. elongatus Schulman, 1953	*Anarhichas lupus*; *Licichthys deuyiculatus*	Barents Sea; White Sea	Urinary bladder	Elongated pyramidal	L: 10.0-13.5 W: 6.0-7.0 T: 7.0-8.5	D: 2.0-3.5	Schulman, 1953
M. meridionalis Evdokimora, 1977	*Merluccius hubbsi*	Southwest Atlantic	Urinary bladder	Ellipsoidal	L: 10.0-11.0 W: 8.0-9.3	L: 3.3 W: 2.7	Evdokimora, 1977
M. cujaeus Sarkar, 1996	*Macrospinosa cuja*	West Bengal, India	Urinary bladder	Spherical	L: 10.5 ± 0.8 (9.0-12.0) W: 9.2 ± 0.8 (8.0-10.0)	D: 3.3 ± 0.4 (3.0-4.0)	Sarkar, 1996

[a] polar capsule; [b]Mean ± SD (Min-Max)

Table 2. *Sinuolinea mai* sp. n. Characteristics of spores found in filefish *Thamnaconus septentrionalis* compared with other *Sinuolinea* spp. L - length; W - width; D - diaminter (all in μm)

Species	Spore size	Polar capsule size	Pseudoplasmodium size	Infection locus	Host	Locality	Data resource
Sinuolinea mai sp. n.	L: 22.4 ± 0.5 (21.7-23.0) [a] W: 19.5 ± 0.5 (18.8-20.2)	D: 5.8 ± 0.4 (5.0 - 6.3)	L: 29.4 W: 25.3	Urinary bladder	*Thamnaconus septentrionalis*	The Yellow Sea, China	This study
S. dimorpha	D: 15.0	D: 4.5	L: 57.0 W: 90.0	Urinary bladder	*Cynoscion regalis*	Beaufort region, U.S.A.	Davis, 1917
S. triangularta	D: 14.0-15.0	D: 5.0-6.5	D: 20.0	Urinary bladder	*Sphaeroides vermicularis*	Sea of Japan	Schulman, 1966
S. magna	D: 19.0-30.0	D: 5.0-7.5	-	Urinary bladder	*Coryphaenoides acrolespis*; *C. pectoralis*	Southern California, U.S.A.	Yoshino and Noble, 1973
S. indica	D: 10.0-13.5	D: 3.0-4.0	L: 20.0-25.0 W: 13.5-17.0	Urinary bladder	*Pseudosciaena coibor*	Hooghly estuary, West Bengal, India	Sarkar, 1997

[a] Mean ± SD (Min-Max)

1932 of southwest Atlantic; *M. cujaeus* Sarkar, 1996 from *Macrospinosa cuja* Ham. in West Bengal, India; *M. cheni* sp. n. from *Thamnaconus septentrionalis* Gunther, 1877 of the Yellow Sea, China (Table 1).

***Sinuolinea mai* sp. n. (Figs. 8-10)**

Diagnosis: trophozoites disporous; spore body inversely pyramidal to spherical with smooth surface, sutural line highly sinuous, thin and slender suture ridge, 22.4 ± 0.5 (21.7-23.0) x 19.5 ± 0.5 (18.8-20.2) μm in size; two spherical polar capsules located anteriorly and conspicuously separated from each other, 5.8 ± 0.4 (5.0-6.3) μm in diameter; coelozic.

Dedication: this species is named after Professor Ma Chenglun, who is Parasitologist and Myxosporologist in the Department of Biology, Chongqing Normal College.

Trophozoites: early stage of plasmodium not observed; late stage drop-like or comma-shaped; *in vivo* cells usually possessing one pseudopodium like amoeba (Fig. 10), always with disporous plasmodium, which measures 29.4 x 25.3 μm.

Spores: body of mature spores inversely pyramidal to subspherical in shape from sutural view; sutural line very sinuous and twisted on its axis (Figs. 8, 9); shell valves thin-walled with smooth surface; spore cavity with binucleated mass of sporoplasm which is often finely granulated; two polar capsules spherical or subspherical, about equal size and located anteriorly far away from each other (Figs. 8, 9); neither iodinophilous vacuole in sporoplasm nor mucous envelope around spore to spot.

Host: *Thamnaconus septentrionalis* Gunther, 1877

Site of infection: urinary bladder.

Locality: coastal waters off Qingdao (36° 08' N, 120° 43' E) of the Yellow Sea, China.

Prevalence: one of 10 fish examined was infected (10%).

Ecological features: salinity about 32‰, water temperature 11-13°C.

Date of sampling: 1998.6.11; 1999.5.23.

Pathogenicity: not apparent.

Type-specimens: one slide as holotype (No. qd-19980611) is deposited in the Laboratory of Protozoology, College of Fisheries, Ocean University of Qingdao, Qingdao, China.

Taxonomic affinities

Class: Myxosporea Bütschli, 1881
Order: Bivalvulida Schulman, 1959
Family: Sinuolineidae Schulman, 1959
Genus: *Sinuolinea* Davis, 1917

Davis (1917) established *Sinuolinea*, in which the spores are spherical or subspherical with 2 nearly spherical polar capsules, and sutural line forms a prominent sinuous ridge around the spore. Since then 15 species were identified (Davis, 1917; Basikalowa, 1932; Tripathi, 1948; Shulman, 1953, 1966; Yoshino and Noble, 1973; Gayevskaya and Kovaleva, 1979; Karatayev and Iskov, 1984, 1985; Ibrahimov, 1988; Moser, Kent and Dennis, 1989; El-Matbouli and Hoffmann, 1994; Sarkar, 1997). All species live in the marine fishes, except *Sinuolinea tetraodoni* El-Matbouli and Hoffmann, 1994.

According to the spore shape, four species, *Sinuolinea dimorpha* Davis, 1917, *Sinuolinea triangularis* Shulman, 1966, *Sinuolinea indica* Sarkar, 1997 and *Sinuolinea magna* Yoshino & Noble, 1973 show similarity with the present species. However, the spores of *S. dimorpha* (Sp. 15.0 μm, Pc. 4.5 μm), *S. triangularis* (Sp. 14.0-15.0 μm, Pc. 5.0-6.5 μm), *S. indica* (Sp. 12.0 μm, Pc. 3.0-4.0 μm) exhibit clear difference in the dimension of spores and the polar capsule from *S. mai* (Sp. 21.7-23.0 x 18.8-20.2 μm, Pc. 5.0-6.3 μm). With reference to dimension, the spore of *S. magna* shows similarity to that of our form, the former is, however, distinctly different from the latter in the shape of spore (spherical), and sutural ridge (thick and strong). In addition, the 4 species mentioned above are obtained from different hosts and regions (Table 2).

Two new species of *Sinuolineidae myxosporean* described in this paper, are from the same host, but they really differ from each other in shape and size of spore. Especially, they have different sutural line, sutural line strongly sinuous in the spore of *S. mai* and sutural line fine straight or slightly sinuous in the spore of *M. cheni*. In view of such differences, the two myxosporeans species are considered as two new species relatively.

Acknowledgements. This work was supported by the "Cheung Kong Scholars Programme", the Scientific and Technological Research Foundation of Chongqing Education Committee (No. 960300) and Chongqing Science and Technology Committee.

REFERENCES

Basikalowa A. (1932) Data on the parasitological studies on Murmansk fish. *Sb. Nauchno-Promysl. Rabot na Murmane, Snabtekhizdat*, 136-153 (in Russian) (not seen in original.)

Davis H. S. (1917) Myxosporidia of the Beaufort region: A systematic and biological study. *Wash.Bull.US Bur. Fish.* **35:** 201-243

Doflein F. (1898) Studien zur Naturgeschichte der Protozoa. III.Über Myxosporidien. *Zool. Jahrb. Abt. Anat.* **11:** 281-350

El-Matbouli M. Hoffmann. R. W. (1994) *Sinuolinea tetraodoni* n. sp.: a myxosporean parasite of freshwater pufferfish *Tetraodon palembangensis* from Southeast Asia - light and electron microscope observations. *Dis. Aquat. Org.* **19:** 47-54

Evdokimova E. B. (1977) Miksosporidii kostistyh ryb Patagonskogo selfa (Atlanticeskoe pobereze Argentiny). *Parazitologiya* **11:** 166-178 (in Russian)

Fantham H. B. Ported A., Richardson L. R. (1940) Some more myxosporidia observed in Canadian fishes. *Parasitology* **32:** 333-353

Gayevskaya A. V., Kovaleva A. A. (1979) New and really encountered species of myxosporidian from the Celtic Sea. *Parazitologiya* **13:** 159-165 (in Russian)

Ibrahimov Sh. R. (1988) A new species of Myxosporea from the gall bladder of *Syngnathus nigrolineatus* Caspian Sea. *Parazitologiya* **22:** 246-247

Kabata Z. (1962) Five new species of myxosporidia from marine fishes. *Parasitology* **52:** 177-186

Karatayev A. K., Iskov M. P. (1984) New myxosporidia species from Black Sea sand-smelt, *Atherina mochon pontica*. *Vest. Zool.* **1:** 59-60 (in Russian with English summary)

Karatayev A. K., Iskov M. P. (1985) *Sinuolinea markevitshi* Karatayev & Iskov nom. n. pro *S. schulmani* Karatayev & Iskov 1984. *Vest. Zool.* **1:** 85 (in Russian)

Kovaleva A. A. (1989) New genus of myxosporidian family Myxoproteidae (Cnidospora, Myxosporea) from the north-western Atlantic. *Zool. Zh.* **68:** 130-132

Kovaleva A. A., Gaevskaya A. V. (1979) Two new species of Myxosporidia of the genus *Myxoproteus* from the Celtic Sea fishes. *Parazitologiya* **13:** 437-439 (in Russian)

Kovaleva A. A., Gaevskaya A. V. (1982) New data on Myxosporidia from the south-western Atlantic fishes. *Parazitologiya* **16:** 353-359 (in Russian)

Kudo R. R. (1920) Studies on myxosporidia. A synopsis of genera and species of myxosporidia. *Ill. Biol. Mongr*. **5:** 1-265

Lom J., Dyková I. (1992) Protozoan Parasites of Fishes. *Development aquaculture and fisheries science* **26,** Elsevier, Amsterdam

Meng Qingxian (1996) Diseases of maricultured animal. Aquaclture Press of China, Beijing, 108-109 (in Chinese)

Moser M. E., Noble E. R. (1977) Three genera of myxosporida (Protozoa) in macrourid fishes. *Int. J. Parasitol.* **7:** 93-96

Moser M., Kent M., Dennis D. (1989) Gall bladder Myxosporea in coral reef fishes from Heron Island, Australia. *Aust. J. Zool.* **37:** 1-13

Sankurathri C. S. (1977) *Conispora renalis* gen. nov. et sp. nov. (Myxosporidia: Wardiidae) from the kidney tubules of pacific hake *Merlucius productus* (Ayres 1855), in coastal waters of British Colubia. *Can. J. Zool*. **55:** 1147-1150

Sarkar N. K. (1996) *Zschokkella pseudosciaena* sp. n. and *Myxoproteus cujaeus* sp. n. (Myxozoa: Myxosporea) from sciaenid fish of Hooghly estuary, West Bengal, India. *Acta Protozool*. **35:** 331-334

Sarkar N. K. (1997) *Sinuolinea indica* sp. n. (Myxosporea: Sinuolineidae) parasitic in the urinary bladder of a sciaenid fish from the Hooghly estuary, West Bengal, India. *Acta Protozool*. **36:** 305-309

Shulman S. S. (1953) New and little known Myxosporidia from the White Sea. *Zool. Zh.* **32:** 384-393 (in Russian)

Shulman S. S. (1966) Myxosporidia of the USSR. Nauka Publs., Moscow-Leningrad (in Russian)

Thelohan P. (1895) Recherches sur les Myxosporidies. *Bull. Sci. Fr. Belg.* **26:** 100-394

Tripathi Y. R. (1948) Some new myxosporidia from Plymouth with a proposed new classification of the order. *Parasitology* **39:** 110-118

Wierzbicka J. (1986) *Paramyxoproteus reinhardti* gen. n. et sp. n. (Bivalvulidea, Myxospora), a parasite of *Reinhardtius hippoglossoides* (Walbaum, 1792). *Acta Protozool.* **25:** 227-234

Yoshino T. P., Noble E. R. (1973) Myxosporida of macrourid fishes from southern California and Mexico. *J. Parasitol.* **59:** 844-850

Yoshino T. P., Moser M. (1974) Myxosporidia (Protozoa) in macrourid fishes (*Coryphaenoides* spp.) of the northeastern Pacific. *J. Parasitol.* **60:** 655-659

Zhao Y., Song W. (1999) Redescription of *Thelohanellus kitauei* Egusa & Nakajima, 1981 (Myxosporea: Thelohaneliidae), parasitic in marine fishes from the Yellow Sea, China. *The Yellow Sea* **5:** 73-76

Zhao Y., Ma C., Song W. (2000) Description of two new species of *Parvicapsula* Shulman, 1953 (Myxosporea: Parvicapsulidae) parasitic in the urinary bladder of marine fishes, *Paralichthys olivaceus* and *Kareius bicoloratus*, from the coast of the Yellow Sea, China. *Acta Protozool.* **39:** 157-162

Received on 12th August, 2000; accepted on 18th December, 2000

Acta Protozool. (2001) 40: 131 - 140

ACTA
PROTOZOOLOGICA

Two New Species of *Mantoscyphidia* Jankowski, 1980 (Ciliophora: Peritrichia), Gill Symbionts of *Haliotis* Linnaeus, 1758 (Mollusca: Archaeogastropoda) from the South Coast of South Africa

Heléne BOTES, Linda BASSON and Liesl L. VAN AS

Department of Zoology and Entomology, University of the Orange Free State, Bloemfontein, South Africa

Summary. Surveys carried out from 1995 to 1999 at the De Hoop Nature Reserve along the south coast of South Africa revealed the presence of scyphidiid peritrichs of the genus *Mantoscyphidia* Jankowski, 1980, occurring in abundance on the gills of *Haliotis spadicea* Donovan, 1808 and *H. midae* Linnaeus, 1758. These species differ from all the known *Mantoscyphidia* species with respect to morphology of the body and nuclear apparatus and are therefore described as two new species, *Mantoscyphidia spadiceae* sp. n. and *Mantoscyphidia midae* sp. n.

Key words: ectosymbiont, *Mantoscyphidia spadiceae* sp. n., *Mantoscyphidia midae* sp. n., marine mollusc, sessiline ciliophoran, scyphidiid peritrich.

INTRODUCTION

Fifteen *Mantoscyphidia* species have so far been found associated with freshwater and marine gastropod hosts. Four are from freshwater: *M. physarum* (Lachmann, 1856) from *Physa*; *M. limacina* (Lachmann, 1856) from *Planorbis*; *M. inclinata* (Lom & Corliss, 1968) from *Cincinnatia* and *M. capitis* (Boitsova, 1976) from an unknown host. The 11 known marine species of *Mantoscyphidia* are the following: *Mantoscyphidia patellae* (Hutton, 1878) from *Patella argentea*; *M. lusitana* (Cuénot, 1891) *emend* Jankowski, 1985 from *Patella vulgata*; *M. fischeri* (Vayssiére, 1885) from *Truncatella truncatula*; *M. littorinae* (Issel, 1918) from an unknown host; *M. hydrobiae* (Kahl, 1933) from *Hydrobia*; *M. ubiquita* (Hirshfield, 1949) from *Acmaea pelta*; *M. acanthophora* (Fish & Goodwin, 1976) from *Gibbula umbilicalis*, *M. bengalensis* (Jamadar & Choudhury, 1988) from *Cerithidea cingulata*; *M. branchi* Van As, Basson & Van As, 1998 from *Patella barbara*; *M. marioni* Van As, Basson & Van As, 1998 from *Nacella delesserti* and *M. fanthami* Basson, Botha & Van As, 1999 from *Oxystele variegata*.

Address for correspondence: Linda Basson, Department of Zoology and Entomology, University of the Orange Free State, PO Box 339, Bloemfontein, 9300, South Africa; Fax: (+2751) 448 8711; E-mail: Bassonl.nw@mail.uovs.ac.za

Surveys of two species of *Haliotis* collected at localities on the south coast of South Africa revealed the presence of two different scyphidiid peritrichs of the genus *Mantoscyphidia*, occurring in abundance on gills of the hosts. The two scyphidiids differ from all known *Mantoscyphidia* species with respect to general body morphology, characteristics of the nuclear apparatus, and host preference and are described here as new species.

MATERIALS AND METHODS

South African haliotids, i.e. *Haliotis spadicea* (venus ears) and *H. midae* (perlemoen) were collected from infratidal pools on the rocky shore and from an abalone aquaculture facility. A total of 225 haliotids were collected from the De Hoop Nature Reserve and from an Abalone Farm at Danger Point near Gansbaai, and examined during March and April over a five-year period from 1995 to 1999.

Haliotids were taken to a field laboratory where body dimensions and mass of the specimens were measured. Gills were dissected, placed on a microscope slide, smeared and examined using a compound microscope. Live specimens of scyphidiid peritrichs were observed to determine body contractility, position of contractile vacuoles and nuclei. Photomicrographs were taken of live specimens in various stages of contraction, for the purpose of measuring body dimensions.

Additionally, wet smears were fixed in Bouin's fluid, and transferred to 70% ethanol. In some cases, they were returned to the laboratory in Bloemfontein for further processing and, in other cases, hematoxylin staining was done in the field laboratory. Mayer's and Harris' Hematoxylin were used to stain the nuclear apparatus and for measuring body dimensions. The details of the infundibulum were studied by staining Bouin's-fixed smears with Protargol, using a combined method as described in Lee, Hunter and Bovee (1985) and Lom and Dyková (1992).

For scanning electron microscopy (SEM), gills were fixed in concentrations of 4 % and 10 % buffered, neutral formalin. In some cases, gills were fixed in Parducz and in 2.5 % glutaraldehyde. In the laboratory in Bloemfontein, the specimens were cleaned by washing gills in tapwater, dehydrated in a series of ethanol concentrations, and critical-point dried. Gills bearing ciliophorans were mounted on stubs, sputter coated with gold, and studied at 5kV and 10kV, using a JOEL WINSEM JSM 6400 scanning electron microscope.

For measurements of live specimens, minimum and maximum values are given, followed in parentheses by the arithmetic mean, standard deviation and number of specimens measured. Measurements based on Bouin's fixed specimens stained with hematoxylin are presented in square brackets. Body length was measured from the scopula to the epistomial disc and body diameter at the widest part of the body. Both macronuclear and micronuclear lengths were measured from adoral to aboral. Description of pellicular striations are from specimens viewed by SEM. The type material is in the collection of the National Museum, Bloemfontein, South Africa.

RESULTS AND DISCUSSION

Mantoscyphidia spadiceae sp. n. (Figs. 2-9)

Type host and locality: *Haliotis spadicea* Donovan, 1080, on gills; De Hoop Nature Reserve, south coast of South Africa (34°28'S, 20°30'E)

Type specimens: holotype, slide 97/04/05-04c (NMBP 235) in the collection of the National Museum, Bloemfontein, South Africa, Paratypes, slides 97/04/07-17 (NMBP 236), 98/04/05-06b (NMBP 237), hematoxylin stained, in the collection of the authors.

Etymology: named after the South African venus ear or siffie, *Haliotis spadicea*, on which the scyphidiid peritrichs occur.

Description

Body cylindrical, widening toward peristome (Figs. 2, 3, 7), extremely contractile. Peristomial disc ranging in shape from flattened to arched, with broad lip (Figs. 4, 6, 7) depending on body contraction. Very prominent peristomial apex (Figs. 4, 7). Body length 70-140 (104.3 ± 21.1, 43) [82-134 (100 ± 12.7, 47)], body diameter 20-40 (31.2 ± 6.7, 43) [26-60 (42 ± 6.5, 47)]. Scopula small (Figs. 3, 7), length 5-15 (9.9 ± 1.7, 43) [1-24 (10.3 ± 6.1, 47)], diameter 20-40 (31.7 ± 7.1, 43) [19-45 (30.2 ± 5.1, 47)].

Pellicular striations in expanded individuals (Figs. 3, 6) approximately 0.3µm apart, adorning whole body, including peristome (Figs. 5, 6) and scopula. Striations evenly spaced and uniform. Bifurcated pattern of striations found in some individuals on body and scopula. Bottom half of peristomial lip with uniform striation pattern in expanded specimens, upper half showing irregular pattern (Figs. 5, 6). Edge of peristome indistinct in contracted individuals, with striations forming a zig-zag pattern (Fig. 6). Trochal band consisting of seven or eight closely associated striations, forming slight elevations (Figs. 2, 3). Pellicular area between trochal band and scopula forming 5-8 elevations depending on degree of contraction.

Adoral zone describing one and one-half turns, about 540° (Figs. 4, 6), before plunging into infundibulum (Fig. 9). Row of pores located between ciliary spiral and peristomial lip (Fig. 6). Buccal apparatus as follows: haplo- and polykinety starting almost at same point, first three kinetosomes of polykinety barren. Haplo- and polykinety divided by pellicular ridge or comb, approximately same width as a kinetosome (Fig. 6). Polykinety

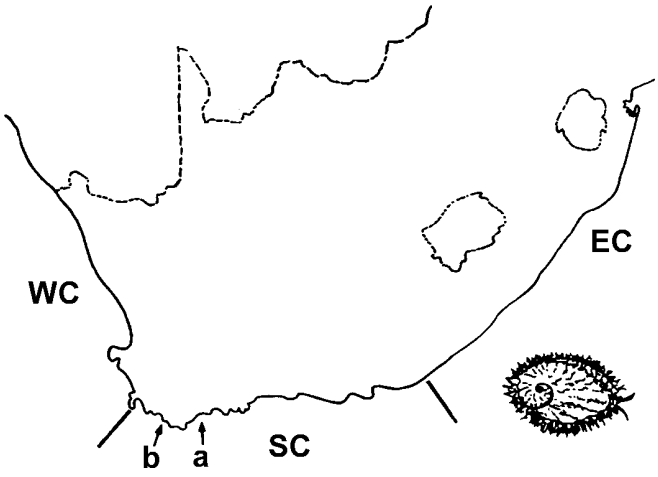

Fig. 1. Map of southern Africa showing the collection localities along the South African coastline. EC - East Coast, SC - South Coast, WC - West Coast, a - De Hoop Nature Reserve, b - Gansbaai

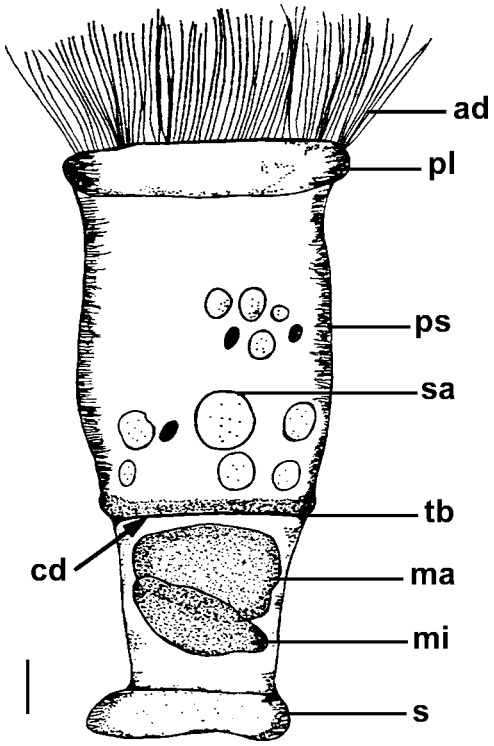

Fig. 2. Microscope projection drawing of *Mantoscyphidia spadiceae* sp. n. occurring on the gills of *Haliotis spadicea* Donovan, 1808, collected from the De Hoop Nature Reserve, South Africa. ad - adoral ciliary spiral, cd - cytoplasmic discontinuity, ma - macronucleus, mi - micronucleus, pl - peristomial lip, ps - pellicle striations, s - scopula, sa - symbiotic algae, tb - trochal band. Scale bar - 10 μm

three kinetosomes wide. Polykinety separates infundibular polykinetids after entering infundibulum (Fig. 9). Haplokinety makes one-half turn (180°), enters infundibulum beyond point at which polykinety enters. Fibrillar structure associated with polykinety. Inside infundibulum, polykinety makes one half turn (180°), haplokinety makes less than one half turn (<180°) before reaching cytostome (Fig. 9). Cytostome not always clearly visible.

Cytoplasm homogenous to granular (Figs. 2, 7, 8). Contractile vacuole present, mostly in adoral third of body. Symbiotic algae occasionally found in cytoplasm, always adoral to trochal band, varying in number and size.

Nuclear apparatus occupies most of area below trochal band (Figs. 2, 7, 8). Discontinuity of cytoplasmic material (Figs. 2, 7) above nuclear apparatus, separating nuclear apparatus from rest of cytoplasm. Nuclear apparatus consists of single, large, spherical to ovoid macronucleus, length 10-25 (19.3 ± 3.4, 30) [11-27 (16.8 ± 3.9, 47)], diameter 20-40 (28.3 ± 5.8, 30) [17-38 (25.8 ± 4.4, 47)] and single, smaller, ovoid micronucleus, length 10-20 (10.8 ± 2.2, 37) [3-15 (10.2 ± 2.2, 47)], diameter 15-40 (22.2 ± 5.6, 37) [12-30 (21.1 ± 3.5, 47)]. Macronucleus adorally broad, tapering somewhat aborally, forming indentation occupied by micronucleus. The latter always situated aboral to macronucleus.

Remarks

Mantoscyphidia spadiceae is the third species of sessiline peritrich described from southern Africa and the first recorded from the genus *Haliotis* Linnaeus, 1758. It can be distinguished from the other species by differences in morphology of the nuclear apparatus, scopula and body shape.

Mantoscyphidia fischeri and *M. hydrobiae* have ribbon- and kidney-shaped macronuclei, respectively (Kahl 1933; and, see Table in Hirshfield 1949). It appears that *M. littorinae* has an oval to sausage-shaped macronucleus, situated in the aboral part of the body (Raabe 1952). *Mantoscyphidia acanthophora* has a C-shaped macronucleus (Fish and Goodwin 1976), which is situated, in the middle to adoral part of the body and a small scopula with cilia, the scopula of *M. spadiceae* also with short cilia, which are grouped together, with a form similar to that of *M. acanthophora*. In *M. branchi*, the scopula is broader with short densely grouped cilia (Van As *et al.* 1998). *Mantoscyphidia bengalensis* also has a small scopula but its macronucleus is conspicuous, cylindrical, and sometimes coiled (Jamadar and Choudhury 1988). In the forms with a coiled macronucleus, the macronucleus fills the entire

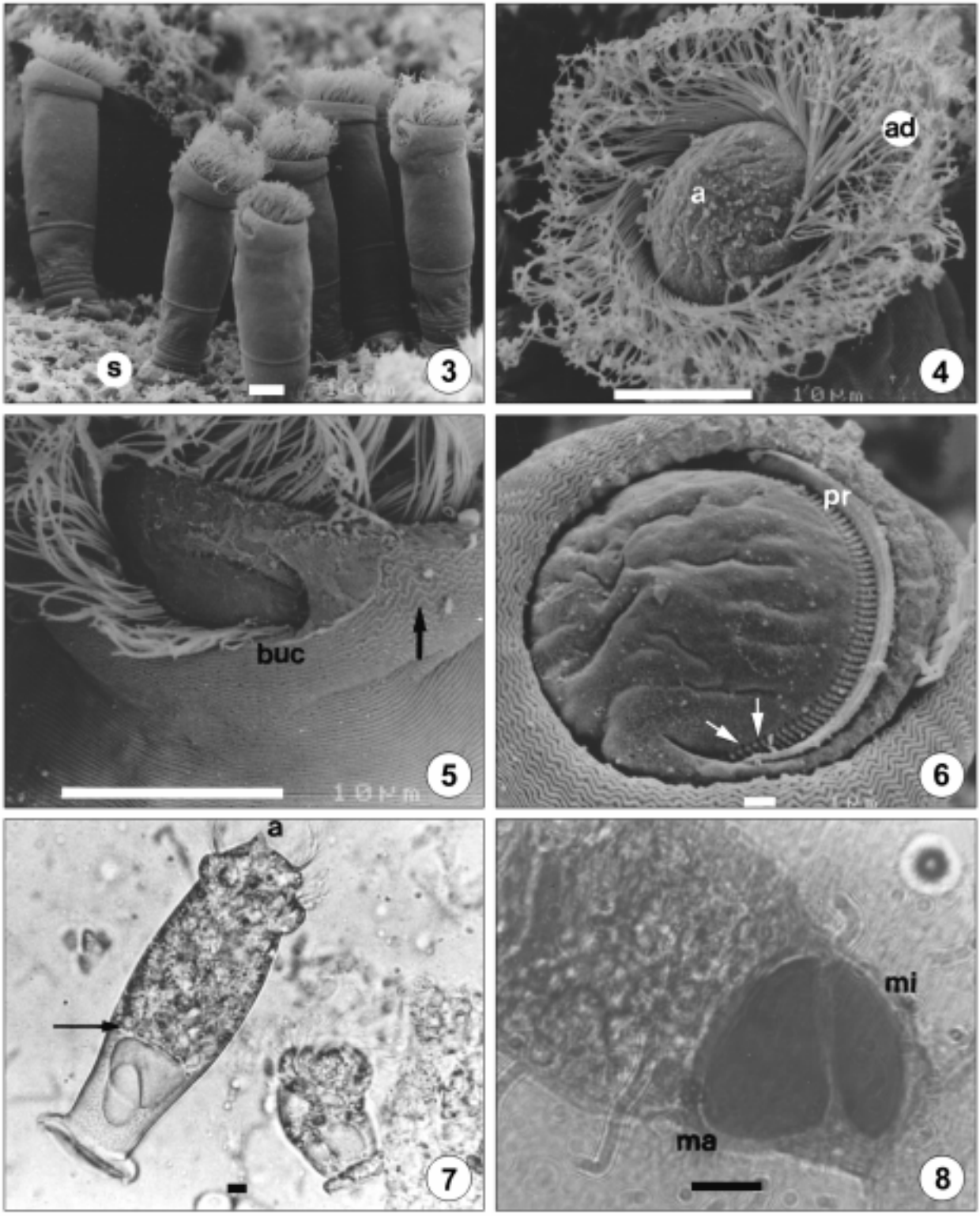

Figs. 3-8. Scanning electron micrographs (**3-6**) and photomicrographs (**7-8**) of specimens of *Mantoscyphidia spadiceae* sp. n. occurring on the gills of *Haliotis spadicea* Donovan, 1808, collected from the De Hoop Nature Reserve, South Africa. **3** - fully expanded specimens; **4** - body expanded, peristome arched; **5** - buccal cavity, uneven zig-zag striations indicated by arrow; **6** - adoral ciliary spiral with kinetosomes. Pores indicated by arrows; **7** - live specimen, discontinuity in cytoplasm indicated by arrow; **8** - hematoxylin stained specimen. a - apex, ad - adoral ciliary spiral; buc - buccal cavity; ma - macronucleus, mi - micronucleus, pr - pellicular ridge, s - scopula. Scale bars - 20 µm (**8**); 10 µm (**3, 4, 5,** 7); 1µm (**6**)

aboral region, and a small micronucleus is located close to the peristome.

In one population of *M. lusitana*, the macronucleus forms a band or is beaded (Cuénot 1891). Another population of *M. lusitana*, described by Madrazo-Garibay and López-Ochoterena (1988) from clams, has a horseshoe-shaped macronucleus adoral to the trochal band. *Mantoscyphidia ubiquita* has a sausage-shaped macronucleus, which is situated in the middle part of the body in expanded and partially contracted forms.

The position and shape of the nuclear apparatus of *M. fanthami* and *M. spadiceae* are similar, but *M. spadiceae* has a much larger macro- and micronucleus than those of *M. fanthami*. The scopula of *M. fanthami* is broader than its body (Basson *et al.* 1999), whilst in the case of *M. spadiceae,* it is as broad as the widest part of the body. As in the case of most of the species of *Mantoscyphidia*, except *M. littorinae*, constriction or narrowing is visible adoral to the scopula in *M. spadiceae*.

***Mantoscyphidia midae* sp. n. (Figs. 10-19)**

Type host and locality: *Haliotis midae*, Linnaeus, 1758, on gills; De Hoop Nature Reserve, south coast of South Africa (34°28'S; 20°30'E)

Type-specimens: holotype, slide 97/04/07-14 (NMBP 238) in the collection of the National Museum, Bloemfontein, South Africa, paratypes, slides 97/03/29-02 (NMBP 239), 97/03/29-09 (NMBP 240), hematoxylin stained, in the collection of the authors.

Etymology: named after the South African perlemoen *Haliotis midae*, on which the scyphidiid peritrichs occur.

Description

Body cylindrical (Figs. 10, 11, 16-18) narrowing toward peristome. Body length 65-150 (86.9 ± 15.9, 81) [81-110 (89.8 ± 8.8, 19)], body diameter 18-45 (28.3 ± 6.1, 81) [22-40 (29.8 ± 5.4, 19)] (Table 2). Peristomial disc ranging from flattened to arched, with broad lip (Figs. 11, 16, 17) where width depends on degree of body contraction. Peristomial apex prominent in expanded specimens (Figs. 16, 17). Scopula broad, flattened and prominent (Figs. 10, 13, 16), length 3-20 (9.1 ± 2.5, 81) [3-28 (10.3 ± 6.3, 19)], diameter 20-50 (34.5 ± 9, 81) [6-50 (32.6 ± 10, 19)].

Pellicular striations in expanded individuals approximately 0.25 µm apart (Figs. 14, 15), adorning whole body, including peristome and scopula. Striations evenly spaced and uniform. Bottom half of peristomial lip with uniform striation pattern in expanded specimens, upper half showing irregular pattern. In contracted individuals, edge of peristome indistinct with striations forming a zigzag pattern. Trochal band consists of four to eight closely associated striations (Table 3), forming slight elevations (Fig. 14). Warren (1991) refers to the trochal band as a slight constriction just above the scopular region of *Mantoscyphidia physarum*.

Adoral zone describes 450° (Fig. 12), before plunging into infundibulum (Fig. 19). Row of pores between ciliary spiral and peristomial lip present but not always prominent. Small buccal cavity. Buccal apparatus as follows: haplo- and polykinety starting almost at same point. Haplo- and polykineties divided by pellicular ridge or comb, approximately same width as a kinetosome. Polykinety three kinetosomes wide. Haplokinety plunges first into infundibulum (Fig. 19). Polykinety divides into infundibular polykinetids after plunging into infundibulum. Impregnable fibrillar structure associated with haplokinety. Both haplo- and polykinety make one turn (360°) inside infundibulum before reaching cytostome (Fig. 19). Cytostome not always clearly visible.

Cytoplasm granular (Figs. 10, 16-18). Contractile vacuole present, always in adoral part of body. Symbiotic algae (Figs. 10, 16, 17) found throughout cytoplasm, varying in number and size.

Nuclear apparatus situated aboral to trochal band, very close to scopula (Figs. 10, 18). Nuclear apparatus consists of single, large, round to ovoid macronucleus, length 10-25 (15.8 ± 4.4, 18) [9-31 (14.5 ± 5.7, 19)], diameter 13-30 (21.4 ± 5.3, 18) [13-41 (20.7 ± 7.3, 19)] and single, smaller, ovoid micronucleus, length 5-15 (8.1 ± 2.7, 25) [5-14 (7.5 ± 2.7, 19)], diameter 8-25 (13.6 ± 4.9, 25) [8-23 (12.8 ± 4.2, 19)]. Micronucleus always found aborally and closely associated with macronucleus. Macronucleus forming indentation, occupied by micronucleus. Nuclear apparatus appear to be surrounded by some granular cytoplasm and symbiotic algae (Figs. 10,16-18).

Remarks

Mantoscyphidia midae can be distinguished from the other species by differences in morphology of the nuclear apparatus, scopula and body.

Mantoscyphidia midae, M. marioni and *M. branchi* all have broad, prominent scopulas. *Mantoscyphidia midae* and *M. fischeri* have similar cylindrical body forms, but differ significantly in shape and location of the macronucleus. The latter has a sausage-shaped macronucleus situated in the adoral region of the body, compared to the macronucleus of *M. midae* that is compact

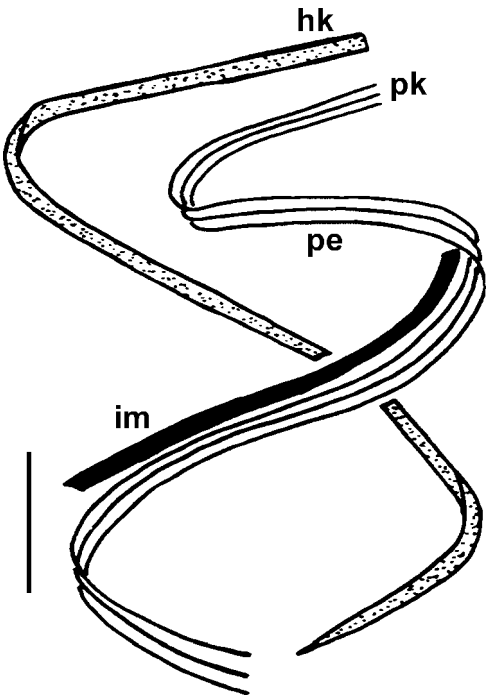

Fig. 9. Buccal infraciliature of *Mantoscyphidia spadiceae* sp. n. occurring on the gills of *Haliotis spadicea* Donovan, 1808, collected from the De Hoop Nature Reserve, South Africa. hk - haplokinety, im - impregnable band, pe - peniculus, pk - polykinety. Scale bar - 1 μm

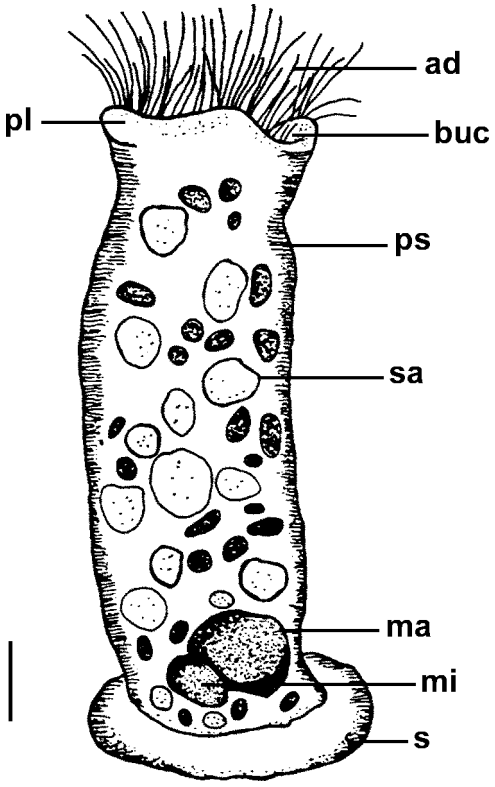

Fig. 10. Microscope projection drawing of *Mantoscyphidia midae* sp. n. occurring on the gills of *Haliotis midae* Linnaeus, 1758, collected from the De Hoop Nature Reserve, South Africa. ad - adoral ciliary spiral, buc - buccal cavity, ma - macronucleus, mi - micronucleus, pl - peristomial lip, ps - pellicle striations, s - scopula, sa - symbiotic algae. Scale bar - 10 μm

in shape and always found aboral to the trochal band. According to Raabe (1952), *M. littorinae* also has a prominent scopula, like that of *M. midae*, but its macronucleus is situated farther adorally from the scopula. Its micronucleus, however, is much smaller than its macronucleus, as is also the case in *M. midae*. *Mantoscyphidia fanthami* has the same cylindrical body form as *M. midae*, but is much longer (101.3 μm and 89.8 μm).

The body of *M. midae* does not widen towards its peristome, like that of *M. spadiceae* but narrows. Both live observations and measurements of hematoxylin stained specimens revealed *M. spadiceae* to have a greater body length than *M. midae* (compare Table 1 and 2). *Mantoscyphidia midae* has a smaller body diameter (28.3 μm), than that of *M. spadiceae* (31.2 μm), and a broader and flatter scopula in relation to body diameter. *Mantoscyphidia midae* also has a vesicular cytoplasm, and has a much higher occurrence of symbiotic algae occurring throughout the body rather than being restricted to the area adoral of the trochal band, as in *M. spadiceae*.

There are significant differences between the infundibula of *M. midae* and *M. spadiceae*, which can be used as distinguishing taxonomic characters (Figs. 9, 19). Furthermore, *M. midae* has striations that are spaced a bit closer together than those of *M. spadiceae*, therefore accounting for the greater total number of striations adorning the body (255.8 and 222.1), even though *M. spadiceae* has a greater average body length. It appears as if the trochal band of *M. midae* includes more striations.

Mantoscyphidia spadiceae has a definite cytoplasmic discontinuity situated adoral to the nuclear apparatus, thus separating the nuclear apparatus from the rest of the cytoplasm. This discontinuity is absent in *M. midae* and the nuclear apparatus appears to be surrounded with symbiotic algae and part of the granular cytoplasm, and thus not separate from the adoral cyto-

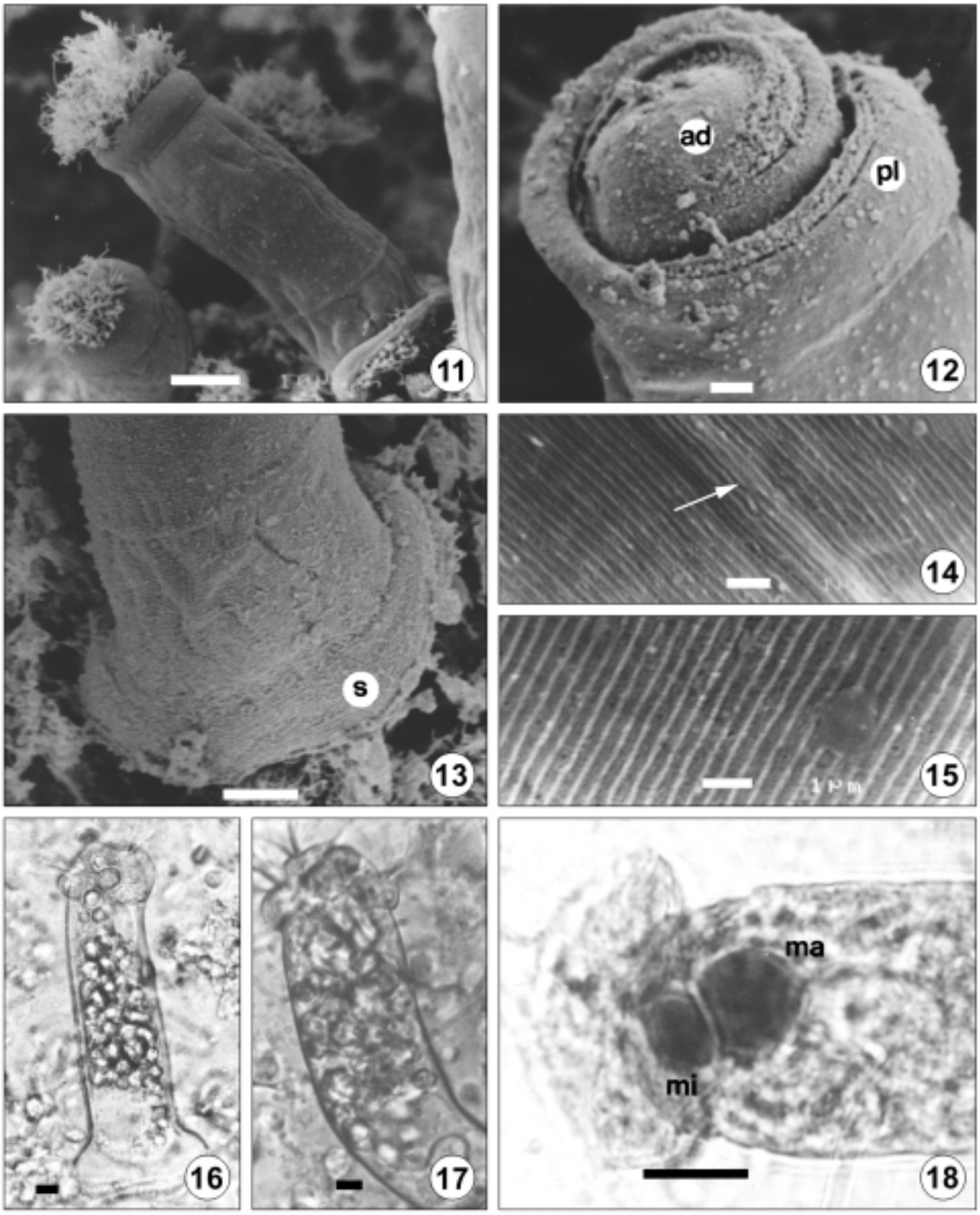

Figs. 11-18. Scanning electron micrographs (**11-15**) and photomicrographs (**16-18**) of specimens of *Mantoscyphidia midae* sp. n. occurring on the gills of *Haliotis midae* Linnaeus, 1758, collected from the De Hoop Nature Reserve, South Africa. **11** - expanded specimen attached to the gill arch; **12** - adoral zone describes 450°; **13** - broad, flattened scopula; **14** - trochal band indicated by arrow; **15** - body striations; **16, 17** - bodies expanded, peristomial discs arched, symbiotic algae distributed throughout body; **18** - hematoxylin stained specimen. ad - adoral ciliary spiral, ma - macronucleus, mi - micronucleus, pl - peristomial lip, s - scopula. Scale bars - 20 µm (**18**); 10 µm (**11, 13, 16, 17**); 1µm (**12, 14, 15**)

Table 1. Variation of body measurements (µm) of hematoxylin stained specimens of *Mantoscyphidia spadiceae* sp. n. occurring on the gills of *Haliotis spadicea* Donovan, 1808 from the De Hoop Nature Reserve, South Africa

	Completely contracted	Partially contracted	Fully expanded
Body length	49-60 (53 ± 4.7,11)	63-80 (72.9 ± 5.5,31)	82-134 (100 ± 12.7,47)
Body diameter	25-43 (34.3 ± 4.8,11)	23-56 (34.5 ± 7.5,31)	26-60 (42 ± 6.5,47)
Scopula length	3-12 (6.8 ± 2.8,11)	2-21 (8.1 ± 4.6,31)	1-24 (10.3 ± 6.1,47)
Scopula diameter	15-38 (27.5 ± 7.7,11)	19-41 (28.2 ± 5.1,31)	19-45 (30.2 ± 5.1,47)
Macronucleus length	8-18 (13.1 ± 3.6,11)	5-22 (14.8 ± 3.5,31)	11-27 (16.8 ± 3.9,47)
Macronucleus diameter	14-33 (20.6 ± 5.1,11)	16-31 (21.1 ± 3.5,31)	17-38 (25.8 ± 4.4,47)
Micronucleus length	4-10 (6.7 ± 1.7,11)	4-12 (8.4 ± 2.1,31)	3-15 (10.2 ± 2.2,47)
Micronucleus diameter	11-17 (12.9 ± 2.3,11)	10-24 (16.2 ± 3.7,31)	12-30 (21.1 ± 3.5,47)

Table 2. Variation of body measurements (µm) of hematoxylin stained specimens of *Mantoscyphidia midae* sp. n. occurring on the gills of *Haliotis midae* Linnaeus, 1758 from the De Hoop Nature Reserve, South Africa

	Completely contracted	Partially contracted	Fully expanded
Body length	45-60 (55.6 ± 4.3,36)	61-83 (69.5 ± 5.9,67)	81-110 (89.8 ± 8.8,19)
Body diameter	17-43 (23.6 ± 4.8, 36)	17-38 (24.9 ± 4.4,67)	22-40 (29.8 ± 5.4,19)
Scopula length	1-18 (5.1 ± 3.7,36)	1-14 (5.9 ± 3.4,67)	3-28 (10.3 ± 6.3,19)
Scopula diameter	13-34 (24.3 ± 5.3,36)	16-43 (27.5 ± 5.4,67)	6-50 (32.6 ± 10,19)
Macronucleus length	5-19 (11 ± 3.1,36)	7-18 (11.1 ± 2.2,67)	9-31 (14.5 ± 5.7,19)
Macronucleus diameter	11-27 (15.5 ± 3.6,36)	10-31 (16.2 ± 4.1,67)	13-41 (20.7 ± 7.3,19)
Micronucleus length	2-12 (5.2 ± 1.8,36)	3-10 (6 ± 1.2,67)	5-14 (7.5 ± 2.7,19)
Micronucleus diameter	7-15 (10.5 ± 2.1,36)	7-16 (10.1 ± 2,67)	8-23 (12.8 ± 4.2,19)

Table 3. Body striations of *Mantoscyphidia spadiceae* sp. n. and *M. midae* sp. n. occurring on the gills of *Haliotis spadicea* Donovan, 1808 and *H. midae* Linnaeus, 1758 from the De Hoop Nature Reserve, South Africa

Number of striations	*M. spadiceae*	*M. midae*
Peristome	19-30 (24.6 ± 3.6,10)	20-42 (26.8 ± 6.8,10)
Peristome to trochal band	92-136 (114.3 ±13.6,10)	127-167 (141.8 ± 11.6,10)
Trochal band	5-12 (7.7 ± 2.6,10)	4-8 (6.2 ± 1.5,10)
Trochal band to scopula	40-103 (58.9 ± 19.5,10)	50-83 (61.3 ± 12.4,10)
Scopula	9-22 (15.8 ± 4.7,10)	14-31 (22.5 ± 4.9,10)
Total number of striations	188-249 (222.1 ± 21.7,10)	238-312 (255.8 ± 23.7,10)

plasm as in the case of *M. spadiceae*. By comparison, *M. midae* specimens have smaller micronuclei than those of *M. spadiceae.* The sizes of their macronuclei do not differ significantly.

Mantoscyphidia spadiceae and *M. midae* do share some similarities, however. Both species have macronuclei that are similar in position and shape, are extremely contractile, and attach to the arch of a gill rather than between gill lamellae. In extremely high infestations, however, the individuals of both species were also observed attached to gill lamellae.

Intraspecific variation

Body measurements of the different stages of contraction for *M. spadiceae* stained material is summarised in Table 1. The shrinkage effect on the nuclear appara-

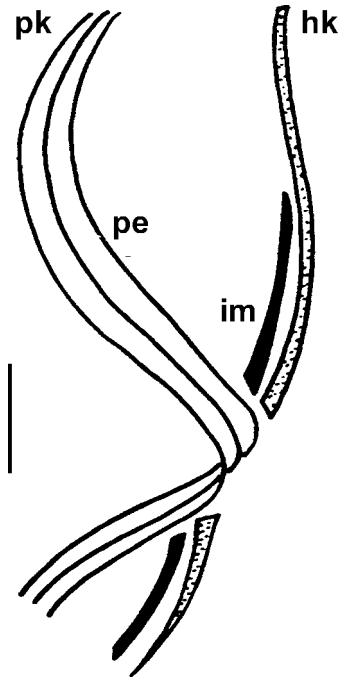

Fig. 19. Buccal infraciliature of *Mantoscyphidia midae* sp. n. occurring on the gills of *Haliotis midae* Linnaeus, 1758, collected from the De Hoop Nature Reserve, South Africa. hk - haplokinety, im - impregnable band, pe - peniculus, pk - polykinety. Scale bar - 1 µm

tus of live specimens vs. hematoxylin stained specimens is as follows: the arithmetic mean of the macronucleus length and diameter of live specimens (fully expanded) was 19.3 µm and 28.3 µm respectively, compared to 16.8 µm and 25.8 µm in hematoxylin stained specimens. This amounts to shrinkage of approximately 13 % and 9 %, respectively. The micronucleus length and diameter showed very little shrinkage between expanded hematoxylin stained and live specimens. Thus, macronucleus length is more affected by shrinkage, as was found in *M. branchi* (Van As *et al*. 1998). As in *M. branchi*, the form and position of the nuclear apparatus of *M. spadiceae* was consistent.

The arithmetic means of the body dimensions of expanded live specimens of *M. spadiceae* (Fig. 7) are slightly higher than those of expanded Bouin's fixed and hematoxylin stained specimens. This is not the case in *M. midae* (Table 2). This information confirms the necessity of including live observations in species descriptions. The body of *M. spadiceae* is extremely contractile, varying from 49 to 134 µm in length (Table 1). The body length of *M. spadiceae* is much greater than that of any other species in the genus, resembling most closely *M. ubiquita*, (body length 30 - 100 µm), and *M. fanthami* (body length 80-130 µm) (Hirshfield 1949, Basson *et al*. 1999).

The number of striations from different parts of the body, counted with the aid of SEM, can be used to describe new scyphidiid species (Van As *et al.* 1995). The number of striations for *M. spadiceae* and *M. midae* is presented in Table 3. Unfortunately this can only be compared to data of *M. branchi*, *M. marioni* and *M. fanthami* as no information on the number of body striations of the other species of *Mantoscyphidia* from marine gastropods is available. *Mantoscyphidia spadiceae, M. midae* and *M. fanthami* have an average total number of 222.1, 255.8 and 262 striations, respectively, whilst *M. branchi* and *M. marioni* have 106.5 and 115.6 striations respectively. This can be ascribed to the greater body length of *M. spadiceae* and *M. fanthami*, and the fact that in both of these species the striations are 0.3 µm apart, whilst in the case of *M. branchi* and *M. marioni* the striations are further (0.5 µm) apart. *Mantoscyphidia midae* has a shorter average body length, but the highest number of striations. This can be attributed to the fact that the body striations are only 0.25 µm apart.

In a comprehensive survey of 19 limpet species representing three genera along the South African coast, the scyphidiid peritrich, *M. branchi*, was found attached to the gills of specimens of all limpet species examined (Van As *et al*. 1998). Similarly, seven of the limpet species were infested with the same *Licnophora* Claparède, 1867 species, namely *L. limpetae* Van As, Van As & Basson, 1999. In a similar investigation of the limpet fauna from a Sub-antarctic Island in the Southern Ocean, one scyphidiid peritrich, *M. marioni* was found associated with the only limpet, *Nacella delesserti* (Phillips, 1849).

Parasitological surveys of the marine gastropod *Oxystele* Philippi, 1847 revealed the occurrence of one scyphidiid peritrich, i.e. *M. fanthami* on the gill filaments. This topshell genus comprises five species endemic to and distributed along the South African coast. *Mantoscyphidia fanthami* was found associated with all five species and occurred along the southern, western and eastern coastline (Basson *et al*. 1999). All the topshells were also infested with the same mobiline species, *Trichodina oxystelis* Sandon, 1965.

The two species in the genus *Haliotis* that were examined, namely *H. spadicea* and *H. midae*, were infested with two distinct species of scyphidiid peritrichs.

This is contrary to what has been found in southern Africa and can perhaps be attributed to the morphological and ecological differences that exist between the hosts.

REFERENCES

Basson L., Botha A., Van As J. G. (1999) *Mantoscyphidia fanthami* sp. n., an ectosymbiont (Ciliophora: Peritrichia) from the gills of the marine gastropod *Oxystele* Philippi, 1847 in South Africa. *Acta Protozool.* **38:** 75-81

Cuénot L. (1891) Infusoires commensaux des *Ligies*, *Patellase* et *Arenicoles*. *Rev. Biol. Nord France* **4:** 81-89

Fish J. D., Goodwin B. J. (1976) Observations on the peritrichous ciliate *Scyphidia ubiquita* from the west coast of Wales and a description of a new species. *J. Zool*. **179:** 361-371

Hirshfield H. (1949) The morphology of *Urceolaria karyolobia* sp. nov. *Trichodina tegula* sp. nov. and *Scyphidia ubiquita* sp. nov. three new species from Southern California limpets and turbans. *J. Morph*. **85:** 1-28

Jamadar Y. A., Choudhury A. (1988) Ciliates of some marine and estuarine molluscs from the Indian coastal region. *Zool. Surv. Ind.* **12:** 1-79

Kahl A. (1933) Ciliata libera et ectocommensalia. In: Die Tierwelt Der Nord-Und Ostsee, (Eds. G. Grimpe and E. Wagler). Lief. 23 (Teil II, c_3), Leipzig, 29-146

Lee J. J., Hunter S. H., Bovee E. C. (1985) Illustrated Guide to the Protozoa. Society of Protozoology. Lawrence, USA

Lom J., Dyková I. (1992) Protozoan Parasites of Fishes. Elsevier, Amsterdam

Madrazo-Garibay M., López-Ochoterena E. (1988) Ciliated protozoans from Mexico. XXXI. Seven species of the *Scyphidia* Dujardin genera (Peritrichida: Oligohymenophorea) and their association with edible clams (Mollusca: Bivalvia) from the Pom Lagoon, Campeche. *An. inst. Cience del Mary Limnol. Univ. Nal. Autón, Mexico*. **15:** 223-228

Raabe Z. (1952) *Ambiphrya miri* g. n. sp. n.-eine Übergangsform zwischen Peritricha Mobilina -und Peritricha Sessilina. *Annls. Univ. Mariae Curie-Sklodowska* **10:** 339-358

Van As L. L., Basson L., Van As J. G. (1998) Two new species of *Mantoscyphidia* Jankowski, 1980 (Ciliophora: Peritrichia) gill symbionts of limpets, from South Africa and the Sub-Antarctic Island, Marion. *Acta Protozool.* **37:** 101-111

Van As L. L., Van As J. G., Basson L. (1995) Procedure for studying sessile ciliophoran symbionts on limpets. *Proc. Elec. Microsc. Soc. southern Afr.* **25:** 69

Warren A. (1991) A scanning electron microscopic study of the morphology of *Scyphidia physarum* Lachmann, 1856 (Ciliophora: Peritrichida). *Scanning Microsc*. **5:** 281-286

Received on 30th March, 2000; accepted 13th December, 2000

Acta Protozool. (2001) 40: 141 - 146

ACTA
PROTOZOOLOGICA

Trichodina cancilae sp. n. (Mobilina: Trichodinidae) from the Gills of a Freshwater Gar, *Xenentodon cancila* (Hamilton) (Belonidae)

Ghazi S. M. ASMAT

Department of Zoology, University of Chittagong, Chittagong, Bangladesh

Summary. A population of a trichodinid ciliate (Mobilina: Trichodinidae) was found in the gills of the freshwater gar, *Xenentodon cancila* (Hamilton) (Belonidae) collected from Kalyani of Nadia District, West Bengal, India and was described as a new species. The specimens are characterized by the shape of denticles being elongated and arched blades; 1 or 2 cut-like notches in the convex side of the blade and the presence of the single non-staining granule at the base of blades and the base of rays; moderate central part; and broad and greatly arched rays. The body diameter ranged from 50.0-74.4 μm, whilst denticle number ranged from 28-32. Approximately 49.5% of the host fishes (213 out of 430) were infested with the ciliate on their gills during September 1995 and December 1997, sometimes in concurrent infestation with *Tripartiella bursiformis* (Davis, 1947) Lom, 1959. The highest percentage of infestation was recorded in December 1996 (73.3%). The variation is recorded and discussed.

Key words: freshwater gar, gills, India, Mobilina, *Trichodina cancilae* sp. n., *Xenentodon cancila*.

INTRODUCTION

In India, studies on the trichodinid ciliates, relatively less so far, is getting momentum in many sectors. As a result, 10 species of trichodinid ciliates representing the genera *Trichodina* Ehrenberg, 1838; *Paratrichodina* Lom, 1963 and *Tripartiella* Lom, 1959 were identified from different freshwater and estuarine Indian fishes (Hagargi and Amoji 1979; Mukherjee and Haldar 1982; Das and Haldar 1987; Das *et al.* 1987; Mishra and Das 1993; Saha *et al*. 1995 a, b; Saha and Haldar 1996, 1997; Asmat and Haldar 1998). The primary objectives of the present study were to identify the trichodinid ciliates inhabiting the freshwater and estuarine fishes and to study on the morphology and taxonomic status of these trichodinids. During the present study, the gills of a freshwater gar, *Xenentodon cancila* (Hamilton) was found to host a dense population of trichodinids. The ciliophoran proved to be a new species and is described here.

Address for correspondence: Ghazi S. M. Asmat, Department of Zoology, University of Chittagong, Chittagong 4331, Bangladesh; Fax: 880-31-726310; E-mail: asmat@globalctg.net

MATERIALS AND METHODS

A total of 430 freshwater gars, *Xenentodon cancila* were examined during September 1995 to December 1997. The host fishes

(10-20 cm, 20-80 g) were collected by fishing nets once in each month from different rivulets of Nadia district of West Bengal, India Gill scrapings were made at the riverside. Air-dried gill scrapings were transported to the laboratory. The slides with trichodinid ciliates were impregnated with Klein's dry silver impregnation technique (Klein 1958). Examinations of preparations were made under the Olympus phase-contrast microscope at x100 magnification. Measurements were made according to the recommendations of Lom (1958), Wellborn (1967), Arthur and Lom (1984) and Van As and Basson (1992). Numerous photomicrographs were made in order to have comprehensive morphological analyses of the ciliates.

RESULTS

Trichodina cancilae sp. n. (Figs. 1-20)

Description

This is a large trichodinid with disc-shaped body and surrounded by a finely striated, wide border membrane. The texture of central area is finely granular and similar as rest of adhesive disc. The denticulate ring consists of 28-32 (29.8 ± 1.2) large denticles. There are 8-12 (10.7 ± 1.0) radial pins per denticle. The adoral cilia described a turn of about 390-395°.

The blade of denticle is broad and curved, filling almost the entire spaces between y+1 axis (Figs.17, 19), sometimes angular (Figs.7, 8), which are also found in newly born individuals (Figs. 13, 14). The tangent point is blunt in most cases, slightly lower than distal margin. The anterior margin is rounded with slightly flattened apex, not touching y+1 axis in most specimens. The apical depression is well developed and never impregnated. But the anterior margin of apical region bears one or two cut-like notches (Figs.1, 3, 7, 8). The anterior blade apophysis is sometimes prominent. The blade connection is well developed. The posterior margin forms narrow, elongated, semilunar curve with deepest point at same level (Figs.17, 18) or lower (Fig.19) than apex. The posterior blade apophysis is not always distinctly visible. The inter-blade space is moderate and often fills with non-impregnable matters.

The central part is moderate to robust, fitting tightly into the preceding denticle with rounded point that extends more than halfway to y-1 axis, sometimes touching this line. The section of central part above and below x-axis is similar. The indentation in lower central part is not always seen.

The ray connection is short and thin with well-developed ray apophysis situated high, pointed in an anterior direction. The ray connection is very delicate with prominent constriction just below ray apophysis. The ray is considerably longer than blade, broad, distinctly grooved with almost same thickness, and rounded end, rarely thin (Fig.1). Typically, ray is slightly curved posteriorly, which is also characteristic of developing individuals (Figs.13, 14, 16), but lying parallel to y-axes. In between ray bases, in many trichodinids, contain non-impregnable pearl-shaped glistening particles (Figs. 9-12).

Intraspecific Variability

Considerable variations among the individuals of the described species concern the shape of blade, orientation of ray, and presence of non-impregnable particles between inter-blade space and ray bases. These variations are not related to body dimensions or seasons of the year, but could be found in a single fish host.

Two types of blade shapes were found in the present species. In one form, the blade is arch-shaped, but with narrow semilunar curve (Figs.6-8), while in others, it is rather spoon-shaped having broad distal end tapering towards central part, giving an erect posture (Figs.4-5). In relation to these shapes, the shape of distal margin, tangent point and semilunar curve also differ. The orientation of ray follows three district patterns. Typically, rays are slightly curved in posterior direction (Fig.17), but in some specimens, rays are anteriorly directed, extending beyond y+1 axis (Fig.19), while in others, rays are oriented posteriorly, extending beyond y-1 axis (Fig.18). The cause of the presence of non-impregnable particles in interblade space and in between ray bases (Figs.9-12) in many specimens is not known. Some developing stages of the species were also found (Figs.13-16).

Type host: *Xenentodon cancila* (Hamilton) (Belonidae).

Type locality: Kalyani of Nadia District, West Bengal, India (23.3°N 88.4°E).

Location: gills.

Etymology: named after the specific name of the type host fish, *Xenentodon cancila* (Hamilton).

Type specimens: holotype, slide XC-1 prepared on 4.3.1996; paratypes on the above mentioned slide and in other slides prepared on different dates in the collection

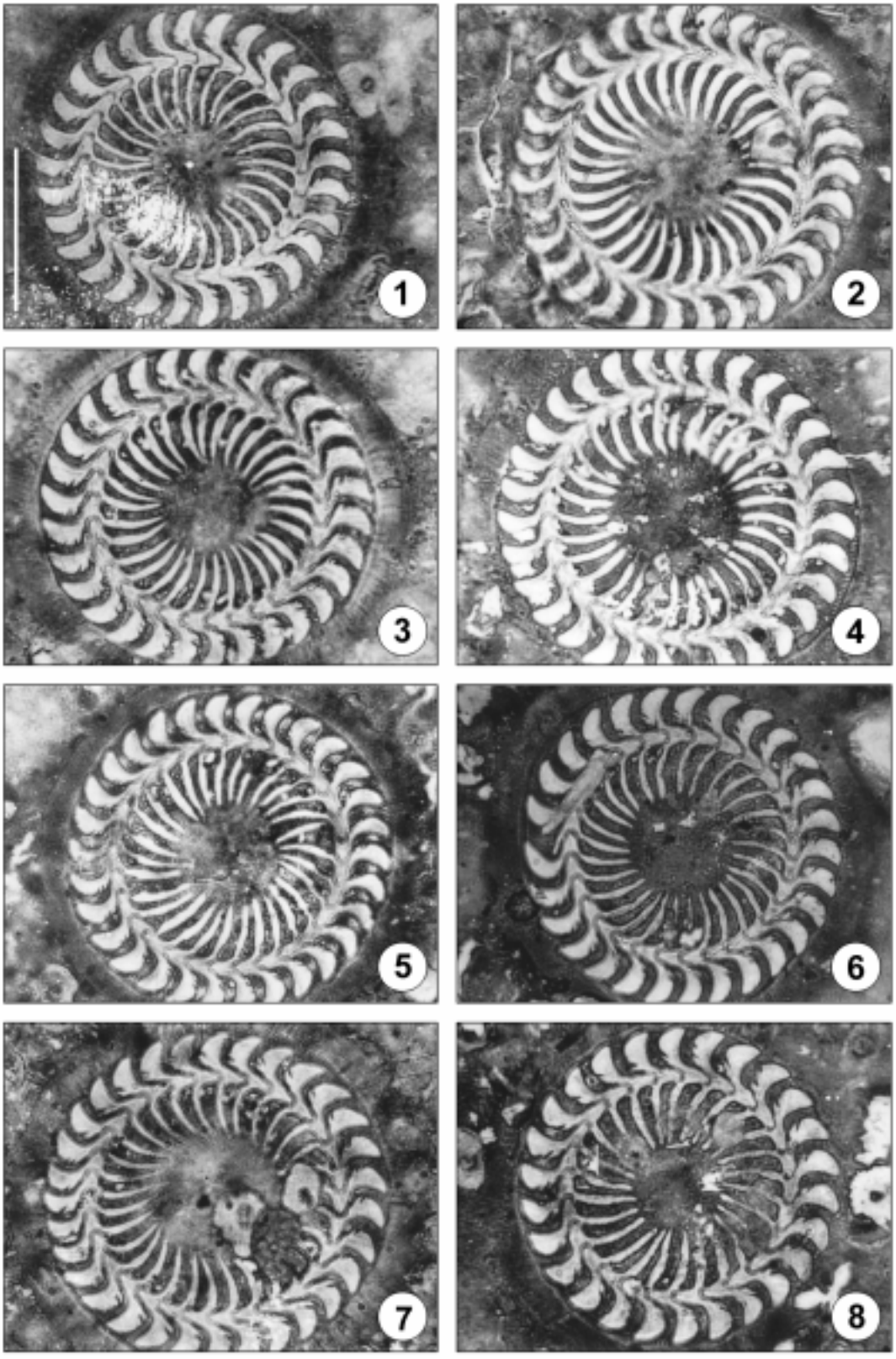

Figs. 1-8. Photomicrographs of *Trichodina cancilae* sp. n. from *Xenentodon cancila* showing the variation in the structure of denticle. Scale bar - 30 μm

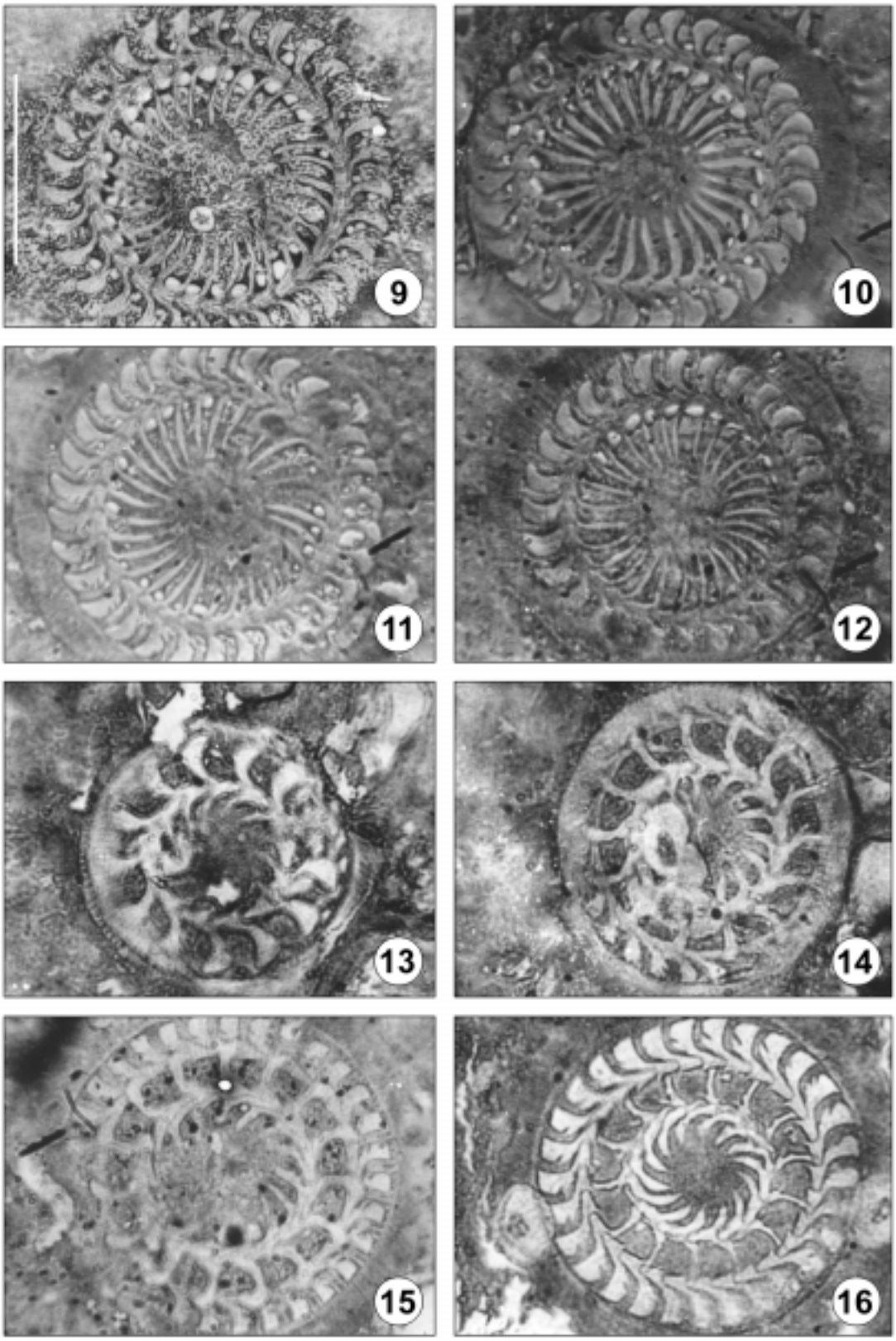

Figs. 9-16. Photomicrographs of *Trichodina cancilae* sp. n. from *Xenentodon cancila* showing the non-impregnated particles between the bases of blade and between the bases of ray (**9-12**) and the developing stages (**13-16**). Scale bar - 30 μm

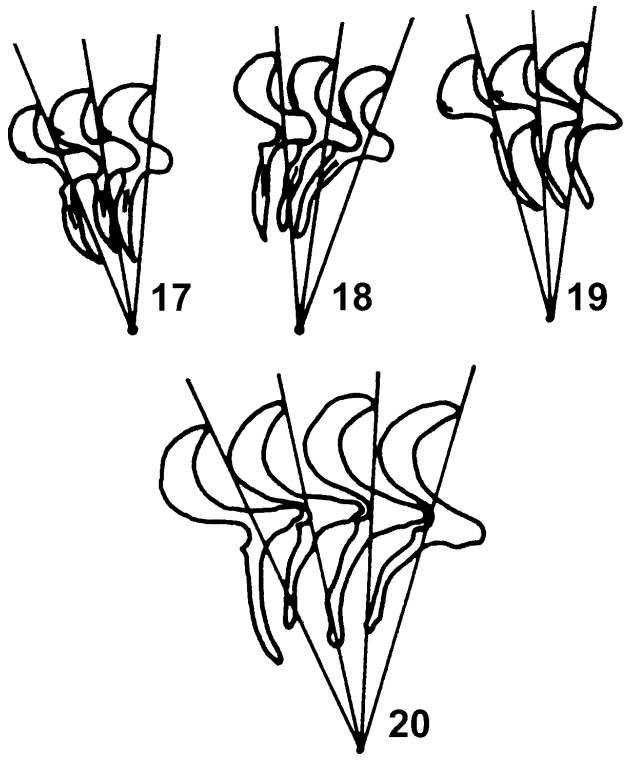

Figs.**17-20.** Diagrammatic drawings of denticles of trichodinids. **16-19** - *Trichodina cancilae* sp. n. from India; **20** - *T. magna* Van As and Basson, 1992 redrawn from Van As and Basson (1992) from South Africa

of the Department of Zoology, University of Chittagong, Chittagong 4331, Bangladesh.

DISCUSSION

As classified by Van As and Basson (1992) the described species falls in the category of large trichodinid with a diameter of 50.0-74.4 (61.9 ± 5.4) µm. *Trichodina cancilae* sp. n. is comparable to *Trichodina magna* Van As and Basson, 1989. However, *Trichodina cancilae* sp. n. differs from the latter species in a number of points of denticle shape, particularly in blade shape, orientation of ray, by the presence of cut-like notches in the convex side of denticle of blade and the presence of the single non-staining granule at the base of the blades and the base of the rays. These characters establish this ciliate as a new species and *Trichodina cancilae* sp. n. is proposed here after the specific name of the type host fish, *Xenentodon cancila* (Hamilton).

The blade of *T. magna* is uniform, regardless of host or locality, but in the present form two types of blade shapes namely arch-shaped and spoon-shaped were noticed, even within a single fish host. The arch-shaped blade forms a narrow semilunar curve rather than larger one as in *T. magna* (Figs.17, 19). The spoon-shaped blade having broad distal end, tapering towards the central part giving an erect posture and which, unlike *T. magna*, have narrow and elongated crescent, at posterior margin. In the spoon-shaped blade, the distal margin is angular, the anterior margin never touches y+1 axis, and the tangent point is also blunt (Fig.18), whilst in the forms having arch-shaped blade, the direction and general blade shape is somewhat similar to those of *T. magna*. Although the shape of apex of blade is similar

Table 1. Morphometric comparison of *Trichodina cancilae* sp. n. and *T. magna* Van As and Basson, 1989. Measurements in µm

Species		*Trichodina cancilae* sp. n. (n=40)	*T. magna* (n=22)
Host		*Xenentodon cancila*	13 species of fish
Locality		Kalyani, West Bengal, India	Capri, South Africa
Location		Gills	Skin, fins
Reference(s)		Present paper	Van As and Basson (1989)
Diameter of body		50.0-74.4 (61.9 ± 5.4)	71.2-111.8 (99.1 ± 9.5)
Diameter of adhesive disc		41.8-60.3 (52.0 ± 5.6)	59.7-94.8 (81.7 ± 8.2)
Diameter of denticulate ring		30.6-46.6 (36.9 ± 4.4)	35.6-57.5 (50.0 ± 4.8)
Diameter of central area		9.7-20.4 (15.3 ± 3.0)	-
Width of border membrane		3.1-6.1 (4.7 ± 0.7)	6.2-13.9 (8.9 ± 1.4)
Number of denticles		28-32 (29.8 ± 1.2)	24-27 (25)
Number of radial pins/denticle		8-12 (10.7 ± 1.0)	10-13 (11)
Dimensions of denticle	span	12.3-23.5 (17.4 ± 2.0)	-
	length	7.1-10.3 (8.7 ± 0.9)	7.4-13.6 (10.9 ± 1.4)
Dimensions of denticle components	ray	6.1-14.3 (9.1 ± 1.4)	7.7-16.0 (13.0 ± 1.7)
	blade	5.1-7.1 (6.1 ± 0.7)	6.0-10.9 (8.6 ± 0.8)
Width of central part		2.0-4.6 (4.0 ± 3.4)	3.7-7.4 (5.6 ± 0.9)
Degree of adoral ciliature		390-395°	400°

in both species, its position in relation to the deepest point is different. In the case of *T. magna,* it is situated lower than deepest point of posterior margin, while in the present form; the apex is situated at same level (Figs.17, 18) or higher than deepest point (Fig.19). The shape and orientation of ray in relation to y-axes also differ in the two species. The ray is thin and of an even thickness throughout in *T. magna* (Fig. 20), but broad and massive, rarely thin, in the presently described species. The orientation of ray follows three patterns in the present form, even within a single fish host. In most cases, the rays are slightly curved posteriorly, but remain parallel to y-axes. Some specimens possess anteriorly directed rays, which extend beyond y+1 axis, as in *T. magna*, while in other forms; the rays are oriented in a posterior direction, extending beyond y-1 axis. Posteriorly oriented rays are also visible in developmental stages (Figs.13, 14). The point of rays, however, is similar in both species. Morphometric comparison between *T. magna* and the presently described species is given in Table 1.

Acknowledgements. The work was carried out in the Department of Zoology, University of Kalyani, West Bengal, India. The author is grateful to Dr. Linda Basson of the Department of Zoology and Entomology, University of Orange Free State, South Africa for critical analysis of the photomicrographs of the specimens and confirming the ciliate as a new species. I am indebted to Professor (Late) K. M. Nurul Huda, Department of Zoology, University of Chittagong for useful advice in improving the manuscript.

REFERENCES

Arthur J. R., Lom J. (1984) Trichodinid Protozoa (Ciliophora: Peritrichida) from freshwater fishes of Rybinsk Reservoir, USSR. *J. Protozool.* **31:** 82-91

Asmat G. S. M., Haldar D. P. (1998) *Trichodina mystusi* - a new species of trichodinid ciliophoran from Indian estuarine fish, *Mystus gulio* (Hamilton). *Acta Protozool.* **37:** 173-177

Das M. K., Haldar D. P. (1987) Urceolariid ciliates of the genus *Tripartiella* invading gills of freshwater cultured carps in India. *Arch. Protistenkd*. **134:** 169-178

Das M. K., Pal R. N., Das P. B. (1987) Preliminary observations on the ecology of animal parasites in estuarine fishes of Deltaic West Bengal. *J. Indian Soc. Coastal Agric. Res.* **5:** 319-323

Hagargi S. S., Amoji S. D. (1979) Occurrence of *Trichodina pediculus* Ehrenberg 1838 on freshwater carps, *Barbus* spp. *Curr. Sci*. **48:** 789-790

Klein B. M. (1958) The dry silver method and its proper use. *J. Protozool*. **5:** 99-103

Lom J. (1958) A contribution to the systematics and morphology of endoparasitic trichodinids from amphibians, with a proposal of uniform specific characteristics. *J. Protozool*. **5:** 215-263

Mishra R. K., Das M. K. (1993) Urceolariid ciliate, *Trichodina reticulata* infesting gills of *Catla catla* in India. *J. Inland. Fish. Soc. India*. **25:** 54-56

Mukherjee M., Haldar D. P. (1982) Observations on the urceolariid ciliates of the genera *Trichodina* and *Tripartiella* in freshwater teleosts. *Arch. Protistenkd.* **126:** 419-426

Saha B. S., Haldar D. P. (1996) First record of *Tripartiella bursiformis* (Davis, 1947) Lom, 1959 (Protozoa: Urceolariidae) from the gills of *Xenentodon cancila* (Hamilton) in the Indian subcontinent. *J. Beng. Nat. Hist. Soc. (NS*). **15:** 11-17

Saha B. S., Haldar D. P. (1997) Observations on the urceolariid ciliates of the genus *Tripartiella* Lom, 1959 parasitising the gills of three freshwater edible fishes of West Bengal, India. *J. Inland Fish. Soc. India*. **29:** 28-36

Saha B. S., Bandopadhyay P. K., Haldar D. P. (1995a) Biodiversity of trichodinid ciliates in freshwater fishes of West Bengal. *Environ. Ecol.* **13:** 814-823

Saha B. S., Bandopadhyay P. K., Haldar D. P. (1995b) First record of *Paratrichodina* sp. (Protozoa: Urceolariidae) from the gills of *Notopterus notopterus* (Pallas) from the Indian subcontinent. *J. Beng. Nat. Hist. Soc. (NS)*. **4:** 35-42

Van As J. G., Basson L. (1989) A further contribution to the taxonomy of the Trichodinidae (Ciliophora: Peritrichida) and a review of the taxonomic status of some fish ectoparasitic trichodinids. *Syst. Parasitol*. **14:** 157-179

Van As J. G., Basson L. (1992) Trichodinid ectoparasites (Ciliophora: Peritrichida) of freshwater fishes of the Zambesi River system, with a reappraisal of host specificity. *Syst. Parasitol*. **22:** 81-109

Wellborn T. L. Jr. (1967) *Trichodina* (Ciliata: Urceolariidae) of freshwater fishes of the Southern United States. *J. Protozool*. **14:** 399-412

Received on 6th June, 2000; accepted on 6th December, 2000

Acta Protozool. (2001) 40: 147 - 151

ACTA
PROTOZOOLOGICA

Trichodina canningensis sp. n. (Ciliophora: Trichodinidae) from an Indian Estuarine Fish, *Mystus gulio* (Hamilton) (Bagridae)

Ghazi S. M. ASMAT*

Department of Zoology, University of Chittagong, Chittagong, Bangladesh

Summary. During the study on the biodiversity of trichodinid ciliates from the state of West Bengal, India, the gills of the Indian estuarine fish, *Mystus gulio* (Hamilton) (Bagridae) was found to be the host to a new species *Trichodina canningensis* sp. n. This ciliate is characterized by reduced blade; stout and robust central part; elongated ray having parallel borders and a large clear circle at the centre containing argentophilic particles. The body diameter ranged from 47.0-56.1 μm, whilst denticle number ranged from 22-29. Approximately 3.6% of the host fishes (6 out of 165) were infested with this ciliate, sometimes in concurrent infestation with *Trichodina mystusi* Asmat and Haldar, 1998 and other species of *Trichodina* from November to January 1996. This trichodinid closely resembles *Hemitrichodina robusta* Basson and Van As, 1989 but differs with slightly developed blade having sharp tangent point and without any protrusion on the distal margin.

Key words: ciliophoran, estuarine fish, India, *Trichodina canningensis* sp. n., trichodinid.

INTRODUCTION

More than 200 species of trichodinid ciliophorans have been reported from the skin, fins, gills, urinary bladder as well as reproductive system of fishes. Despite the abundance of trichodinids they have been little studied in India since the early work of Annandale (1912). As a result, 12 species of trichodinid ciliates representing the genera *Trichodina* Ehrenberg, 1838; *Paratrichodina* Lom, 1963; *Tripartiella* Lom, 1959 were identified from different freshwater and estuarine Indian fishes (Hagargi and Amoji 1979; Mukherjee and Haldar 1982; Das and Haldar 1987; Das *et al.* 1987; Mishra and Das 1993; Saha *et al.* 1995a, b; Saha and Haldar 1996, 1997; Asmat and Haldar 1998; Basu and Haldar 1998). During the course of the present investigation on the biodiversity of trichodinid ciliates in various freshwater and estuarine fishes in the state of West Bengal, an estuarine fish, *Mystus gulio* (Hamilton) has been found to be a host to a new species of *Trichodina.*

Address for correspondence: Ghazi S. M. Asmat, Department of Zoology, University of Chittagong, Chittagong 4331, Bangladesh; Fax: 880-31-726310; E-mail: asmat@globalctg.net

* The work was carried out at Protozoology Laboratory, Department of Zoology, University of Kalyani, Kalyani 741235, West Bengal, India

MATERIALS AND METHODS

The host fishes were collected from the river Matla (Latitude 21.5°N Longitude 88.5°E) at Canning, South 24-Parganas District, about 30 km south of Calcutta, which regularly receives saline water from the Bay of Bengal during high tide.

A total of 165 host fishes were examined during September 1995 to December 1997. The fishes (12-16 cm x 20-120 gm) were collected by fishing nets. Gill scrapings were made at the riverside. Air-dried scrapings were transported to the laboratory. The slides with trichodinid ciliates were impregnated with Klein's dry silver impregnation technique (Klein 1958). Examinations of preparations were made under the Olympus phase-contrast microscope at x100 magnification. Measurements were made according to the recommendations of Lom (1958), Wellborn (1967), Arthur and Lom (1984) and Van As and Basson (1992). Photomicrographs were made in order to have comprehensive morphological analyses of the ciliates.

DESCRIPTION OF THE SPECIES

Trichodina canningensis sp. n. (Figs. 1-12, Table 1)

The trichodinid is medium-sized and disc-shaped, 47.0-56.1 (51.1 ± 2.8). There are 7-10 (8.5 ± 0.8) radial pins per denticle. The centre of the adhesive disc is a clear circle, which is surrounded by an undulating or notched heavily impregnated perimeter and somewhat elevated from the rest of adhesive disc (Fig. 6). There are few to many dark argentophilic particles scattered in the circle (Figs. 1, 2, 6, 7).

The denticulate ring consists of 22-29 (25.4 ± 2.1) denticles. The blades are reduced and angular with truncated distal margins, which are parallel to the border membrane, sometimes slightly sloped anteriorly. In some malformed specimens the blades appear as warts or are absent altogether (Fig.7). The tangent point is sharp and situated slightly lower than the distal margin. The anterior surface of the blade is slightly curved and extends more than half of the space to the y axis (Figs. 9-11). The apex is not always prominent because of the impregnation of the apical depression, giving a notch-like appearance at the base of blade. The anterior blade apophysis is not clearly visible. The posterior margin of blade forms a narrow semilunar curve with the deepest point at same level as anterior notch. The blade connection is short and well developed. The posterior blade apophysis is prominent.

The central part is robust, flat and rectangularly triangular in shape with a bluntly pointed end and wider than the length of blade (Table 1). The point of the central part is fitted tightly into the following denticle, almost touching the y-1 axis (Figs. 9-11) and sometimes extends beyond this line. The section of the central part above the x-axis is more convex. Indentation in the lower central part is not prominent.

The ray apophysis is present, sometimes prominent and directed obliquely in an upward direction (Figs. 6, 7). The ray connection is short and wide. The ray is broad and straight with a distinct central groove (Fig.1), but appears as whip-like filaments in younger specimens (Fig. 8). The ray gradually tapers to a rounded point (Figs.1, 3, 4, 6) and remains parallel to y axes (Figs.7, 9). The tip of the ray sometimes touches the boundary of the clear circle.

The exact turn of the adoral ciliary spiral could not be detected.

Type host: *Mystus gulio* (Hamilton) (Bagridae).

Type locality: river Matla (Latitude 21.5° N Longitude 88.5° E) at Canning, South 24-Parganas District, West Bengal, India.

Location: gills.

Etymology: named after the place of collection of the type host fish, *Mystus gulio* (Hamilton).

Type specimens: holotype, slide MG-1 prepared on 15.01.1996, paratypes in the above mentioned slide and in other slides prepared on different dates in the collection of the Protozoology Laboratory, Department of Zoology, University of Kalyani, Kalyani 741235, West Bengal, India.

DISCUSSION

Trichodinids are distinguished by the silver nitrate impregnated adhesive disc. The combination of large clear central area, reduced blade, well-developed ray and robust central part of the trichodinid from *Mystus gulio*, made it unique among the described trichodinids The only species could be compared is the member of a different genus, i.e. *Hemitrichodina robusta* Basson and Van As, 1989 (Fig.12). The genus *Hemitrichodina* with its only species *H. robusta* is characterized by the denticulate ring consisting of denticles with well-developed rays and central parts, but number of blades is reduced. The adoral ciliary spiral in *Hemitrichodina* describes an arc of more than 360°, but less than two full circles. Basson and Van As (1989) originally described *H. robusta* from the host fish, *Marcusenius macrolepidotus* from the Olifants River system in the eastern Transvaal, South Africa. Later, Van As and Basson (1992) also recorded it from two other host fish, *Hepsettus odoe* from the Lake Liambesi and *Micralestes acuitidens* from the Zambesi River in South Africa. The

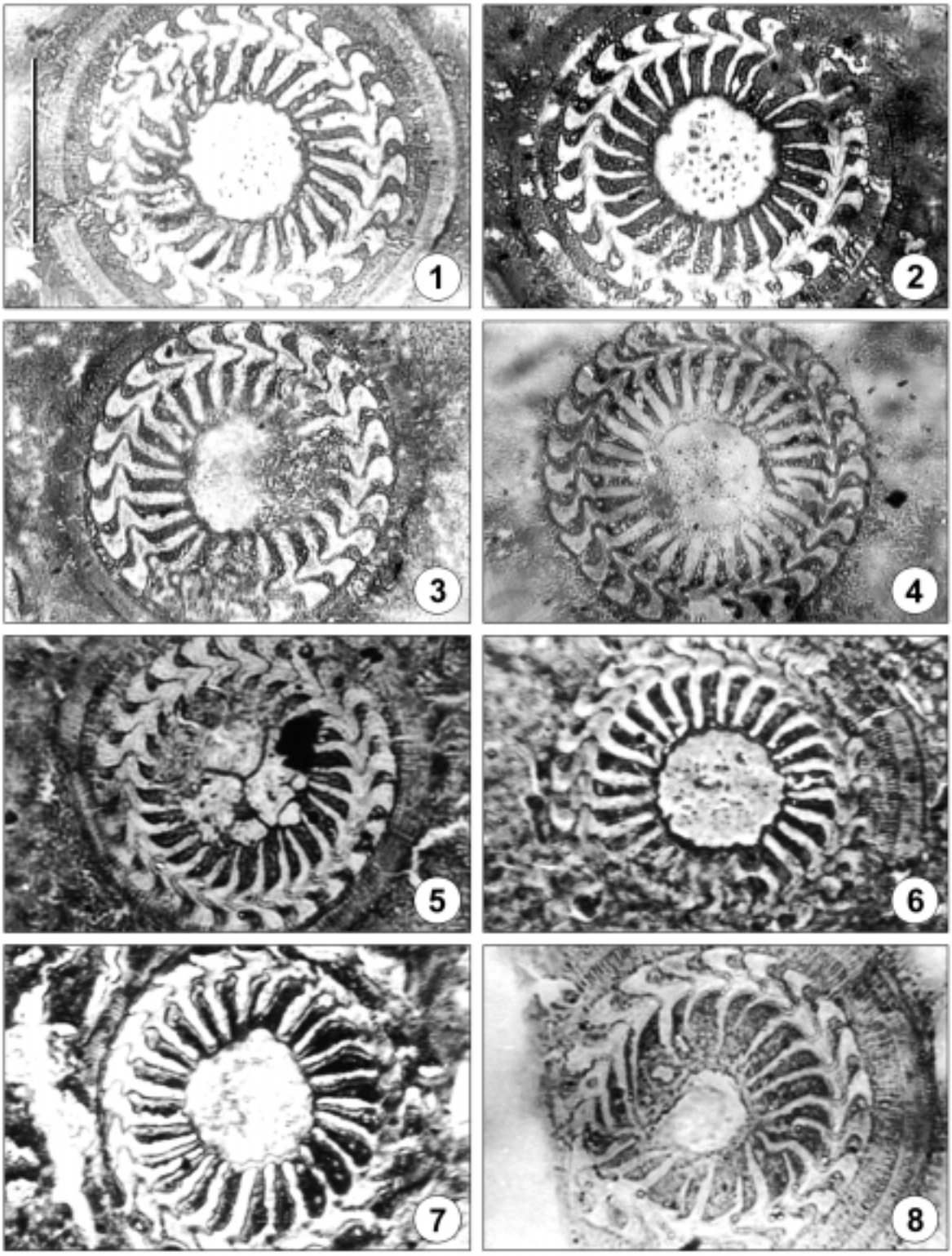

Figs.1-8. Photomicrographs of silver nitrate impregnated adhesive discs of *Trichodina canningensis* sp. n. from *Mystus gulio* showing variation in appearance. Scale bar - 30 μm

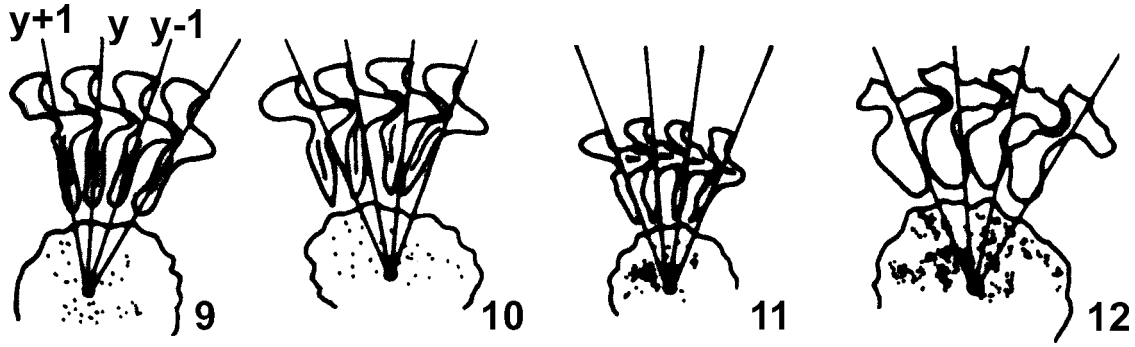

Figs. 9-12. Diagrammatic drawings of denticles of trichodinids. **9-11** - *Trichodina canningensis* sp. n. from India; **12** - *Hemitrichodina robusta* Basson and Van As, 1989; redrawn from Basson and Van As (1989) from South Africa

Table. 1. Morphometric comparison between *Trichodina canningensis* sp. n. and *Hemitrichodina robusta* Basson and Van As, 1989

Species	*Trichodina canningensis* sp. n. n=14	*Hemitrichodina robusta*
Reference	Present paper	Basson and Van As (1989)
Host	*Mystus gulio*	*Marcusenius macrolepidotus, Micralestes acutidens, Hepsettus odoe*
Location	Gills	Skin, fins, occasionally gills
Geographic Locality	Matla River, Canning, West Bengal, India	Olifants River, Loskop Dam, Eastern Transvaal, South Africa
Diameter of:		
body	47.0-56.1 (51.1 ± 2.8)	52.3-82.7 (63.8 ± 7.1)
adhesive disc	40.8-47.9 (43.9 ± 2.1)	42.9-70.1 (53.2 ± 6.2)
denticulate ring	28.6-35.7 (32.5 ± 2.1)	27.3-44.9 (33.5 ± 4.2)
central area	11.2-17.8 (15.3 ± 1.8)	-
clear area	10.2-16.3 (14.2 ± 1.5)	12.4-20.0 (16.0 ± 2.0)
Width of border membrane	3.1-4.1 (3.6 ± 0.4)	4.5-6.8 (5.6 ± 0.8)
Number of:		
denticles	22-29 (25.4 ± 2.1)	18-24 (23.0)
radial pins/denticle	7-10 (8.5 ± 0.8)	8-11 (9.0)
Dimensions of denticle:		
span of denticle	11.2-14.8 (12.9 ± 0.9)	-
length of:		
denticle	7.1-8.2 (7.3 ± 0.8)	6.9-10.9 (8.6 ± 1.1)
ray	5.6-8.6 (7.1 ± 0.9)	4.9-10.0 (6.7 ± 1.3)
blade	1.5-3.1 (2.6 ± 0.5)	3.0-5.3 (4.0 ± 0.5)
width of central part	2.0-3.6 (3.1 ± 0.4)	2.4-4.1 (3.0 ± 0.5)
Degree of adoral ciliature	-	405-450°

described trichodinid in having reduced blade; stout and robust central part; elongated ray having parallel borders and a large clear circle at the centre containing argentophilic particles closely resembles *H. robusta*. However, the new species differs from *H. robusta* in having blades not as reduced as recorded by Basson and Van As (1989) but slightly developed with sharp tangent point and without any protrusion on distal margin. The species

under discussion is also distinct from *H. robusta* in having straight and gradually tapered ray and of smaller body dimensions (Table 1).

Acknowledgements. The work was carried out in the Department of Zoology, University of Kalyani, West Bengal, India. The author is grateful to Dr. Jiří Lom of the Czech Academy of Science at České Budjéovice, Dr. J. G. Van As and Dr. Linda Basson of the Department of Zoology and Entomology, University of Orange Free State, South Africa, who examined the photomicrographs and confirms the status of the ciliate as a new species of *Trichodina*.

REFERENCES

Annandale N. (1912) Preliminary description of a freshwater medusa from the Bombay Presidency. *Rec. Indian Mus.* **7:** 253-256

Arthur J. R., Lom J. (1984) Trichodinid protozoa (Ciliophora: Peritrichida) from freshwater fishes of Rybinsk Reservoir, USSR. *J. Protozool.* **31:** 82-91

Asmat G. S. M., Haldar D. P. (1998) *Trichodina mystusi*-a new species of trichodinid ciliophoran from Indian estuarine fish, *Mystus gulio* (Hamilton). *Acta Protozool.* **37:** 173-177

Basson L., Van As J. G. (1989) Differential diagnosis of the genera in the family Trichodinidae (Ciliophora: Peritrichida) with the description of a new genus ectoparasitic on freshwater fish from Southern Africa. *Syst. Parasitol.* **13:** 153-160

Basu S., Haldar D. P. (1998) Comparative study on prevalence of protozoan parasites in pure and hybrid carps. *Environ. Ecol*. **16:** 584-587

Das M. K., Haldar D. P. (1987) Urceolariid ciliates of the genus *Tripartiella* invading gills of freshwater cultured carps in India. *Arch. Protistenkd*. **134:** 169-178

Das M. K., Pal R. N., Das P. B. (1987) Preliminary observations on the ecology of animal parasites in estuarine fishes of Deltaic West Bengal. *J. Indian Soc. Coastal Agric. Res.* **5:** 319-323

Hagargi S. S., Amoji S. D. (1979) Occurence of *Trichodina pediculus* Ehrenberg 1838 on freshwater carps, *Barbus* spp. *Curr. Sci*. **48:** 789-790

Klein B. M. (1958) The dry silver method and its proper use. *J. Protozool*. **5:** 99-103

Lom J. (1958) A contribution to the systematics and morphology of endoparasitic trichodinids from amphibians, with a proposal of uniform specific characteristics. *J. Protozool.* **5:** 215-263

Mishra R. K., Das M. K. (1993) Urceolariid ciliate, *Trichodina reticulata* infesting gills of *Catla catla* in India. *J. Inland. Fish. Soc. India*. **25:** 54-56

Mukherjee M., Haldar D. P. (1982) Observations on the urceolariid ciliates of the genera *Trichodina* and *Tripartiella* in freshwater teleosts. *Arch. Protistenkd.* **126:** 419-426

Saha B. S., Haldar D. P. (1996) First record of *Tripartiella bursiformis* (Davis, 1947) Lom, 1959 (Protozoa: Urceolariidae) from the gills of *Xenentodon cancila* (Hamilton) in the Indian subcontinent. *J. Beng. Nat. Hist. Soc. (NS*). **15:** 11-17

Saha B. S., Haldar D. P. (1997) Observations on the urceolariid ciliates of the genus *Tripartiella* Lom, 1959 parasitising the gills of three freshwater edible fishes of West Bengal, India. *J. Inland Fish. Soc. India*. **29:** 28-36

Saha B. S., Bandyopadhyay P. K., Haldar D. P. (1995a) Biodiversity of trichodinid ciliates in freshwater fishes of West Bengal. *Environ. Ecol.* **13:** 814-823

Saha B. S., Bandopadhyay P. K., Haldar D. P. (1995b) First record of *Paratrichodina* sp. (Protozoa: Urceolariidae) from the gills of *Notopterus notopterus* (Pallas) from the Indian subcontinent. *J. Beng. Nat. Hist. Soc. (NS)*. **4:** 35-42

Van As J. G., Basson L. (1989) A further contribution to the taxonomy of the Trichodinidae (Ciliophora: Peritrichida) and a review of the taxonomic status of some ectoparasitic trichodinids. *Syst. Parasitol.* **14:** 157-179

Van As J. G., Basson L. (1992) Trichodinid ectoparasites (Ciliophora: Peritrichida) of freshwater fishes of the Zambesi system, with a reappraisal of host specificity. *Syst. Parasitol*. **22:** 81-109

Wellborn T. L. Jr. (1967) *Trichodina* (Ciliata: Urceolariidae) of freshwater fishes of the Southeastern United States. *J. Protozool.* **14:** 399-412

Received on 6th September, 2000; accepted on 11th January, 2001

Acta Protozool. (2001) 40: 153 - 157

ACTA
PROTOZOOLOGICA

Short Communication

Alterations of Photophobic Motile Response in *Stentor* by Cyclic Guanosine 3', 5'- Monophosphate-elevating Agents

Mirosława WALERCZYK and Stanisław FABCZAK

Department of Cell Biology, Nencki Institute of Experimental Biology, Polish Academy of Sciences, Warszawa, Poland

Summary. The effects of exogenous cyclic nucleotides and modulators of the cyclic nucleotide signaling pathway on the step-up photophobic response have been studied in the ciliate *Stentor coeruleus*. To attain this, the latency time for the ciliary stop response and the ciliary reversal duration has been estimated using microscope videorecording and dark-field macro-photography. Membrane-permeable, slowly hydrolyzable analogs of cyclic GMP, 8-Br-cGMP and db-cGMP, significantly increase the latency time of ciliary stop response and decrease the period of ciliary reversal. By contrast, cyclic AMP analogs, 8-Br-cAMP or db-cAMP, had no measurable effect on the photophobic response parameters. The effects of the exogenous cGMP are mimicked by the application of the non-specific PDE inhibitor IBMX or zaprinast, a specific cGMP-PDE inhibitor. These behavioral observations suggest that *in vivo*, the internal level of presumed cGMP, but not cAMP, is possibly a limiting factor for the time course of the motile avoiding response of *Stentor*, and they further support the hypothesis that cGMP metabolism may play a role in photosignal transduction in these cells.

Key words: cGMP phosphodiesterase, ciliary stop and reversal response, cyclic nucleotide analogs, cyclic nucleotide phosphodiesterase inhibitors, photophobic response, phototransduction, *Stentor coeruleus*.

Abbreviations: cAMP = adenosine 3', 5'- cyclic monophosphate; 8-Br-cAMP = 8-bromo-cAMP; db-cAMP = N^6, 2'-o-dibutyryl-cAMP; cGMP = guanosine 3', 5'- cyclic monophosphate; 8-Br-cGMP = 8-bromo-cGMP; db-cGMP = N^6, 2'-o-dibutyryl-cGMP; DMSO = dimethyl sulfoxide; PDE = cyclic nucleotide phosphodiesterase; IBMX = 3-isobutyl-l-methylxanthine; zaprinast = 1,4-dihydro-5- [2-propoxyphenyl]-7H-1,2,3-triazolo [4,5-d]pyrimidine-7-one.

INTRODUCTION

The avoidance of an illuminated area by ciliate *Stentor coeruleus* results from a step-up photophobic response (Tartar 1961). This motile response may be elicited by a spatial or temporal increase in light intensity and it consists of a delayed stop of forward swimming, a period of ciliary reversal during which cell moves backwards and turns to one side, and subsequent stop of movement followed by resumption of forward swimming in a new direction (Wood 1976, Song *et al.* 1980, Fabczak *et al.* 1993b). The ciliary reversal in *Stentor* is caused, as in other ciliates, by an action potential, triggered, in turn, by a delayed depolarizing photoreceptor potential (Wood 1976, Fabczak *et al.* 1993b). The generation of receptor potential is a consequence of light absorption by numerous blue-green subpellicular pigment granules, arranged in longitudinal strips between

Address for correspondence: Stanisław Fabczak, Department of Cell Biology, Nencki Institute of Experimental Biology, ul. Pasteura 3, PL-02-093 Warszawa, Poland; Fax: (4822) 822 53 42; E-mail: sfabczak@nencki.gov.pl

each pair of ciliary rows (Tartar 1961, Tao *et al.* 1994). These granules contain stentorin, a hypericin derivative, as a chromophore (Møller 1962, Tao *et al.* 1994, Song 1995). At present, little is known about functional link between photoreceptors and the bioelectrical events preceding the observed photomotile behavior of *Stentor*. In preliminary studies, we suggested an existence a signaling chain in *Stentor*, which may involve cGMP as a second messenger (Fabczak *et al.* 1993a). In this paper, we have used a microscope videorecording system and pharmacological approach to further investigate the role of cGMP metabolism in the light-dependent motile responses in the ciliate *Stentor coeruleus*.

MATERIALS AND METHODS

Stentor coeruleus ciliates were grown in 0.5 l Petri dishes in a manner previously described (Koprowski *et al.* 1997). For cell harvesting, a chosen dish was placed on a dark or moderate illuminated background and then it was lighted from one side. In a short time, most ciliates collect at the side opposite to the light source (negative photodispersal effect). Thus, accumulated cells were transferred with a pipette to fresh culture medium devoid of nutritional components, referred to as a control medium. The selected cell sample was then placed in an appropriate solution filling a test chamber, located on a microscope stage. Each recording session of cell movements was performed usually after 60 min of cell adaptation to darkness and applied test solution. A constant temperature of 22°C of the solution filling recording chamber was maintained automatically throughout the experiment by an electronic device, based on a semiconductor Peltier element (Fabczak 1990). Test solutions containing derivatives of cGMP or cAMP were prepared simply by its addition to control medium, prepared daily from stock solution. Cyclic nucleotide PDE inhibitors, IBMX and zaprinast, were first dissolved in ethanol and DMSO, respectively, and then added to the control solution. The maximal final concentrations of both solvents in test solutions were 0.1% and the same amount of the solvents was included in the control solution for each series of experiments. All cyclic nucleotide analogs, 8-Br-cGMP, db-cGMP, 8-Br-cAMP and db-cAMP and IBMX were purchased from Sigma, whereas zaprinast was obtained from Alexis. All chemicals were of analytical reagent grade.

The photostimulation and video recordings of cell swimming pattern were carried out with methods described elsewhere (Fabczak *et al.* 1994, Fabczak 2000a). The effects of the tested substances on cell photobehavior were achieved by measurements of photophobic response parameters, such as latency of stop response (T_{CRL}, time between cell entry into light spot from a dark background and stop of cell forward swimming) and duration of backward swimming (T_{CRD}, time of ciliary reversal) expressed as percentage change in relation to the control values (taken arbitrarily as 100%).

A dark-field and low-magnification photography was used for an illustration of cell motility pattern under different experimental conditions (Ferguson 1957, Dryl 1958).

RESULTS AND DISCUSSION

To test the effects of cyclic nucleotides on cell photophobic movement, both the T_{CRL} and T_{CRD} parameters of photophobic responses were evaluated in cells exposed to dibutyryl- or 8-bromo-substituted cyclic nucleotide analogs, 8-Br-cAMP and 8-Br-cGMP or db-cAMP and db-cGMP. These compounds, being lipophilic analogs of cAMP and cGMP, possess considerable membrane permeability and are relatively poorly hydrolyzed by cyclic nucleotide PDEs (Braumann and Jastorff 1985, Zimmerman *et al.* 1985, Krass *et al.* 1997). When 8-Br-cGMP or db-cGMP analogs in final concentrations between 0.25 and 2.00 mM were applied to *Stentor via* bath addition, the time course of photophobic response underwent significant alterations in a dose-dependent manner (Fig. 1). In cells treated by 2 mM 8-Br-cGMP for 5 min, the T_{CRL} value was increased two-fold and T_{CRD} reduced by about 73% compared with controls (Fig. 1A). As illustrated in Fig. 3A-D, the inhibitory effect of cGMP was larger with prolongation of incubation time. The influence of db-cGMP analog on the cell response latency or ciliary reversal duration was also very large (Fig. 1B) but somewhat lower than that of 8-Br-cGMP, probably due to differences in membrane permeability or metabolic turnover of a particular cyclic nucleotide analog by PDEs. In contrast, both 8-Br-cAMP and db-cAMP analogs were ineffective at the same applied concentrations and incubation.

These results demonstrate that application of membrane-permeable cGMP analogs, which are expected to increase intracellular cGMP levels, significantly modulates the light avoiding motile behavior of *Stentor* cells. The negative results obtained using membrane-permeable cAMP analogs serve, as a control, to evidence the specificity of the action of cGMP on cell photobehavior. These might indicate that, *in vivo,* the level of presumed cGMP, but not cAMP, in *Stentor* is perhaps a limiting factor for the cGMP signaling pathway and increased cGMP levels might suppress the signaling chain efficiency. This might demonstrate a direct or indirect causal connection between the kinetics of the signaling process and time course of the cell motile response to light. A slower processing of light signals resulting from cGMP accumulation could lengthen the T_{CRL} and decrease T_{CRD} periods. On the other hand, a higher efficiency of signal pathway could lead to a shortening and prolongation of the T_{CRL} and T_{CRD} response parameters,

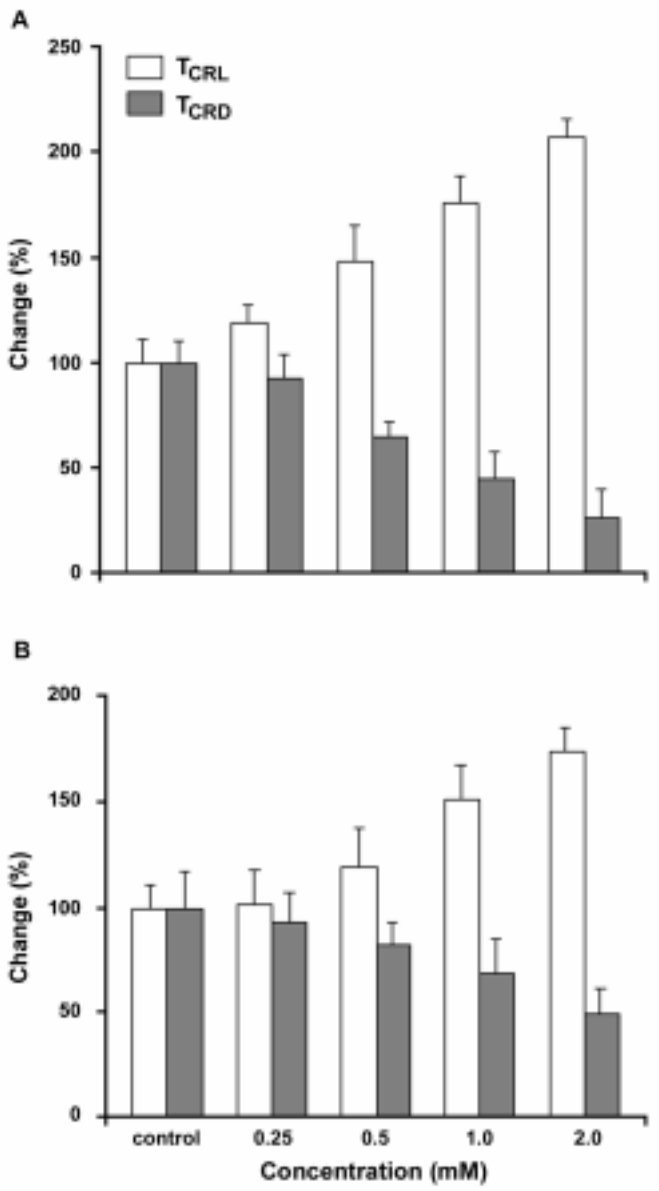

Fig. 1. Effect of 8-Br-cGMP (A) and db-cGMP (B) analogs on photophobic response elicited with standard white light stimuli (5 x 10^{-4} Wcm^{-2}). The ciliary stop response latency (T_{CRL}) and duration of backward swimming (T_{CRD}) were determined in dark-adapted cells in control medium and in this medium supplemented with cGMP analogs at the indicated concentrations. All data (in percent) are given as mean ± S.E of measurements on 60-80 cells

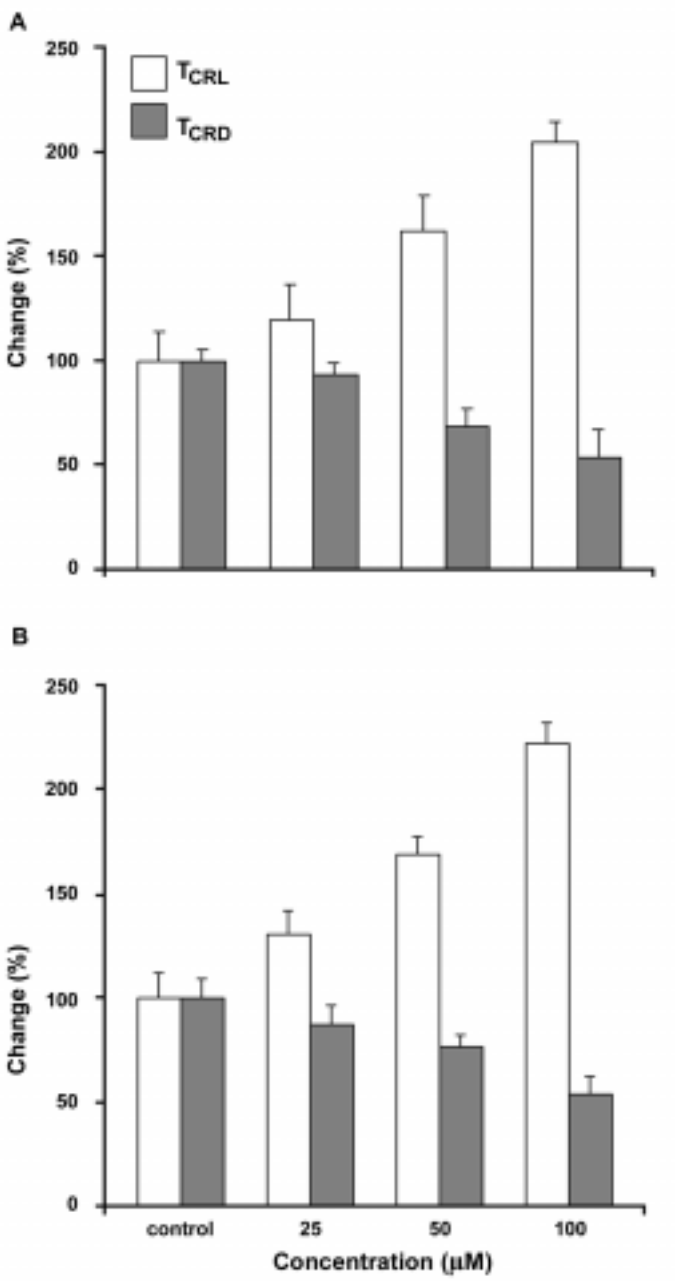

Fig. 2. Effect of IBMX (A) and zaprinast (B) on photophobic response. The T_{CRL} and T_{CRD} values were estimated in control medium including appropriate solvent concentrations (ethanol or DMSO) and in medium supplemented with IBMX and zaprinast at the indicated concentrations. Other details as for Fig. 1

respectively. This closely resembles earlier behavioral observations on the reciprocal relationship between the response latency and duration of ciliary reversal in *Stentor*, when photophobic responses were elicited with light stimuli of variable intensity (Fabczak *et al.* 1993a). Thus, the photophobic response of prolonged T_{CRL} and decreased T_{CRD} can be obtained under both experimental circumstances - when signal turnover is disturbed by an application of cGMP-elevating agents, as found in the present experiments, or during cell stimulation with light stimuli of low fluence rates, as observed earlier (Fabczak *et al.* 1993a).

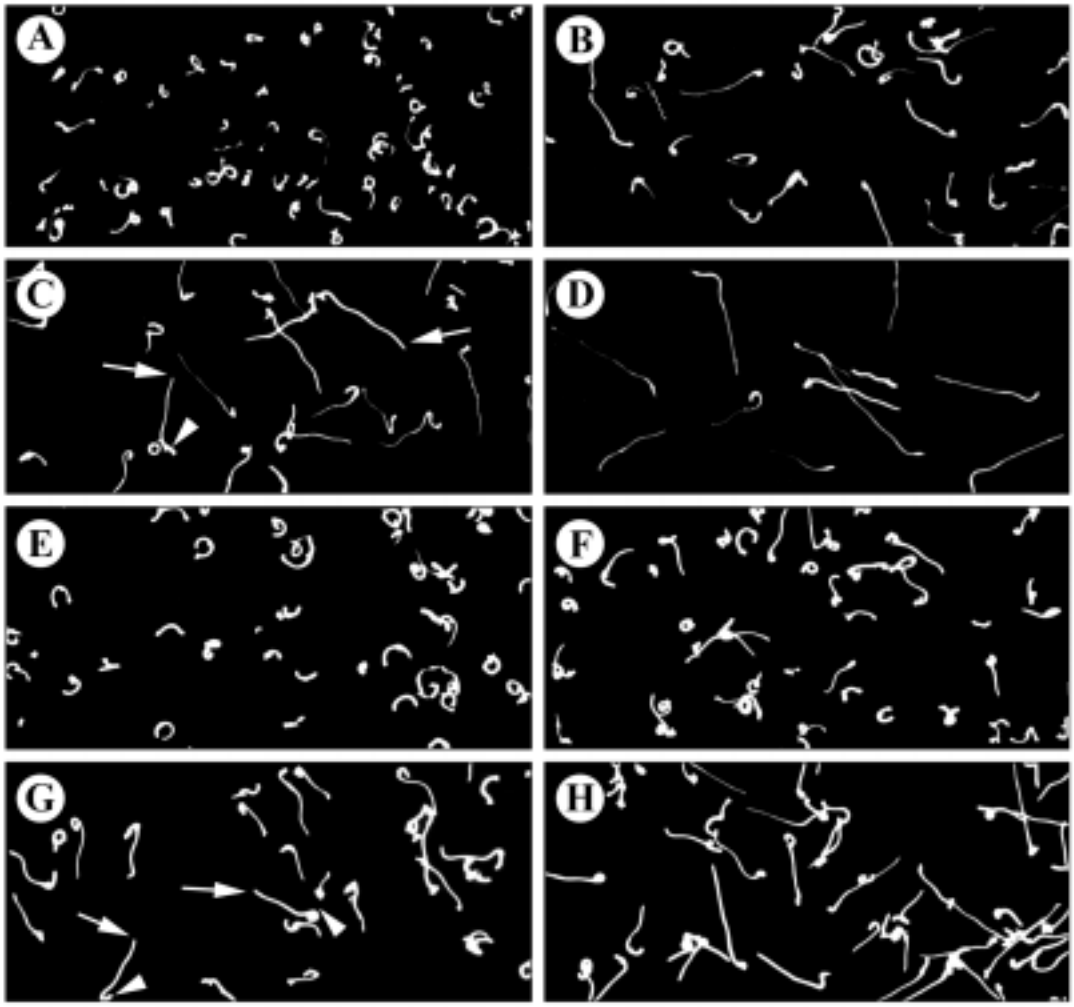

Fig. 3. Dark-field and low-magnification photographs of *Stentor* photobehavior (motility tracks) under different experimental conditions. The photophobic response of dark-adapted cells to standard light stimulus in control medium (A) and in the presence of 3 mM 8-Br-cGMP analog (B-D) applied for 1 min (B), 10 min (C) and 30 min (D) or in control medium supplemented with 0.1% ethanol (E) and in the presence of 25 μM IBMX (F-H) applied for 1 min (F), 10 min (G) and 30 min (H). Arrows and arrowheads in (C) or (G) indicate the onset of light stimulus and ciliary reversal, respectively. The photographs were taken with an exposure time of 6 s

To verify whether *Stentor* cells contain an endogenous enzymatic pathway for cGMP metabolism, we externally applied a non-specific PDE inhibitor, IBMX and a specific cGMP PDE inhibitor, zaprinast (Amer and Kriegbaum 1975, Goldberg and Haddox 1977, Turko *et al.* 1999). IBMX and zaprinast are known to effectively raise the intracellular concentration of cGMP, as a consequence of inhibition of cGMP degradation by PDE, when cGMP synthesis catalyzed by a guanylate cyclase remains unaffected (Goldberg and Haddox 1977, Burns *et al*. 1992). Both of these agents applied at micromolar concentrations (25-100 μM) modulated T_{CRL} similarly to the effects of cGMP analogs (Fig. 2). An application of IBMX (Fig. 2A) or zaprinast (Fig. 2B) at a concentration of 100 μM extended the T_{CRL} two-fold and more than 2,2-fold, respectively, whereas T_{CRD} was decreased in both cases by about 46% compared with those photoresponse parameters in appropriate control solutions (Figs. 2A,B). As in the case of cGMP analogs, an increase in the incubation time caused more pronounced inhibitory effects of IBMX (Fig. 3E-H). No toxic effects for either drug were observed, as judged by the continuing regular cell swimming at the inhibitor concentrations used. These observations indicate that a decrease in PDE activity in *Stentor* may cause changes in cytoplasmic cGMP levels and, as a consequence, the photophobic response coupled to the cGMP messenger might be suppressed.

Since the inhibitory effects of the used compounds, cGMP analogs and antagonists to cyclic nucleotide PDE are presumably due to the accumulation of internal cGMP in *Stentor*, the decrease in cellular cGMP concentration is considered to be implicated in the cell phobic response to light stimuli. This supposition is consistent with the recently reported preliminary results of *in vivo* estimation of endogenous cyclic nucleotide levels in *Stentor* cells using highly specific cyclic nucleotide radioimmunoassay (Walerczyk *et al.* 2000, Walerczyk and Fabczak 2001). These experiments evidently show that, in dark-adapted cells following illumination, a decrease in intracellular cGMP level occurs. The measured alterations in cGMP levels were observed to be suppressed strongly by cyclic nucleotide PDE inhibitors, such as IBMX or theophylline (Darcy and Fisher 1990). Moreover, a presence of cGMP-activated channels and 63 kD protein that specifically bind cGMP were confirmed in ciliate cortex fraction with an electrophysiological patch-clamp and immunochemical methods, respectively (Fabczak 2000b, Walerczyk *et al.* 2000). Also in *Stentor* cells, a transducin-like G-protein was detected using α-transducin antibody (Fabczak *et al.* 1993a). Based on the presented findings, it appears that the photosensitive unicellular organism *Stentor, as* in olfactory- and photo-receptor cells (Fesenko *et al.* 1985, Nakamura and Gold 1987), possess biochemical machinery that involve events from light absorption by photoreceptor pigments (hypericin-like stentorin) *via* G-protein-coupled phosphodiesterase activation to directly modulate membrane cGMP-gated ion channels.

Acknowledgments. This work represents a part of the Ph. D. thesis project (of M. W.) and was supported by Committee for Scientific Research Grant 6-P04C-011-19 (to S. F.).

REFERENCES

Amer M. S., Kriegbaum W. E. (1975) Cyclic nucleotide phosphodiesterase properties: Activators, inhibitors, structure-activity relationship and possible role in drug development. *J. Pharmacol. Sci.* **64:** 1-64

Braumann T., Jastorff B. (1985) Physicochemical characterization of cyclic nucleotides by reversed phase high-performance liquid chromatography. II. Quantitative determination of hydrophobicity. *J. Chromatogr.* **350:** 105-118

Burns F., Rodger I. W., Pyne N. J. (1992) The catalytic subunit of protein kinase A triggers activation of the type V cyclic GMP-specific phosphodiesterase from guinea-pig lung. *Biochem. J.* **283:** 487-491

Darcy P. K., Fisher P. R. (1990) Pharmacological evidence for a role for cyclic AMP signaling in *Dictyostelium discoideum* slug behavior. *J. Cell Sci.* **96:** 661-887

Dryl S. (1958) Photographic registration of movement of protozoa. *Bull. Acad. pol. Sci. Cl. II Sér. Sci. biol.* **6:** 429-430

Fabczak H. (2000a) Contribution of phosphoinositide-dependent signaling to photomotility of *Blepharisma* ciliate. *J. Photochem. Photobiol.* **55:** 120-127

Fabczak H. (2000b) Protozoa as a model system for studies of sensory light transduction: mechanism of photophobic response in the ciliate *Stentor* and *Blepharisma. Acta Protozool.* **39:** 171-181

Fabczak H., Park P. B., Fabczak S., Song P.-S. (1993a) Photosensory transduction in ciliates. II. Possible role of G-protein and cGMP in *Stentor coeruleus. Photochem. Photobiol.* **75:** 702-706

Fabczak S. (1990) Free potassium and membrane potential in cells of *Blepharisma japonicum. Acta Protozool.* **29:** 179-185

Fabczak S., Fabczak H., Tao N., Song P.-S. (1993b) Photosensory transduction in ciliates. I. An analysis of light-induced electrical and motile responses in *Stentor coeruleus. Photochem. Photobiol.* **57:** 696-701

Fabczak S., Fabczak H., Song P.-S. (1994) Ca^{2+} ions mediate the photophobic response in *Blepharisma* and *Stentor. Acta Protozool.* **33:** 93-100

Ferguson M. L. (1957) Photographic technique for quantitative physiological studies of *Paramecium* and other motile cells. *Physiol. Zool.* **30:** 208-215

Fesenko E. E., Kolesnikov S. S., Lyubarski A. L. (1985) Induction of cyclic-GMP of cation conductance in plasma membrane of retinal rod outer segment. *Nature* **313:** 310-313

Goldberg N. D., Haddox M. K. (1977) Cyclic GMP metabolism and involvement in biological regulation. *Annu. Rev. Biochem.* **46:** 823-896

Koprowski P., Walerczyk M., Groszyńska B., Fabczak H., Kubalski A. (1997) Modified patch-clamp method for studying ion channels in *Stentor coeruleus*. *Acta Protozool.* **36:** 121-124

Krass J. D., Jastorff B., Genieser H.-G. (1997) Determination of lipophilicity by gradient elution high-performance liquid chromatography. *Anal. Chem.* **69**: 2575-2581

Møller K. M. (1962) On the nature of stentorin. *Comp. Rend. Trav. Lab. Carlsberg* **32:** 471-497

Nakamura T., Gold G. H. (1987) A cyclic nucleotide-gated conductance in olfactory receptor cilia. *Nature* **325:** 442-444

Song P.-S., Hader D.-P., Poff K. L. (1980) Step-up photophobic response in the ciliate *Stentor coeruleus. Arch. Microbiol*. **126:** 181-186

Song P.-S. (1995) The photomechanical responses in the unicellular ciliates. *J. Photosci.* **2:** 31-35

Tao T., Deforce L., Romanowski M., Meza-Keuthen M. S., Song P.-S., Furuya M. (1994) *Stentor* and *Blepharisma* photoreceptors: structure and function. *Acta Protozool*. **33:** 199-211

Tartar V. (1961) The Biology of *Stentor.* In: International Series of Monographs on Pure and Applied Biology, (Ed. G. A. Kerkut), Pergamon Press, Oxford, London, New York, Paris, **5:** 11-25

Turko I. V., Ballard S. A., Francis S. H., Corbin J. D. (1999) Inhibition of cyclic GMP-binding cyclic GMP-specific phosphodiesterase (Type 5) by sildenafil and related compounds. *Mol. Pharmacol.* **56:** 124-130

Walerczyk M., Fabczak H., Fabczak S. (2000) Cyclic cGMP-gated channels are present in ciliate *Stentor coeruleus*. *Post. Hig. Med. Doświad*. **54:** 329-339

Walerczyk M., Fabczak S. (2001) Pharmacological evidence for a role for cyclic GMP signalling in *Stentor coeruleus* motile behavior. *Photochem. Photobiol.* (in press)

Wood D. C. (1976) Action spectrum and electrophysiological responses correlated with the photophobic response of *Stentor coeruleus. Photochem. Photobiol*. **24:** 261-266

Zimmerman A. L., Yamanaka G., Eckstein F., Baylor D. D., Stryer L. (1985) Interaction of hydrolysis-resistant analogs of cyclic GMP with the phosphodiesterase and light sensitive channel of retinal rod outer segment. *Proc. Natl. Acad. Sci. USA* **82:** 8813-8817

Received on 14th March, 2001; accepted March 23rd, 2001

Acta Protozool. (2001) 40: 159 - 160

ACTA
PROTOZOOLOGICA

Short Communication

Membranous Whorl Associated with the Mitochondrion of *Leishmania mexicana*

Anabella SEBASTIAN[1], Hector J. FINOL[2] and Felix TEJERO[1]

[1]Section of Parasitology, Institute of Tropical Zoology, Faculty of Sciences, Central University of Venezuela, Caracas and [2]Center for Electron Microscopy, Faculty of Sciences, Central University of Venezuela, Caracas, Venezuela

Summary. Recent studies carried out in our laboratory had shown a singular structure in the mitochondrion of *Leishmania mexicana* during its *in vitro* development. This particular structure looks like a membranous whorl.

Key words: *Leishmania mexicana*, membranous whorl, mitochondrion, parasite.

We have observed that during the development of the Trypanosomatidae (specially *L. mexicana*) a portion of the mitochondrion proliferates, and assumes the form of elaborated convoluted structures with rough endoplasmic reticulum elements occupying, regularly arranged, grooves into the mitochondrial mass. Similar submicroscopic patterns had been described earlier. Indeed, Vickerman and Preston (1976), suggested that this labyrinth could be a mitochondrial system in a compact condition, ready for expansion after multiplication. In addition, Pannese (1966) and Ghadially (1997), had described membranous whorls in vertebrate mitochondria of ganglion neuroblasts and renal cells, respectively. They suggested that these membranous processes might be related to new mitochondrion formation.

In our *L. mexicana* samples (Deane *et al*. 1966), this arrangement was found in association with the mitochondrial envelope (Fig. 1). Apparently, patterns in such a manner could represent a mitochondrial transformation related to autolytic processes. The assembly itself seems to involve changes linked to the development of dense osmiophilic layers, the membranous whorl formation, as well as the transformation of such structures into lysosomal bodies, which eventually can be converted in myelin-like figures. These *L. mexicana* whorls could be acting like a storage area of mitochondrial envelope derived from condensed forms. We have seen that during the *in vitro* development of *L. mexicana* in LIT medium (Docampo *et al.* 1974), organellar ultrastructure takes different complexity arrangements. Probably, it is

Address for correspondence: Felix Tejero, Apartado 60006, Chacao, Caracas 1060, Venezuela; Fax: +58(212)2645213; E-mail: ftejero@reacciun.ve

Fig. 1. This electron micrograph shows a mitocondrial membranous whorl in a *Leishmania mexicana* promastigote. Scale bar - 4, 2 µm

consequence of the medium chemical composition, stages of development occurring in the culture, metabolic changes, and/or continuous series of organellar degeneration, among others.

Whorl formation in trypanosomatids has only been reported in *Crithidia fasciculata* (Hill *et al.* 1968) and *Trypanosoma raiae* (Vickerman and Preston 1976). Therefore, it is necessary to continue this line of investigation in order to establish if these arrays are present in other members of the family and/or order.

Acknowledgements. This work was supported by grant # 03-10-4169-98 from the Consejo de Desarrollo Científico y Humanístico de la Universidad Central de Venezuela.

REFERENCES

Deane M., Chaves J., Torrealba J. W., Torrealba J. F. (1966) Aislamiento de leishmanias de la médula ósea y de la sangre de una paciente con leishmaniasis tegumentaria difusa. *Gaceta Méd. Caracas* **74:** 367-371

Docampo R., Boiso J. F., Stoppani A. O. M. (1974) Diferencias metabólicas en *Trypanosoma cruzi* dependientes de las condiciones de cultivo. *Rev. Asoc. Arg. Microbiol*. **6:** 7-14

Hill G. C., Brown C. A., Clark M. V. (1968) Structure and function of mitochondria in *Crithidia fasciculata*. *J. Protozool.* **15:** 102-109

Pannese E. (1966) Structures possibly related to the formation of new mitochondria in spinal ganglion neuroblast. *J. Ultrastruct. Res.* **15:** 57-65

Ghadially F. N. (1997) Ultrastructural Pathology of the Cell and Matrix. vol. 1. 4 ed. Butterworth-Heinemann, Boston

Vickerman K., Preston T. M. (1976) Comparative cell biology of the Kinetoplastida. In: Biology of the Kinetoplastida, (Eds. W. H. R. Lumsden and D. A. Evans). Academic Press, London **1:** 35-130

Received and accepted on 27th March, 2001

Acta Protozool. (2001) 40: 161 - 167

ACTA
PROTOZOOLOGICA

Short Communication

Chloroplast Ultrastructure of *Euglena cuneata* Pringsheim, *E. deses* Ehrenberg and *E. mutabilis* (Euglenophyceae): Taxonomic Significance

Bożena ZAKRYŚ[1], Jaume CAMBRA-SANCHEZ[2] and Patricia L. WALNE[3]

[1]Department of Plant Systematics and Geography, Warsaw University, Warszawa, Poland; [2]Department of Vegetal Biology, Barcelona University, Barcelona, Spain; [3]Department of Botany, University of Tennessee, Knoxville, USA

Summary. For the first time the "unilateral" pyrenoids of *Euglena* were studied by transmission electron microscopy in three taxa: *E. deses* var. *deses* Ehrenberg, *E. deses* Ehr. var. *intermedia* Klebs and *E. mutabilis* Schmitz. The presence of pyrenoids in *E. deses* var. *intermedia* has been uncertain. Our investigations show that these three taxa have chloroplasts with pyrenoids. Centrally or laterally located in each plastid, the pyrenoid matrix is penetrated by a few thylakoids (*E. deses*) or by many (*E. mutabilis*).

The chloroplast morphology and ultrastructure of *Euglena cuneata* Pringsheim were also studied for the first time. The species has one stellate, axial chloroplast with pyrenoid and the pyrenoid matrix forms a net-like pattern; no thylakoids penetrate the pyrenoid.

Key words: chloroplast, *Euglena, E. cuneata, E. deses, E. mutabilis,* pyrenoid, systematics, taxonomy, ultrastructure.

INTRODUCTION

The identification of *Euglena* taxa has been based largely on morphological characters at the light-microscopic level, but especially on the historically important criterion of chloroplasts (their number, size, location; presence or absence of pyrenoids; number, morphology and location of paramylon grains). Many authorities have acknowledged chloroplast characteristics as the major criteria for the establishment of an intrageneric classification for *Euglena* (Dangeard 1901; Lemmermann 1913; Chu 1946; Gojdics 1953; Huber-Pestalozzi 1955; Pringsheim 1956; Zakryś 1986, 1997).

For most of the species of *Euglena*, however, details about the chloroplast are insufficiently known and described, a particular concern for the taxa for which plastid organization or pyrenoid presence are not visible in the light microscope, thus necessitating more detailed examination by transmission electron microscopy.

Of special interest for this investigation are three species of the genus *Euglena* for which chloroplast ultrastructure is not described: *E. cuneata, E. deses and E. mutabilis.* Light-microscopic observations to date on these organisms (Gojdics 1953, Huber-Pestalozzi 1955, Pringsheim 1956, Popova 1966, Péterfi 1986, Zakryś 1986, Zakryś and Walne 1994, Németh 1997, Kim *et al.* 1998, Zhi *et al.* 1999, Dillard 2000) have not allowed definitive determinations about the number of

Address for correspondence: Bożena Zakryś, Department of Plant Systematics and Geography, Warsaw University, Aleje Ujazdowskie 4, PL-00-478 Warszawa, Poland; E-mail: Zakrys@mercury.ci.uw.edu.pl

the plastids (*E. cuneata*) or the presence and organization of pyrenoids (*E. cuneata, E. deses and E. mutabilis*).

The purpose of this investigation is thus twofold:

(1) To document chloroplast number and morphology for *E. cuneata,* for which ultrastructural details have been unreported, and to compare these data to other known species with similar chloroplast organization: *E. geniculata, E. myxocylindracea, E. stellata, E. tristella* and *E. viridis*.

(2) To study the ultrastructure of "unilateral" pyrenoids and to document their presence for *E. mutabilis* and two varieties of *E. deses.*

MATERIALS AND METHODS

Cultures

Three strains of *Euglena* were obtained from the Sammlung von Algenkulturen (SAG), Göttingen, Germany: *E. cuneata* Pringsheim, strain # 26.93 (authentic strain); *E. deses* var. *deses* Ehrenberg strain # 1224-19b, *E. mutabilis* Schmitz, strain # 1224-9b. One strain of *E. deses* var. *intermedia* was isolated from Poland (Warsaw Botanical Garden). Clones derived from each strain were cultured in liquid media (3C - Starr 1978) and under identical conditions in a growth chamber maintained at 19° C and 16 : 8 h L/D, *ca* 27 µmol photons m^{-2} s^{-1} provided by cool-white fluorescent tubes. Two-week-old cultures were used for the electron-microscopic studies.

Transmission electron microscopy

Actively swimming cells were harvested by low-speed centrifugation and fixed in 2% glutaraldehyde buffered with 0.05 M sodium cacodylate, pH 7.2, for 1 h at 4° C. After several rinses in buffer, the samples were post-fixed in buffered 2% OsO_4 also for 1 h at 4° C, followed by dehydration in a graded ethanol/acetone series and embedment in Spurr's low-viscosity resin. Thin sections were cut with a diamond knife on a Reichert Ultracut-E ultramicrotome and were stained sequentially with uranyl acetate and lead citrate, prior to examination in a Hitachi H-600 transmission electron microscope.

RESULTS

The cells of *Euglena cuneata* have axial chloroplasts often obscured other cellular structures and organelles. The plastids are not readily discernible or only faintly so in the light microscope, thus necessitating more detailed examination by transmission electron microscopy, as described below.

Euglena cuneata Pringsheim. The chloroplast is a single, stellate and elongate structure, which fills the entire axial part of the cell displacing the nucleus from a central position towards the periplast (light microscope observations). The chloroplast contains a large central pyrenoid (Figs. 1, 2, 4). An integral part of the plastid, the pyrenoid is not surrounded by a defining membrane and is readily identifiable by its matrix, which forms a net-like pattern, composed of areas of high and low electron opacity (Figs. 2-6). No thylakoids penetrate the pyrenoid.

Euglena deses Ehrenberg. Since there is discrepancy in the literature about the occurrence of pyrenoids in this species, we used one strain obtained from an algal culture collection identified as *E. deses* var. *deses* (with small paramylon grains only - Figs. 7, 11, 12, 14, 15) and one strain isolated from Poland which has both large and small paramylon grains in the cells (*E. deses* var. *intermedia* - Figs. 8-10, 13). In both varieties (var. *typica* and var. *intermedia)* the plastid organization is identical, and each chloroplast contains a pyrenoid. The pyrenoids are rather small and not always located in the center of chloroplasts (Figs. 7-12). The pyrenoid matrix is penetrated by a few thylakoid pairs that are continuous with the typical euglenoid triplet lamellae (Figs. 13-15, arrowheads).

Euglena mutabilis Schmitz. In cells of *E. mutabilis* the chloroplasts are much larger compared with those of *E. deses*, the pyrenoids are scarcely visible and then mostly when the cells are kept in good growth conditions. For this study we used only one strain of *E. mutabilis* obtained from an algal culture collection. The main part of each large chloroplast contains a pyrenoid (Figs. 16-18). Centrally located in the plastid, the pyrenoid matrix is penetrated by numerous thylakoid triplets that are continuous with lamellar quadruplets in the chloroplast stroma. The quadruplet lamellae traverse the matrix parallel to each other at regular distances, creating a pattern (Figs. 18-20).

DISCUSSION

Our investigation shows that *Euglena cuneata* has a similar chloroplast structure to *E. geniculata, E. myxocylindracea, E. stellata, E. tristella* and *E. viridis* (Haller 1959; Mignot 1965, 1966; Buetow 1968; Leedale 1968; Dragos *et al.* 1979; Péterfi *et at.*1979; Zakryś and Walne 1998). The major difference among these species is chloroplast number (one per cell in *E. cuneata, E. myxocylindracea, E. stellata* and *E. viridis*; two in *E. geniculata*; three in *E. tristella).*

Euglena cuneata differs from the rest of the taxa in two aspects: (a) the pyrenoid is large and its matrix

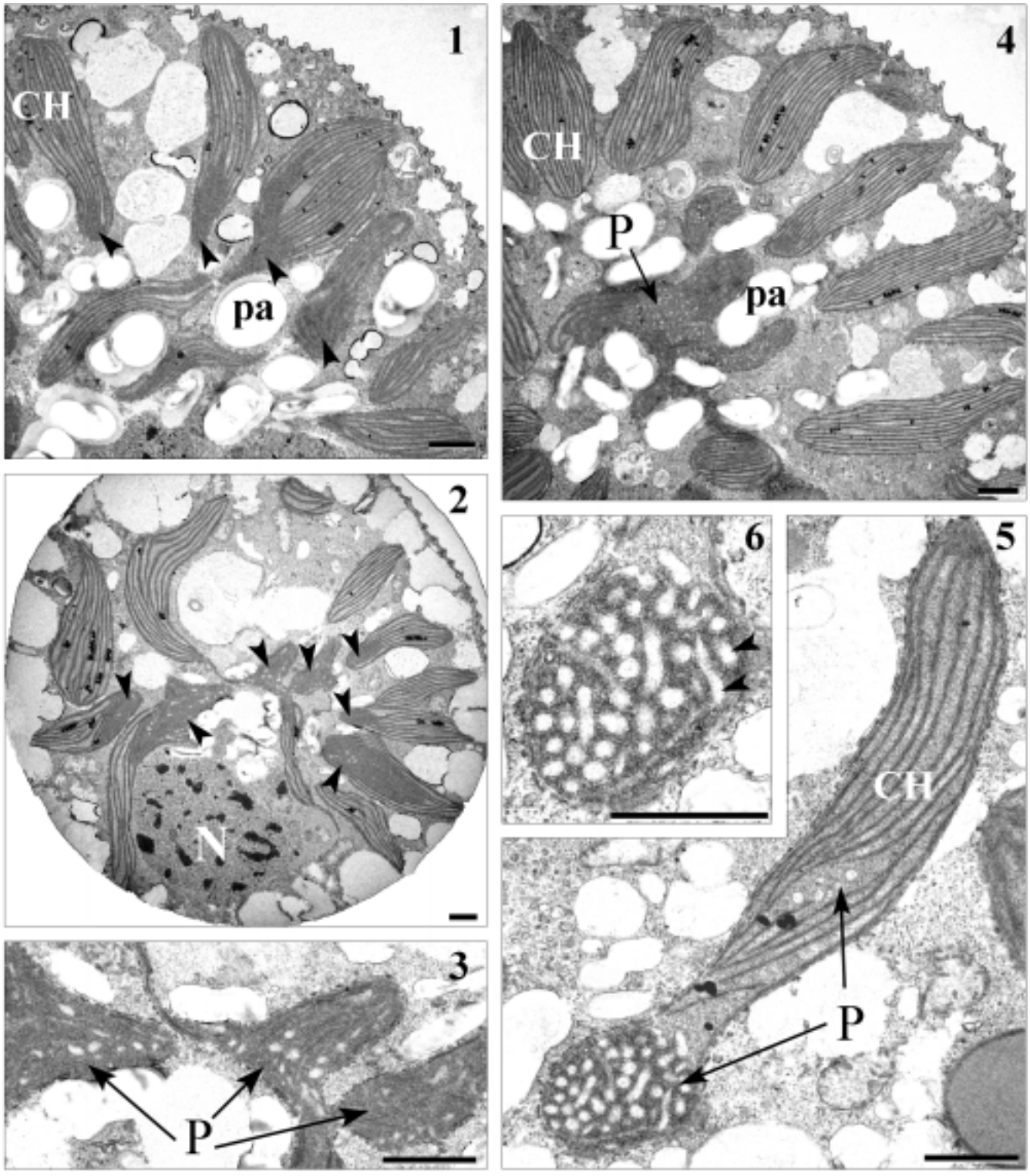

Figs. 1-6. *Euglena cuneata*; **1, 2, 4** - transverse sections through various levels of cell show single chloroplast (CH) with pyrenoid (P and arrows), nucleus (N), and paramylon grains (pa); **3, 5, 6** - higher magnification of pyrenoid (P) shows net-like structure of the matrix. Scale bars - 1 μm

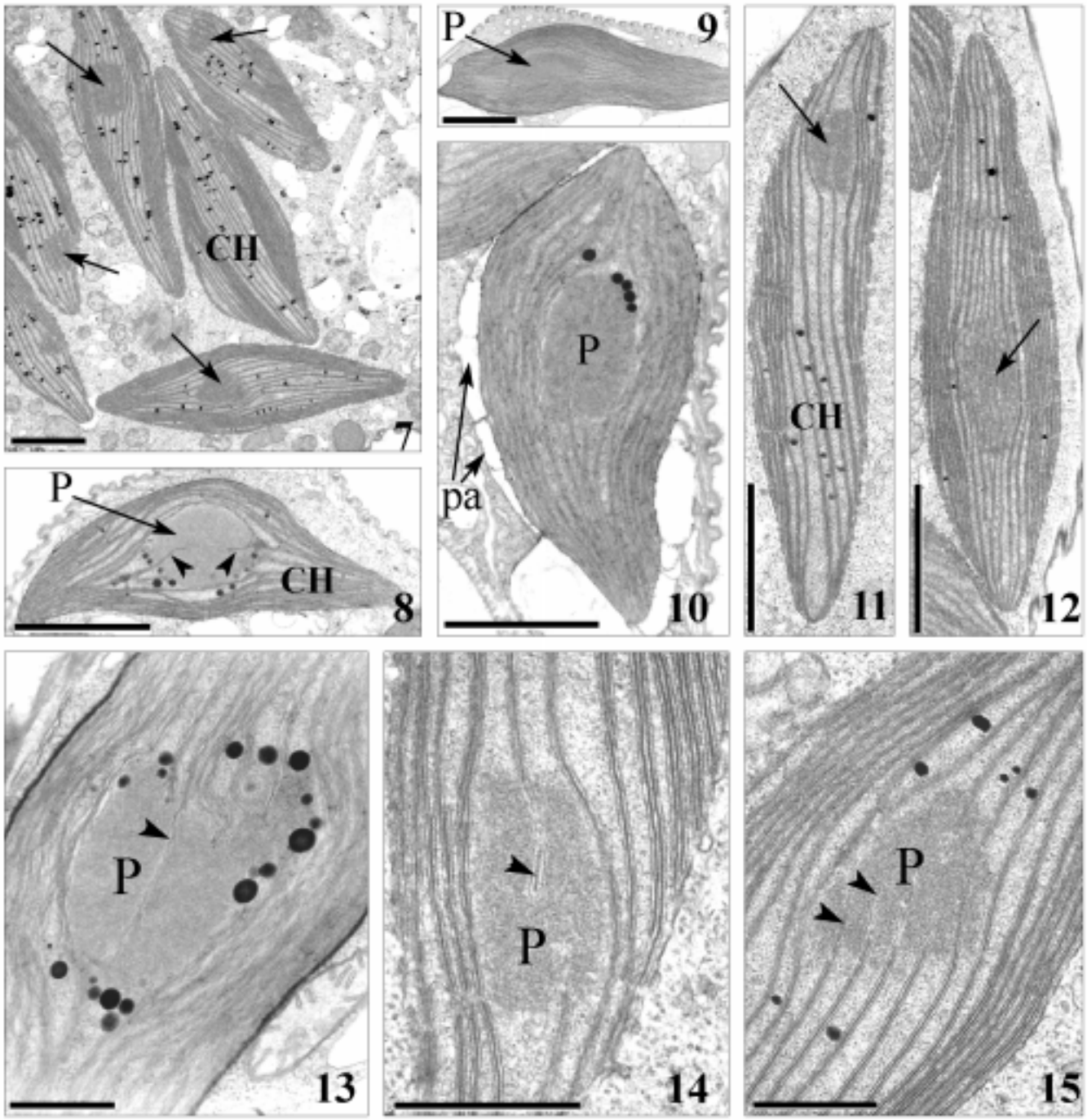

Figs. 7-15. *Euglena deses*; **7-12** - chloroplasts (CH) with pyrenoids (P and arrows) and paramylon cap (pa) in var. *deses* (7, 11, 12) and var. *intermedia* (8-10), scale bars - 5 µm; **13-15** - higher magnification of pyrenoids (P) showing matrices traversed by thylakoids (arrows) in var. *intermedia* (13) and var *deses* (14, 15), scale bars - 0.5 µm

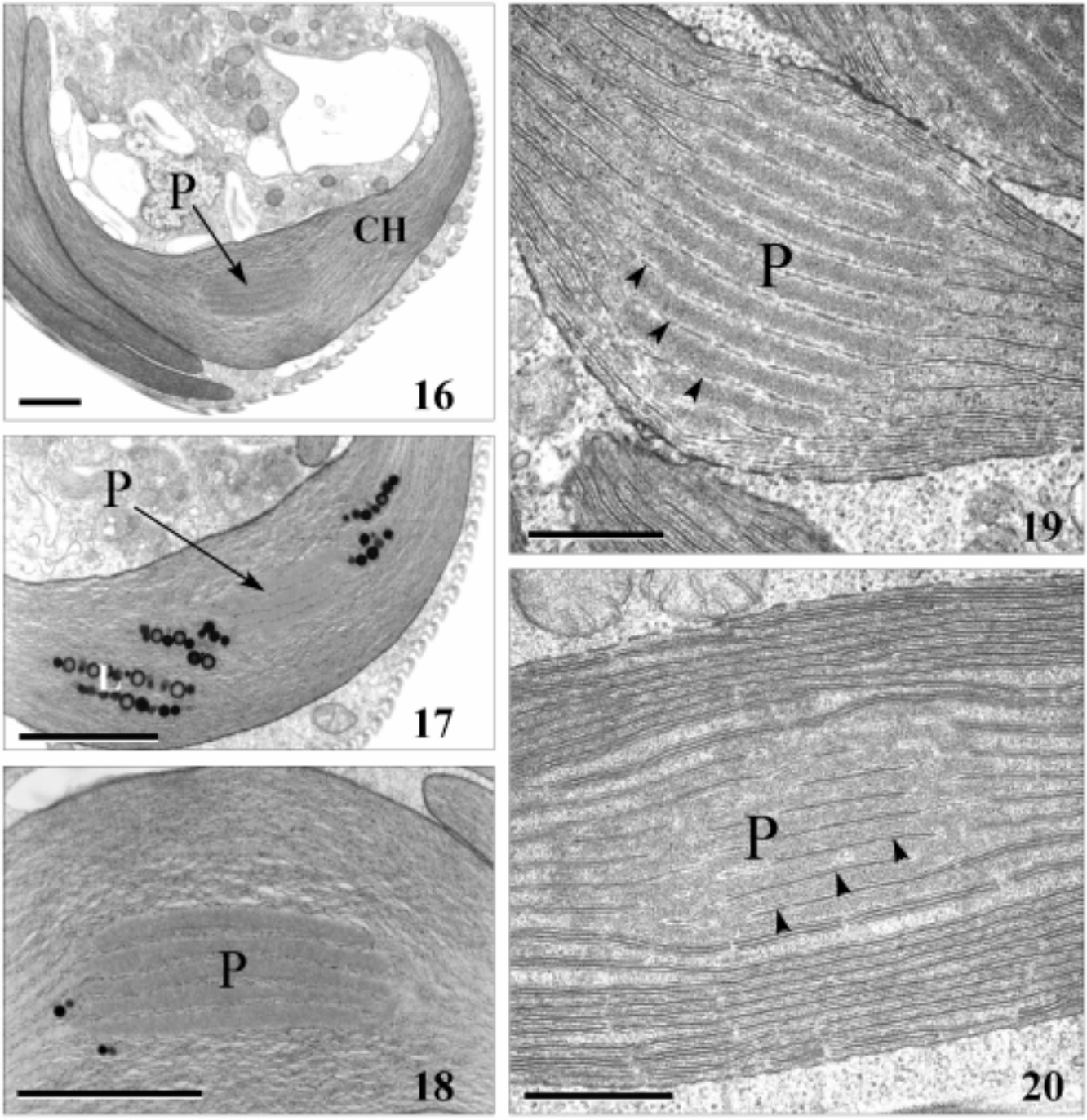

Figs. 16-20. *Euglena mutabilis*; **16-18** - transverse views of chloroplasts (CH) with pyrenoids (P) and lipid granules (L), paramylon grains (pa), scale bars - 5μm; **19, 20** - higher magnification of pyrenoids (P) showing matrices traversed by parallel thylakoids (arrows), scale bars - 0.5 μm

forms a net-like pattern (Figs. 1, 2, 4-6); (b) the main part of its single chloroplast containing the pyrenoid is large and long, displacing the nucleus from a central position towards the periplast (light microscope observations).

Except for the original descriptions of *E. cuneata* (Pringsheim 1956), and two floristic reports about its occurrence (one from Rumania - Péterfi 1986, and one from China - Zhi 1999), there is no written information about the taxa. Such paucity of information is understandable since *E. cuneata* is very rare, also because it may have been mistaken for similar species as *E. stellata* or *E. viridis.* Fortunately the authentic strain is still available from algal culture collections, so this study could be carried out.

Two varieties of *E. deses* were also examined to explore the existing contradictions concerning the presence or absence of pyrenoids in var. *deses* (with only small paramylon grains) and in var. *intermedia* (with small and large paramylon grains). Some authors (Gojdics 1953, Pringsheim 1956, Popova 1966, Németh 1997, Zhi *et al.* 1999, Dillard 2000) observed pyrenoids in the cells of the *typical* variety only. Some other authors could not see pyrenoids in the cells of both varieties (Huber-Pestalozzi 1955, Zakryś 1986, Zakryś and Walne 1994, Kim *et al.* 1998, Wołowski 1998). Both strains were studied by light microscopy and no pyrenoids were observed in any cell. The electron- microscopic results however show that in both varieties the pyrenoids are present and the plastid organization is identical. Only in a few cases in both varieties, flat "paramylon caps" in association with the pyrenoids were observed. The caps were situated on one side of the chloroplasts (Fig. 10). Such "one sided paramylon caps" are apparently formed in good growth conditions and disappear when the environment changes, but their presence is interpreted as a presence of pyrenoids. It may explain the erratic occurrence or observation of the "unilateral" pyrenoids in the light microscope. Nevertheless, additional experimental research is necessary to understand these phenomena.

"Unilateral" pyrenoids also reported in *E. mutabilis,* are hardly visible in the light microscope, although the chloroplasts are much larger compared with those of *E. deses*. It is not even possible to see them when the strains are kept on synthetic media in culture for many years, and in this study the pyrenoids were not observed either. But their presence was confirmed by electron microscopy. No "paramylon caps" were observed, although numerous paramylon grains were noted on the curved side of the chloroplasts (Fig. 16). The caps were not probably formed, because the strain was kept in culture for many years. It would be interesting to examine a strain just taken from a natural habitat.

Our ultrastructural results thus suggest taxonomic reassignments among some of the *Euglena* species studied here. Using the intra-generic classification proposed by Zakryś (1986) one more taxa, *E. cuneata* should now be added to those presently classified in the Subgenus *Euglena*, which is characterized by axial chloroplasts with pyrenoids. Moreover, two other taxa, *E. deses* var. *deses* and *E. deses* var. *intermedia,* should be now classified in the Subgenus *Calliglena*, which is characterized by parietal (or partly so), never axial chloroplasts with pyrenoids (Zakryś 1986).

It is clear that additional research is essential for the requisite taxonomic revision of *Euglena* species, termed "*Euglena viridis* Group, Subgenus *Euglena,* in which *E. myxocylindracea, E. stellata, E. viridis,* and now *E. cuneata* are classified. Current proposed relationships among the members of the group need to be verified by additional approaches, especially the use of molecular methods.

Some molecular data have been obtained recently but only for two species - *E. stellata and E. viridis,* however, the data are contradictory. Whereas the pair of species have 82,7% of RAPD and 88,5% of RFLP bands in common and each clustering method reveals this two-element cluster (Zakryś *et al.* 1997), their SSU rDNA sequences are distinct, having diverged by 13% from each other (Linton *et al.* 2000). Such investigations will be the focus of future research.

Acknowledgements. This work was supported by grant from the Polish Committee for Scientific Research (KBN 6 PO4C 016 17). We thank Prof. Dr. U. G. Schlösser, Sammlung von Algenkulturen (SAG), Göttingen, Germany, for providing the *Euglena* strains. We acknowledge the Electron Microscopy Laboratory at University of Barcelona for technical assistance with the project.

REFERENCES

Buetow D. E. (1968) Morphology and ultrastructure of *Euglena.* In: The Biology of Euglena I. (Ed. D. E. Buetow). Academic Press, London-New York, 109-184

Chu S. P. (1946) Contributions to our knowledge of the genus *Euglena*. *Sinensia* **17:** 75-34

Dangeard P. A. (1901) Recherches sur les Eugléniens. *Le Botaniste* **8:** 97-360

Dillard G. E. (2000) Freshwater algae of the Southeastern United States. Part 7: Pigmented *Euglenophyceae*. Bibliotheca Phycologica. Gebr. Borntraeger, Berlin-Stuttgart

Dragos N., Péterfi L. S., Craciun C. (1979) Fine structure of *Euglena.* II. *Euglena stellata* Mainx and *Euglena viridis* Ehrenberg. *Nova Hedwigia* **31:** 223-246

Gojdics M. (1953) *The genus Euglena*. The University of Wisconsin. Press, Madison

Haller D. E. G. (1959) Structure submicroscopique *d'Euglena viridis. Archs Sci. Genéve,* **12:** 309-340

Huber-Pestalozzi P. (1955) Das Phytoplankton des Süsswassers. In: Die Binnengewässer 4. (Ed. A. Thienemann). E. Schweizerbart'sche Verlagsbuchhandlung, Stuttgart 1-606

Kim J. T. S., Boo S. M., Zakryś B. (1998) Floristic and taxonomic accounts of the genus *Euglena* (*Euglenophyceae)* from Korean fresh waters. *Algae* **13:** 173-197

Lemmermann E. (1913) *Eugleninae.* In: Die Süsswasserflora Deutschlands, Österreichs, und der Schweiz. G. Fisher, Jena, 215-274

Leedale G. F. (1968) Ultrastructure. In: The Biology of Euglena III. (Ed. D. E. Beutow). Academic Press, London-New York, 1-27

Linton E. W., Nudelman M. A., Conforti V., Triemer R. E. (2000) A molecular analysis of the Euglenophytes using SSU rDNA. *J. Phycol.* **36:** 740-746

Mignot J. P. (1965) Ultrastructure des Eugléniens I. Étude de la cuticule chez différentes espéces. *Protistologica* **1:** 5-15

Mignot J. P. (1966) Structure et ultrastructure de quelques Euglénomonadines. *Protistologica* **2:** 51-117

Németh J. (1997) A Guide for the identification of *Euglenophyta* occurring in Hungary. I. Vizi Természet-És Környezetvédelem (in Hungarian)

Péterfi L. S. (1986) Algal flora of Salicea I. *Euglenophyta. Contributii Botanice, Cluj-Napoca*, 13-28

Péterfi L. S., Dragos N., Craciun C. (1979) Fine structure of *Euglena.* I. *tristella* Ch. *Nova Hedwigia* **31:** 197-221

Popova T. G. (1966) Euglenovyje vodorosli. Vyp. 2 (*Euglenophyta.* Part 2). Flora sporovych rastenij SSSR 9. Izd. Nauka, Moskva - Leningrad (in Russian)

Pringsheim E. G. (1956) Contributions towards a monograph of the genus *Euglena. Nova Acta Leopoldina* **18:** 1-168

Starr R. C. (1978) The culture collection of algae at the University of Texas at Austin. *J. Phycol*. **14(Suppl.):** 47-100

Wołowski K. (1998) Taxonomic and environmental studies on Euglenophytes of the Kraków-Częstochowa upland (Southern Poland). *Fragm. Flor. Geogot.* Suppl. **6(Suppl.):** 3-192

Zakryś B. (1986) Contribution to the monograph of Polish members of the genus *Euglena* Ehrenberg 1830. *Nova Hedwigia* **42:** 494-540

Zakryś B., Walne P. L. (1994) Floristic, taxonomic and phytogeographic studies of green *Euglenophyta* from southeastern United States, with emphasis on new and rare species. *Arch. Hydrobiol. Suppl. Algol. Studies* **72:** 71-114

Zakryś B. (1997) The taxonomic consequences of morphological and genetic variability in Euglena agilis Carter (Euglenophyta): Species or clones in *Euglena*?. *Acta Protozool.* **36:** 157-169

Zakryś B., Walne P. L. (1998) Comparative ultrastructure of chloroplasts in the Subgenus *Euglena* (Euglenophyta): Taxonomic significance. *Cryptogamie, Algol.* **19:** 3-18

Zakryś B., Moraczewski I., Kucharski R. (1997) The species concept in *Euglena* in the light of DNA polymorphism analyses. *Arch. Hydrobiol. Suppl. Algol. Studies* **86:** 51-79

Zhi Z. X., Wang Q. X., Xie S. L., Dai J., Chen L. (1999) Flora Algarum Sinicsrum Aquae Dulcis. Tomus VI: *Euglenophyta*. Academiae Sinicae: Science Press (in Chinese)

Received and accepted on 28th March, 2001

INSTRUCTIONS FOR AUTHORS

Acta Protozoologica is a quarterly journal that publishes current and comprehensive, experimental, and theoretical contributions across the breadth of protistology, and cell biology of lower Eukaryote including: behaviour, biochemistry and molecular biology, development, ecology, genetics, parasitology, physiology, photobiology, systematics and phylogeny, and ultrastructure. It publishes original research reports, critical reviews of current research written by invited experts in the field, short communications, book reviews, and letters to the Editor. Faunistic notices of local character, minor descriptions, or descriptions of taxa not based on new, (original) data, and purely clinical reports, fall outside the remit of *Acta Protozoologica.*

Contributions should be written in grammatically correct English. Either British or American spelling is permitted, but one must be used consistently within a manuscript. Authors are advised to follow styles outlined in The CBE Manual for Authors, Editors, and Publishers (6th Ed., Cambridge University Press). Poorly written manuscripts will be returned to authors without further consideration.

Research, performed by "authors whose papers have been accepted to be published in *Acta Protozoologica* using mammals, shall have been conducted in accordance with accepted ethical practice, and shall have been approved by the pertinent institutional and/or governmental oversight group(s)"; this is Journal policy, authors must certify in writing that their research conforms to this policy.

Nomenclature of genera and species names must agree with the International Code of Zoological Nomenclature (ICZN), International Trust for Zoological Nomenclature, London, 1999; or the International Code of Botanical Nomenclature, adopted by XIV International Botanical Congress, Berlin, 1987. Biochemical nomenclature should agree with "Biochemical Nomenclature and Related Documents" (A Compendium, 2nd edition, 1992), International Union of Biochemistry and Molecular Biology, published by Portland Press, London and Chapel Hill, UK.

Except for cases where tradition dictates, SI units are to be used. New nucleic acid or amino acid sequences will be published only if they are also deposited with an appropriate data bank (e.g. EMBL, GeneBank, DDBJ).

All manuscripts that conform to the Instructions for Authors will be fully peer-reviewed by members of Editorial Board and expert reviewers. The Author will be requested to return a revised version of the reviewed manuscript within four (4) months of receiving the reviews. If a revised manuscript is received later, it will be considered to be a new submission. There are no page charges, but Authors must cover the reproduction cost of colour illustrations.

The Author(s) of a manuscript, accepted for publication, must transfer copyrights to the publisher. Copyrights include mechanical, electronic, and visual reproduction and distribution. Use of previously published figures, tables, or brief quotations requires the appropriate copyright holder's permission, at the time of manuscript submission; acknowledgement of the contribution must also be included in the manuscript. Submission of a manuscript to *Acta Protozoologica* implies that the contents are original, have not been published previously, and are not under consideration or accepted for publication elsewhere.

SUBMISSION

Authors should submit manuscript to: Dr Jerzy Sikora, Nencki Institute of Experimental Biology, ul. Pasteura 3, 02-093 Warszawa, Poland, Fax: (4822) 8225342; E-mail: jurek@nencki.gov.pl or j.sikora@nencki.gov.pl.

At the time of submission, authors are encouraged to provide names, E-mails, and postal addresses of four persons who might act as reviewers. Extensive information on *Acta Protozoologica* is available at the website: **http://www.nencki.gov.pl/ap.htm**; however, please do not hesitate to contact the Editor.

Hard copy submission: Please submit three (3) high quality sets of text and illustrations (figures, line drawing, and photograph). When photographs are submitted, arranged these in the form of plate. A copy of the text on a disk or CD should also be enclosed, in PC formats, preferably Word for Windows version 6.0 or higher (IBM, IBM compatible, or MacIntosh). If they do not adhere to the standards of the journal the manuscript will be returned to the corresponding author without further consideration.

E-mail submission: Electronic submission of manuscripts by e-mail is acceptable in PDF format only. Illustrations must be prepared according to journal requirement and saved in PDF format. The accepted manuscript should be submitted as a hard copy with illustrations (two copies, one with lettering + one copy without lettering) in accordance with the standards of the journal.

ORGANIZATION OF MANUSCRIPTS

Text: Manuscripts must be typewritten, double-spaced, with numbered pages (12 pt, Times Roman). The manuscript should be organized into the following sections: Title, Summary, Key words, Abbreviations, Introduction, Materials and Methods, Results, Discussion, Acknowledgements, References, Tables, and Figure legends. Figure legends must contain explanations of all symbols and abbreviations used. The Title Page should include the title of the manuscript, first name(s) in full and surname(s) of author(s), the institutional address(es) where the work was carried out, and page heading of up to 40 characters (including spaces). The postal address for correspondence, Fax and E-mail should also be given. Footnotes should be avoided.

Citations in the text should be ordered by name and date but not by number, e.g. (Foissner and Korganova 2000). In the case of more than two authors, the name of the first author and *et al.* should be used, e.g. (Botes *et al.* 2001). Different articles by the same author(s) published in the same year must be marked by the letters a, b, c, etc. (Kpatcha *et al.* 1996a, b). Multiple citations presented in the text must be arranged by date, e.g. (Small 1967, Didier and Detcheva 1974, Jones 1974). If one author is cited more than once, semicolons should separate the other citations, e.g. (Lousier and Parkinson 1984; Foissner 1987, 1991, 1994; Darbyshire *et al.* 1989).

Please observe the following instructions when preparing the electronic copy: (1) label the disk with your name; (2) ensure that the written text is identical to the electronic copy; (3) arrange the text as a single file; do not split it into smaller files; (4) arrange illustrations as separate files; do not use Word files; *.TIF, *.PSD, or *.CDR graphic formats are accepted; (5) when necessary, use only italic, bold, subscript, and superscript formats; do not use other electronic formatting facilities such as multiple font styles, ruler changes, or graphics inserted into the text; (6) do not right-justify the text or use of the hyphen function at the end of lines; (7) avoid the use of footnotes; (8) distinguish the numbers 0 and 1 from the letters O and l; (9) avoid repetition of illustrations and data in the text and tables.

References: References must be listed alphabetically. Examples for bibliographic arrangement:

Journals: Flint J. A., Dobson P. J., Robinson B. S. (2003) Genetic analysis of forty isolates of *Acanthamoeba* group III by multilocus isoenzyme electrophoresis. *Acta Protozool.* **42:** 317-324

Books: Swofford D. L. (1998) PAUP* Phylogenetic Analysis Using Parsimony (*and Other Methods). Ver. 4.0b3. Sinauer Associates, Sunderland, MA

Articles from books: Neto E. D., Steindel M., Passos L. K. F. (1993) The use of RAPD's for the study of the genetic diversity of *Schistosoma mansoni* and *Trypanosoma cruzi*. In: DNA Fingerprinting: State of Science, (Eds. S. D. J. Pena, R. Chakraborty, J. T. Epplen, A. J. Jeffreys). Birkhäuser-Verlag, Basel, 339-345

Illustrations and tables: After acceptance of the paper, drawings and photographs (two copies one with lettering + one copy without) must be submitted. Each table and figure must be on a separate page. Figure legends must be placed, in order, at the end of the manuscript, before the figures. Figure legends must contain explanations of all symbols and abbreviations used. All line drawings and photographs must be labelled, with the first Author's name written on the back. The figures should be numbered in the text using Arabic numerals (e.g. Fig. 1).

Illustrations must fit within either a single column width (86 mm) or the full-page width (177 mm); the maximum length of figures is 231 mm, including the legend. Figures grouped as plates must be mounted on a firm board, trimmed at right angles, accurately mounted, and have edges touching. The engraver will then cut a fine line of separation between figures.

Line drawings should be suitable for reproduction, with well-defined lines and a white background. Avoid fine stippling or shading. Prints are accepted only in *.TIF, *.PSD, and *.CDR graphic formats (Grayscale and Colour - 600 dpi, Art line - 1200 dpi) on CD. Do not use Microsoft Word for figure formatting.

Photographs should be sharp, glossy finish, bromide prints. Magnification should be indicated by a scale bar where appropriate. Pictures of gels should have a lane width of no more than 5 mm, and should preferably fit into a single column.

PROOF SHEETS AND OFFPRINTS

After a manuscript has been accepted, Authors will receive proofs for correction and will be asked to return these to the Editor within 48-hours. Authors will be expected to check the proofs and are fully responsible for any undetected errors. Only spelling errors and small mistakes will be corrected. Twenty-five reprints (25) will be furnished free of charge. Additional reprints can be requested when returning the proofs, but there will be a charge for these; orders after this point will not be accepted.

Indexed in: Current Contents, Biosis, Elsevier Biobase, Chemical Abstracts Service, Protozoological Abstracts, Science Citation Index, Librex-Agen, Polish Scientific Journals Contents - Agric. & Biol. Sci. Data Base at: **http://psjc.icm.edu.pl**, Microbes.info "Spotlight" at **http://www.microbes.info**, and electronic version at Nencki Institute of Experimental Biology website in *.PDF format at http://www.nencki.gov.pl/ap.htm now free of charge.

ACTA
PROTOZOOLOGICA

ORIGINAL ARTICLES

SHORT COMMUNICATIONS

2001 MAY
VOLUME 40 NUMBER 2